



**Illinois State Water Survey**  
HYDROLOGY DIVISION

---

SWS Contract Report 518

**HYDROLOGIC MODELING OF THE FOX RIVER WATERSHED**

*by*

*H. Vernon Knapp, Terry W. Ortel, and Robert S. Larson*  
*Office of Surface Water Resources and Systems Analysis*

Prepared for the  
Illinois Department of Transportation, Division of Water Resources

Champaign, Illinois

November 1991

# **HYDROLOGIC MODELING OF THE FOX RIVER WATERSHED**

By  
H. Vernon Knapp, Terry W. Ortel, and Robert S. Larson

Prepared for the  
Illinois Department of Transportation, Division of Water Resources

Illinois State Water Survey  
2204 Griffith Drive  
Champaign, Illinois 61820-7495

November 1991

This report was printed on recycled and recyclable paper.

# CONTENTS

	Page
Introduction.....	1
Purpose of Modeling.....	3
Acknowledgments.....	3
Description of the Fox River Watershed.....	4
Lakes and Reservoirs.....	7
Precipitation.....	8
Precipitation Gages.....	9
Frequency of Heavy Rainfall.....	9
Soil Type.....	11
Available Soils Information.....	11
Geographic Distribution.....	13
Land Use.....	13
Available Data.....	13
Geographic Distribution.....	17
Streamflow.....	17
Available Streamflow Information.....	17
Historical Flooding.....	17
Model Development and Calibration.....	24
Desired Attributes of the Rainfall-Runoff Model.....	24
Model Structure.....	25
Component 1: Soil-Moisture Modeling for Land Use and Soil Types.....	26
PACE Soil-Moisture Modeling.....	26
Modifications to the PACE Soil-Moisture Component.....	29
Implementation of PACE to Land-Use and Soil Type Combinations.....	30
Separation of Subsurface Flow into Interflow and Baseflow.....	34
Soil-Moisture Modeling Output.....	34
Component 2: Modeling Watershed Hydrograph Response.....	34
Variations in Hydrologic Response to Storm Rainfall.....	34
Regression Analysis.....	36
Using Regression Coefficients to Estimate Watershed Hydrographs.....	37
Regionalization of Hydrograph Response.....	40
Estimation of Baseflow.....	43
Simulation of Sub-Watershed Hydrographs.....	44
Comparison of Simulated and Observed Hydrographs for Sub-Watersheds.....	44
Estimation of Six-Hour Hydrograph Values.....	56
Component 3: Channel and Reservoir Routing.....	57
Channel Routing.....	58
Reservoir Routing.....	60
Application to the Fox River Upstream of Wilmot.....	61
Application to Nippersink Creek.....	69
Application to the Fox River from Wilmot to South Elgin.....	70
Analysis of Modeling Results.....	73
Comparison of Observed and Estimated Streamflow Records.....	73
Annual Flows.....	73
Average Monthly Flows.....	75
Daily Flows.....	75
Annual Maximum Flows.....	78
Use of the Model for Near Real-Time Forecasting.....	84
Recommended Modifications to the Precipitation Gage Network.....	85
Summary.....	87
References.....	88

## LIST OF FIGURES

	Page
Figure 1. Aerial photograph of the southern portion of the Fox Chain of Lakes	2
Figure 2. Location of the Fox River watershed in Illinois and Wisconsin, and the limits of study	5
Figure 3. Major lakes and streams in the Fox River watershed	6
Figure 4. Stream profile of the Fox River and major tributaries	7
Figure 5. Location of precipitation gages in and near the Fox River watershed	10
Figure 6. Geographic distribution of soils in the Fox River watershed	14
Figure 7. Location of streamgaging stations in and near the Fox River watershed	19
Figure 8. Inflow flood hydrographs for the Chain of Lakes: November and December 1982	22
Figure 9. Inflow flood hydrographs for the Chain of Lakes: September and October 1986	22
Figure 10. Components of the Fox River Hydrologic Model	27
Figure 11. Daily amounts of a) surface runoff, and b) subsurface flow, from soil types A, B1, B2, C, and D: Lake Geneva, September 1986	33
Figure 12. Portion of computed subsurface flow resulting in baseflow	41
Figure 13. Relationship between watershed drainage area and surface runoff hydrographs	42
Figure 14. Observed versus estimated flow: Poplar Creek, 1974	52
Figure 15. Observed versus estimated flow: Poplar Creek, 1979	52
Figure 16. Observed versus estimated flow: Boone Creek, 1974	53
Figure 17. Observed versus estimated flow: Boone Creek, 1979	53
Figure 18. Observed versus estimated flow: Root River Canal, 1976	54
Figure 19. Observed versus estimated flow: Root River Canal, 1974	54
Figure 20. Example of the estimation of six-hour streamflows from daily values	57
Figure 21. Schematic diagram of routing elements for the Fox River upstream of Wilmot	62
Figure 22. Cross section of Nippersink Creek downstream of the Spring Grove gage	63
Figure 23. Cross section of Nippersink Creek near the Spring Grove gage	64
Figure 24. Cross section of Nippersink Creek upstream of the Spring Grove gage	64
Figure 25. Depth of flow versus cross-sectional area for Nippersink Creek	65
Figure 26. Cross-sectional area versus discharge for Nippersink Creek	65
Figure 27. Relationship between Muskingum K and discharge	67
Figure 28. Relationship between Muskingum X and discharge	67
Figure 29. Schematic diagram of routing elements for Nippersink Creek	69

## List of Figures Concluded

	Page
Figure 30. Schematic diagram of routing elements for the Fox River between Wilmot and South Elgin.....	71
Figure 31. Observed versus estimated flow: Fox River at Wilmot, 1979.....	76
Figure 32. Observed versus estimated flow: Fox River at Wilmot, 1986.....	76
Figure 33. Observed versus estimated flow: Nippersink Creek near Spring Grove, 1979.....	77
Figure 34. Observed versus estimated flow: Nippersink Creek near Spring Grove, 1986.....	77
Figure 35. Frequency of daily flows: Fox River at Wilmot.....	79
Figure 36. Frequency of daily flows: Nippersink Creek near Spring Grove.....	79
Figure 37. Prediction of the total inflow entering the Chain of Lakes, based on four rainfall prognoses.....	85

## LIST OF TABLES

Table 1. Channel Slopes for Streams in the Fox River Watershed.....	4
Table 2. Surface Area and Storage Capacity for the Fox Chain of Lakes.....	8
Table 3. Lists of Daily Precipitation Gages in and Near the Fox River Watershed.....	9
Table 4. Magnitude and Frequency of Heavy 24-Hour Precipitation by Season, Northeastern Illinois.....	11
Table 5. Soil Associations in the Illinois Portion of the Fox River.....	12
Table 6. Soil Associations in the Wisconsin Portion of the Fox River.....	12
Table 7. Examples of Land Use in the Illinois Portion of the Fox River.....	15
Table 8. Examples of Land Use in the Wisconsin Portion of the Fox River.....	16
Table 9. List of USGS Stream Gages in the Fox River Watershed Area.....	18
Table 10. Major Flood Peaks Recorded at the Fox River at Algonquin, Fox River at Wilmot, and Nippersink Creek near Spring Grove.....	20
Table 11. Maximum Discharges Observed at Gages on Smaller Streams in or near the Fox River Watershed.....	23
Table 12. Estimates of the 100-Year Flood Peak from Flood Insurance Studies Conducted for Streams in the Fox River Watershed.....	23
Table 13. Example of the Annual Distribution of Surface Runoff and Subsurface Flow Estimated by the PACE Soil-Moisture Component for Different Land Uses: Soil Types B1 and C.....	32
Table 14. Example of the Annual Distribution of Surface Runoff and Subsurface Flow Estimated by the PACE Soil-Moisture Component for Different Soil Types.....	32

## LIST OF TABLES (concluded)

	Page
Table 15. Example of PACE Model Output _____	35
Table 16. Streamgage Records Used in Hydrograph Regression Analysis.....	38
Table 17. Calibrated Coefficients of Surface Runoff from Sub-Watersheds___	38
Table 18. Sub-Watersheds in the Fox River Basin.....	45
Table 19. Land Use and Soil Type Combinations for Each Watershed (by fraction of the watershed) _____	47
Table 20. Hydrograph Parameters for Sub-Watersheds.....	50
Table 21. Annual Peak Flow Series (cfs) for Selected Sub-Watersheds.....	55
Table 22. Routing Parameter Reach Types.....	62
Table 23. Fox River Routing Parameter Relations.....	66
Table 24. Climatic Data Used in Reservoir Routing.....	68
Table 25. Nippersink Creek Routing Parameter Relations.....	70
Table 26. Average Annual Flows for the Fox River and Nippersink Creek: Observed versus Estimated Flow.....	74
Table 27. Average Monthly Flow for the Fox River and Nippersink Creek: Observed versus Estimated Flow, Calendar Years 1974-1987.....	75
Table 28. Error in Simulated Daily Flows.....	80
Table 29. Annual Maximum Daily Flows for the Fox River at Wilmot: Observed versus Estimated Flow.....	81
Table 30. Annual Maximum Daily Flows for Nippersink Creek near Spring Grove: Observed versus Estimated Flow.....	82
Table 31. Ranked Series of Annual Maximum Flows for the Fox River at Wilmot and Nippersink Creek near Spring Grove: Observed versus Estimated Flow.....	83

## INTRODUCTION

The Fox Chain of Lakes is a series of interconnected glacial lakes in northeastern Illinois. Both the Chain of Lakes and the Fox River downstream of the lakes have long been popular for boating, fishing, and other recreational activities. McHenry Dam, located on the Fox River downstream of the lakes, was originally constructed in 1907 to raise and regulate pool levels in the Fox Chain of Lakes for boating purposes. Gate facilities were added during a reconstruction of the dam in 1939. The gates provide greater flexibility in regulating lake stages and outflow from the lakes, but the primary objective of gate operation remains the maintenance of the recreational pool.

Over the years, there has been considerable residential development along the flat shoreline of the lakes and river (figure 1). Along with the development has come increasing interest in the management of the gates at McHenry Dam for flood-control benefits. However, the required methods of gate operation for flood control are not straightforward — in part because the dam's ability to reduce flooding damage is limited by hydraulic characteristics of the Fox River. An additional consideration is the potential impact that flood-control operation has on other uses of the Chain of Lakes, such as recreation and the maintenance of aquatic habitat. Flood-control operation of the dam has attempted to minimize overbank flooding both upstream and downstream of the dam without negative impact on recreation. Within this objective, and given the available amount of flow information in the watershed, gate management has appeared to have reasonably successful results. However, a search for better methods to improve gate operation for flood control is desired.

Flood-control concerns prompted previous studies in 1962 and 1984. The 1962 study by the Illinois Division of Water Resources, formerly the Division of Waterways, concluded that the major controlling factor in the determination of upstream or downstream flooding is not the operation of McHenry Dam, but is the limited hydraulic conveyance of the channel both upstream and downstream of McHenry Dam. Several alternative measures were presented, including channel enlargement, construction of upstream reservoirs, and flood levees; but each was considered either economically impractical or incapable of significantly reducing flood damage.

A study by the U.S. Army Corps of Engineers (1984) recommended the installation of additional floodgates at the McHenry and Algonquin Dams to help improve the channel's ability to convey greater flood flow. A major purpose of the proposed gates was the reduction of storage in the lakes prior to the arrival of a flood. Proper management of the gates would require a flood forecast system that provides lead-time and sufficiently estimates the magnitude of an approaching flood. Insufficient information was supplied with the Corps of Engineers'



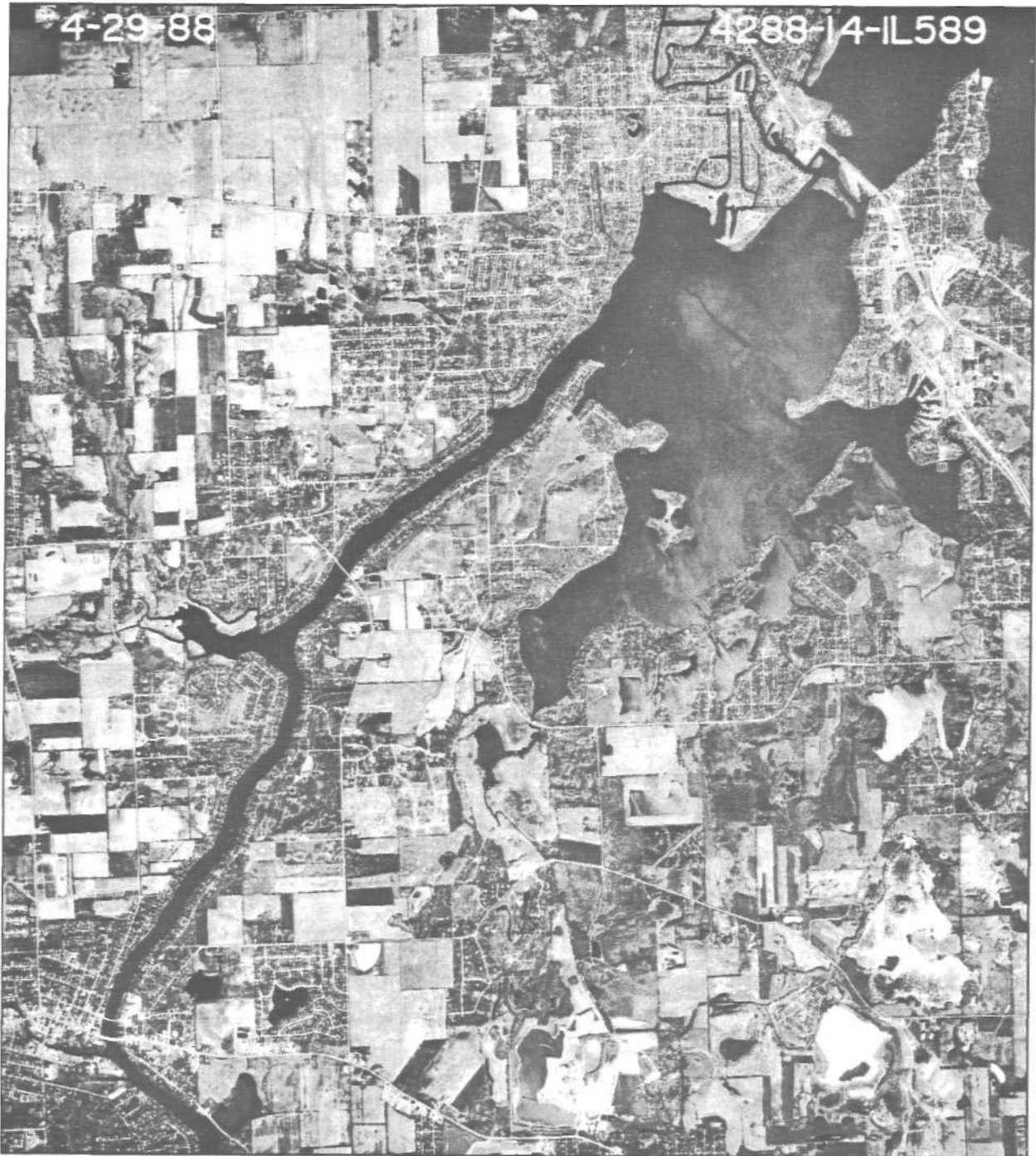


**Figure 1. Aerial photograph of the southern portion of the Fox Chain of Lakes (photograph courtesy of the Illinois Department of Transportation, Division of Water Resources)**

recommendation to determine the amount of lead-time needed for reduction in the Chain of Lakes storage or the effect of the hydraulic changes on flood hydrographs.

### **Purpose of Modeling**

The development and evaluation of a flood-control management policy for McHenry Dam requires both accurate forecasts of inflows into the Chain of Lakes and a method to evaluate how different gate operations will affect lake levels and flows downstream. Two models are proposed for use in this evaluation: 1) a rainfall-runoff watershed model and 2) an unsteady flow-routing model to simulate the hydraulics of both the lake and the Fox River. The development of the rainfall-runoff watershed model is described in this report. The unsteady flow-routing model for the Chain of Lakes and Fox River was developed concurrently by the Illinois Division of Water Resources.

The rainfall-runoff watershed model two proposed uses: 1) operational forecasting, providing forecasts of inflow into the Fox Chain of Lakes for up to five days; and 2) simulating streamflow conditions throughout the watershed for historical storms and for hypothetical rainfall conditions. Using hypothetical rainfall, rainfall-runoff is evaluated for storms.

When used in simulation mode, the output from the rainfall-runoff model will be used as input to the unsteady flow-routing model to estimate flow and stage in the Chain of Lakes and the Fox River downstream to South Elgin. Using forthcoming simulation analyses, it is anticipated that the response of the lake level and downstream flow levels to changes in gate openings will be sufficiently understood to produce management policy that will minimize upstream and downstream flood damage. The benefit of adding additional gates to the McHenry and Algonquin Dams can also be evaluated using this simulation analysis.

The model developed in this study was designed specifically for use in planning and operational forecasting for the Chain of Lakes and the Fox River downstream to South Elgin. Use of this model without further modification may not be appropriate for other purposes, such as evaluating the flood hydrology along smaller tributaries within the Fox River watershed.

### **Acknowledgments**

This study was supported by the Illinois Department of Transportation, Division of Water Resources, with William W. Rice as project coordinator. The investigation was prepared under the general supervision of Richard G. Semonin, Chief of the Illinois State Water Survey; John M. Shafer, Hydrology Division Head; and Krishan P. Singh, Director of the Office of Surface Water Resources and Systems Analysis. Linda J. Hascall prepared the illustrations and the report was edited by Eva C. Kingston.

## DESCRIPTION OF THE FOX RIVER WATERSHED

The Fox River is a tributary to the Illinois River, located in northeastern Illinois and southeastern Wisconsin. The Fox River watershed (figure 2) has a total area of approximately 2,658 square miles (sq mi), 938 sq mi of which are in Wisconsin. This report is concerned with that portion of the Fox River lying upstream of South Elgin, where the drainage area is 1,555 sq mi. The two principal tributaries to the Fox River in the study reach are Honey Creek, with a drainage area of 264 sq mi, and Nippersink Creek (205 sq mi). Other major streams in the watershed (figure 3) are White River (111 sq mi), Mukwonago River (88 sq mi), Wind Lake Canal (84 sq mi), Sugar Creek (63 sq mi), Squaw Creek (46 sq mi), and Poplar Creek (44 sq mi).

The topography of the Fox River basin is developed on glacial till and glacial outwash. Throughout much of the watershed, the glacial moraines produce an uneven rolling topography that frequently has depressions with limited external drainage. Lakes often form in these depressions, and when no surface outlet is available, water from these lakes may be discharged into shallow aquifers rather than directly into streams (Cotter et al., 1969).

The Fox River watershed is gently rolling with moderate land slopes and channel slopes (table 1). Along the Fox River in the central portion of the watershed (between Waukesha, Wisconsin and Algonquin, Illinois), the terrain is low-lying and flat. The channel slope of the Fox River in the 50-mile reach between Burlington and Algonquin is especially mild, averaging

**Table 1. Channel Slopes for Streams in the Fox River Watershed**

	Drainage Area (sq mi)	Channel Slope (ft/mi)
<u>Wisconsin</u>		
Fox River at Waukesha	126.	4.0
Mukwonago River	74.	3.7
Honey Creek	85.	3.9
Sugar Creek	76.	5.1
Wind Lake Drainage Ditch	98.	1.8
Eagle Creek	16.3	5.9
*Root River Canal	57.0	6.3
*Menomonee River	34.7	6.7
*Jackson Creek	9.0	18.8
<u>Illinois</u>		
Boone Creek	23.3	6.2
Flint Creek	36.8	8.3
Crystal Creek	27.2	13.5
Ferson Creek	51.7	13.3
Poplar Creek	35.2	9.1

**Note:** An asterisk denotes stream located adjacent to the Fox watershed.

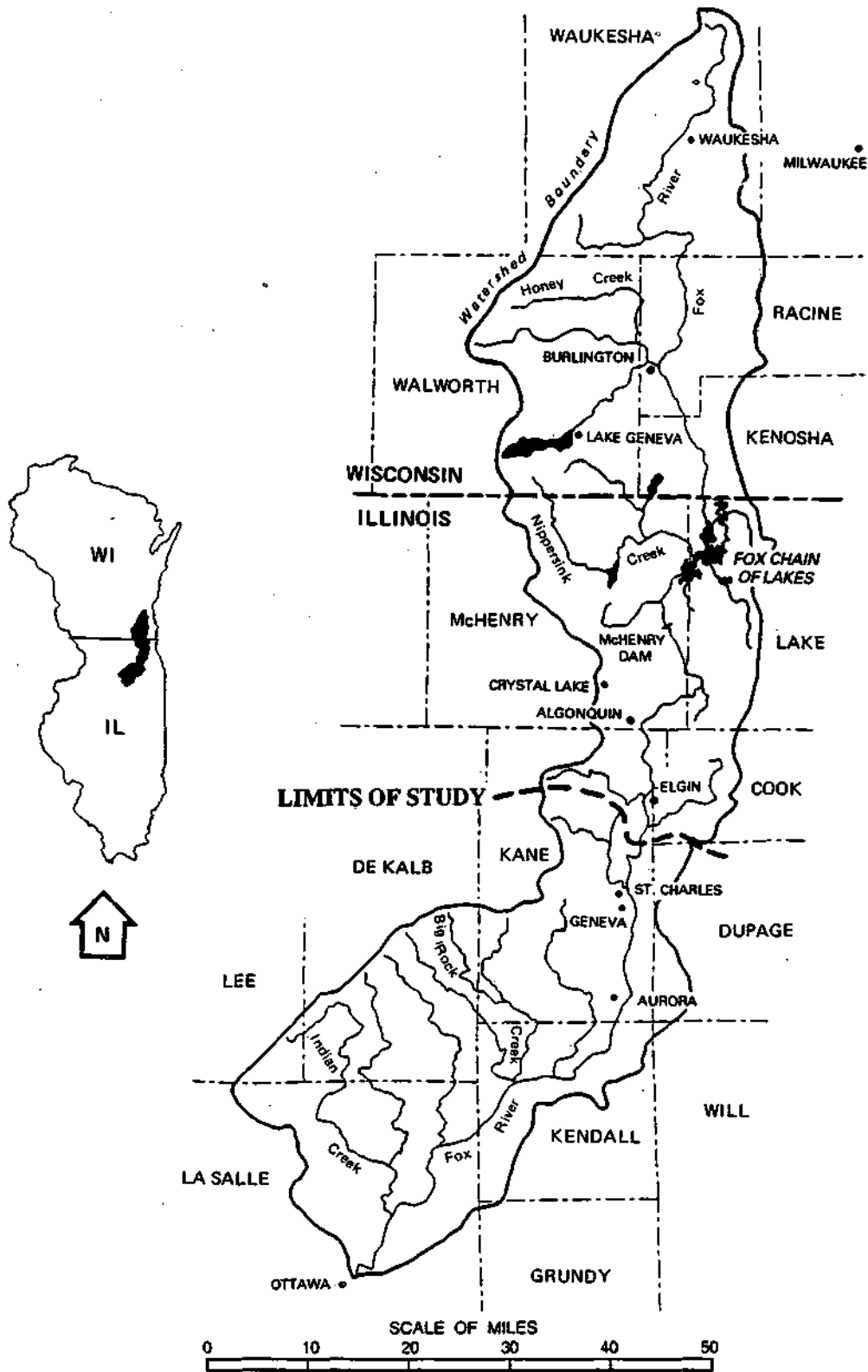


Figure 2. Location of the Fox River watershed in Illinois and Wisconsin, and the limits of study

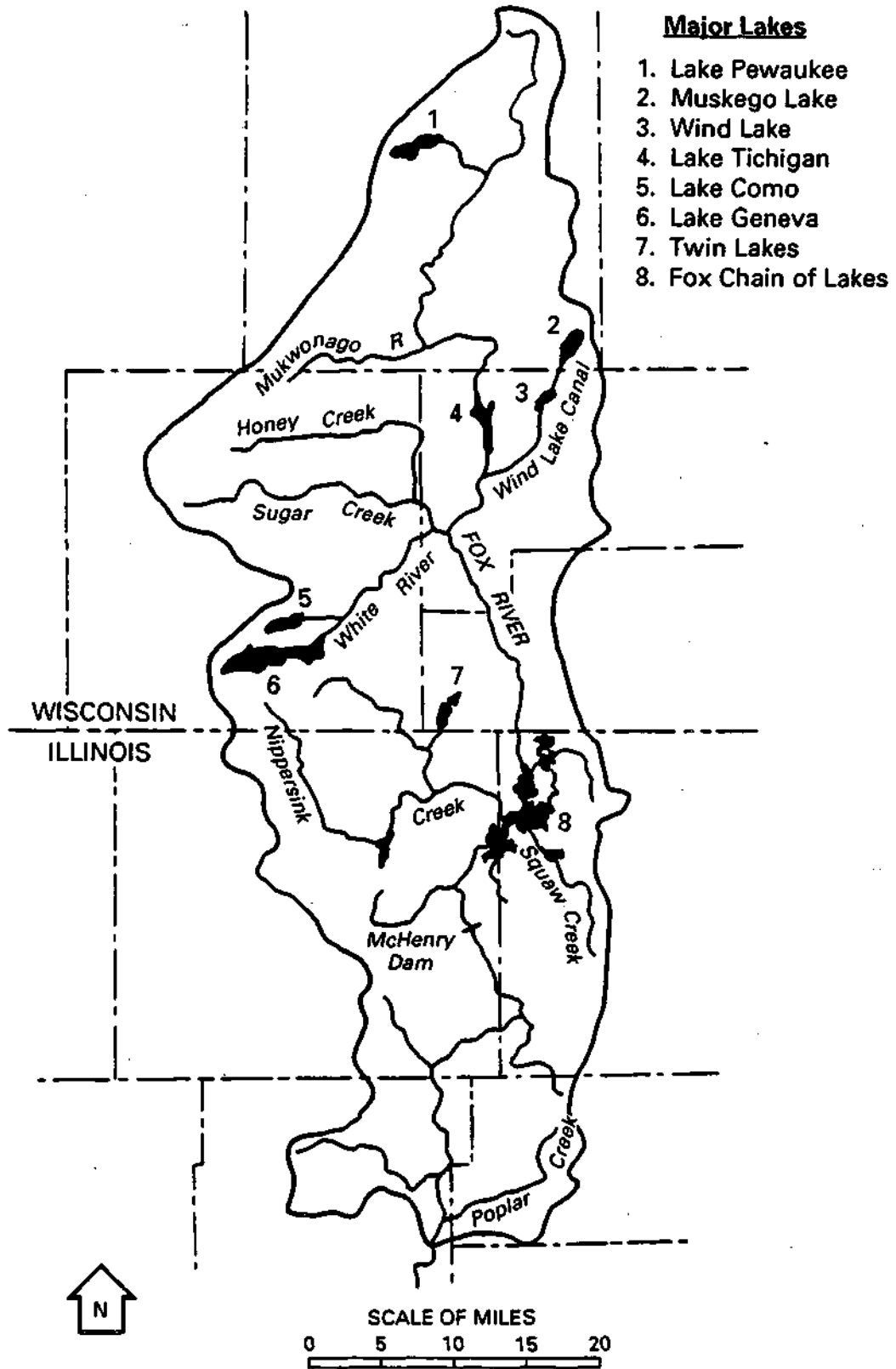


Figure 3. Major lakes and streams in the Fox River watershed

less than 0.5 feet per mile. This is illustrated in the channel profile of the Fox River given in figure 4. The mild slope and low-lying areas produce many wetlands and marshes. It is also in this area that the Chain of Lakes occur. As a result of the mild slopes and marshy areas, which provide additional detention storage, water generally moves slowly through both the watershed and the Chain of Lakes.

### Lakes and Reservoirs

The Fox River watershed has approximately 60 naturally occurring lakes that have a surface area larger than 100 acres (U.S. Army Corps of Engineers, 1976). The Fox Chain of Lakes contains nine of these prominent lakes: Fox Lake, Nippersink Lake, Pistakee Lake, Petite Lake, Grass Lake, Channel Lake, Bluff Lake, Lake Marie, and Lake Catherine. The nine interconnected lakes have a combined surface area of 7,700 acres and storage capacity of approximately 44,000 acre-feet at the normal recreation pool level. The storage capacity in the Chain of Lakes for a range of pool levels is given in table 2. The difference in storage between the normal pool level and the highest recorded pool level is approximately 38,000 acre-feet. This

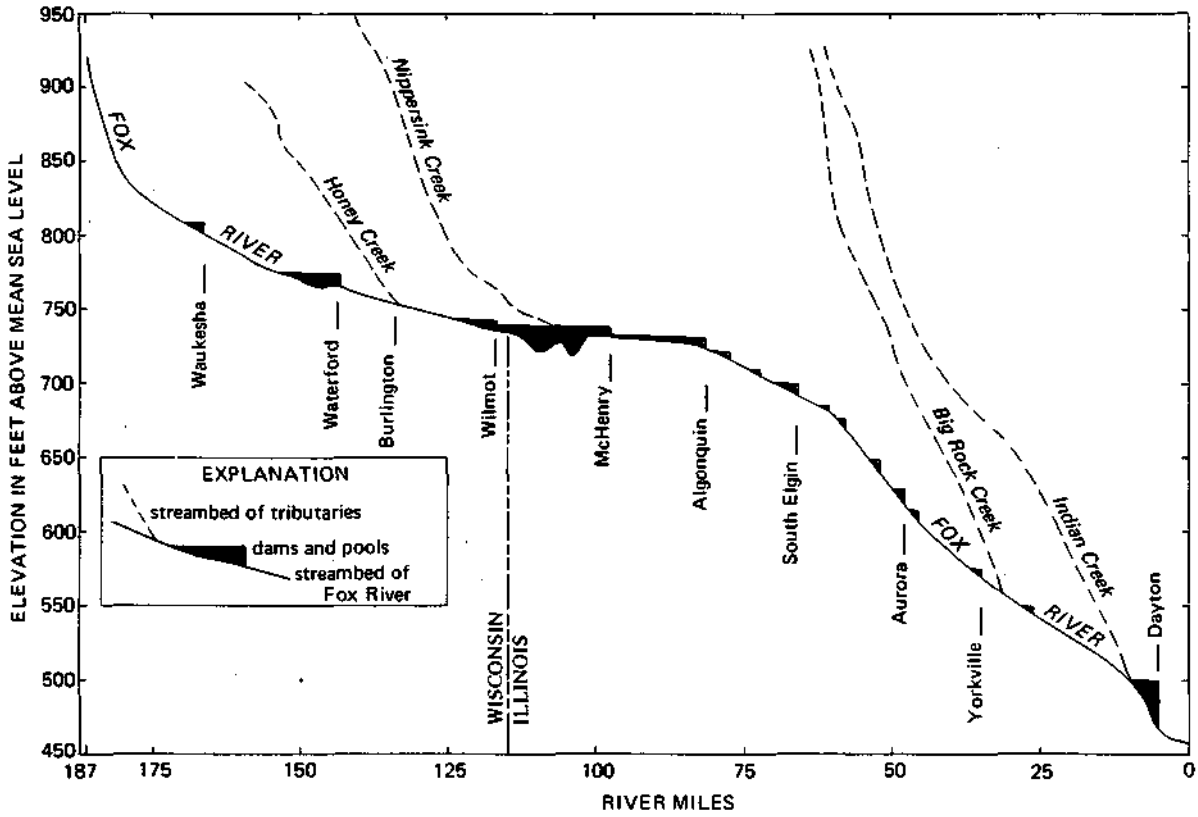


Figure 4. Stream profile of the Fox River and major tributaries

**Table 2. Surface Area and Storage Capacity for the Fox Chain of Lakes**

<u>Elevation of Pool Level (feet) [NGVD]<sup>a</sup></u>	<u>Water Surface Area (acres)</u>	<u>Storage Capacity (acre-feet)</u>
735.0	6,100	31,000
736.8 <sup>b</sup>	7,700	44,000
738.0	10,000	54,000
740.55 <sup>c</sup>	11,900	82,000

**Notes:** <sup>a</sup> National Geodetic Vertical Datum

<sup>b</sup> normal recreational pool level

<sup>c</sup> level of highest recorded flood

difference in storage is equivalent to the volume of water that would result from a uniform 0.3"-inch rainfall over the entire watershed. This is only a small portion of the total volume of water that would flow through the lakes during a major flood.

Other large natural lakes in the Fox River watershed (figure 3) are Lake Geneva, having a surface area of 5,262 acres, Muskego Lake (2,496 acres), Lake Pewaukee (2,496 acres), Twin Lakes (1,300 acres), Lake Tichigan (1,133 acres), Lake Como (946 acres), and Wind Lake (936 acres).

Almost all of the naturally occurring lakes have some type of man-made outlet, which has been added to control pool levels. But the outflows from several lakes flow through flat wetland areas, subject to backwater effects, where the natural conditions often still control the rate of outflow. A great percentage of the lakes occur in small watersheds; collectively, they provide considerable storage in the watershed, but separately they have a very small effect on the flow in primary streams. The model includes routing procedures for the lakes listed above as well as the following smaller lakes: Crystal Lake, Island Lake, Slocum Lake, Round Lake, Loon Lake, Camp Lake, Phantom Lake, Eagle Springs Lake, Lake Beulah, and Echo Lake.

### **Precipitation**

The average annual precipitation for the Fox River watershed is 33 inches, ranging from 30 inches in the northern portions of the basin to 35 inches near Elgin. Average precipitation is greatest in June and July and least in January and February. Average precipitation during the warm-season months (April to September) accounts for approximately 63% of the annual total.

### *Precipitation Gages*

Table 3 lists the precipitation stations in and near the Fox River watershed, as well as the time of measurement. The location of these gages, approximately one gage for every 200 sq mi, is shown in figure 5. Only two gages in the watershed (Eagle and McHenry Lock and Dam) are continuous recording stations that provide hourly or sub-hourly data. Gages at Milwaukee and Chicago O'Hare also provide hourly and sub-hourly data. The remaining stations measure daily precipitation for the 24-hour period since the last measurement, not for calendar days. It is possible, and for some gages likely, that the precipitation is recorded on the calendar day after it actually occurred.

An additional description of the precipitation gage network and recommended modifications to the network are provided in the section: "Use of the Model for Near Real-Time Forecasting."

### *Frequency of Heavy Rainfall*

Table 4 lists the magnitude and frequency of 24-hour rainfall for northeastern Illinois (Huff and Angel, 1989). The frequency of heavy rainfall is significantly greater in the summer months (June to August) than in other seasons.

**Table 3. Daily Precipitation Gages in and Near the Fox River Watershed**

<u>Gage Name</u>	<u>Years of Record</u>	<u>Time of Measurement</u>	<u>Weighted Percent of Watershed</u>
Germantown, WI	1943-present	8 am	2
Oconomowoc, WI	1938-present	4 pm	< 1
Waukesha, WI	1890-present	midnight	13
West Allis, WI	1951-present	midnight	<1
Mt. Mary College, WI	1946-present	5 pm	< 1
Union Grove, WI	1940-present	10 am	3
Burlington, WI	1945-present	8 am	14
Eagle, WI*	1948-present	midnight	9
Fort Atkinson, WI	1942-present	8 am	<1
Lake Geneva, WI	1944-present	7 pm	19
Antioch, IL	1921-present	7 am	8
Lake Villa, IL	1984-present	midnight	< 1
McHenry Lock & Dam, IL *	1975-present	7 am	16
Marengo, IL	1866-present	7 am	1
Barrington, IL	1963-present	8 am	8
Elgin, IL	1908-present	7 am	6
Clinton, WI	1941-present	4 pm	0
Milwaukee, WI *	1927-present	midnight	0
Chicago O'Hare, IL *	1958-present	midnight	0

**Note:** An asterisk denotes continuous recording precipitation gages.



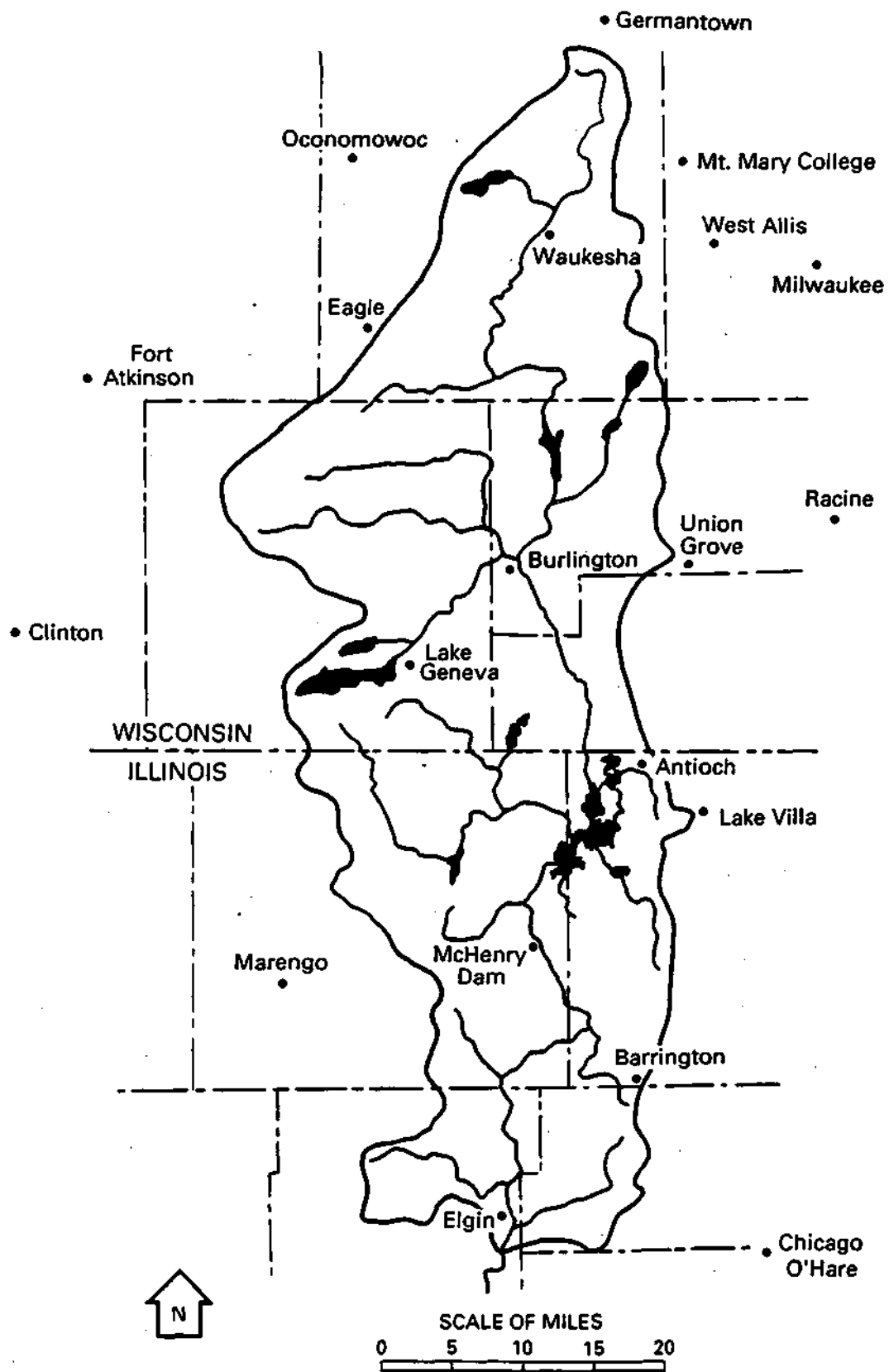


Figure 5. Location of precipitation gages in and near the Fox River watershed

**Table 4. Magnitude and Frequency of Heavy 24-Hour Precipitation by Season, Northeastern Illinois**

	<i>Estimated Recurrence Interval</i>					
	2-yr	5-yr	10-yr	25-yr	50-yr	100-yr
Summer	2.61	3.34	4.07	5.18	6.20	7.43
Fall	1.92	2.55	3.12	4.04	4.80	5.74
Spring	1.92	2.39	2.82	3.53	4.13	4.85
Winter	1.09	1.44	1.79	2.26	2.65	3.18
ANNUAL	3.04	3.80	4.47	5.51	6.46	7.58

### Soil Type

Soils greatly influence the hydrology of an area because they affect runoff and infiltration of precipitation. Low soil permeability contributes to rapid surface runoff and low infiltration; high soil permeability allows rapid infiltration of precipitation and decreases surface runoff. This infiltrated water becomes either ground-water recharge or interflow (subsurface storm runoff). The permeability of the lower layers of the soil (as differentiated from the top layers) is therefore a distinct parameter affecting runoff hydrology.

#### *Available Soils Information*

Information on soil type for the Illinois portion of the Fox River watershed was obtained using the Division of Energy and Natural Resources Illinois Geographic Information System (DENR-IGIS). The source of the soils information used in the DENR-IGIS coverage is the "General Soil Map of Illinois" developed by the University of Illinois Agricultural Experiment Station (1982). The Illinois mapping, developed at a scale of 1:500,000, identifies 50 different soil associations in the entire state. Twelve of these soil associations (table 5) occur in the study area. Also provided in table 5 are the hydrologic soils groups correlated to these specific soil associations by the Soil Conservation Service (SCS). The SCS hydrologic soil classification is comprised of four groups: A, B, C, and D. Soils in hydrologic group A are highly permeable soils having a low amount of direct surface runoff. The permeability for soil groups B, C, and D is progressively less, such that soils in hydrologic group D have the lowest permeability and have high rates of runoff.

Data on Wisconsin soil types were obtained from the Southeastern Wisconsin Regional Planning Commission (SEWRPC) via the Illinois Division of Water Resources (table 6). The Wisconsin information identifies the soils based on the hydrologic soil group classification used by the SCS. The SEWRPC soil information, developed from detailed soil maps, estimates the total area for each soil type.

**Table 5. Soil Associations in the Illinois Portion of the Fox River**

<u>Soil Association</u>	<u>Percent of Fox Watershed Covered</u>	<u>Hydrologic Soil Group</u>
Casco-Fox-Ockley	20	B1
Morley-Blout-Beecher	19	C
Houghton-Palms-Muskego	10	D
Kidder-McHenry	9	B1
Griswold-Ringwood	9	B1
Plano-Proctor-Worthen	9	B2
Saybrook-Dana-Drummer	2	B2
Varna-Elliott-Ashkum	3	C
St. Charles-Camden-Drury	6	B2
Dodge-Russell-Miami	6	B2
St. Clair-Nappanee-Frankfort	1	D
Lorenzo-Warsaw-Wea	6	B1

*Distribution for Specific Watersheds*

<u>Watershed Name</u>	<u>Hydrologic Soil Group</u>				
	<u>A</u>	<u>B1</u>	<u>B2</u>	<u>C</u>	<u>D</u>
Poplar Creek	0	9	2	85	4
Flint Creek	0	3	24	65	7
Tyler Creek	0	16	77	0	7
Spring Creek	0	44	18	33	5
Boone Creek	0	80	15	0	5
Nippersink Creek	1	58	28	3	10
Squaw Creek	0	0	12	68	13
ILLINOIS TOTAL	0	45	22	22	11

**Table 6. Soil Associations in the Wisconsin Portion of the Fox River**

<u>Watershed Name</u>	<u>Hydrologic Soil Group</u>				
	<u>A</u>	<u>B1</u>	<u>B2</u>	<u>C</u>	<u>D</u>
Mukwonago River	18	63	5	5	9
Honey Creek	6	62	5	7	20
Sugar Creek	2	51	12	10	25
White River	6	45	20	8	21
Wind Lake Drainage Canal	0	0	15	50	35
Eagle Creek	0	3	6	60	31
Fox River above Waukesha	0	3	47	26	24
WISCONSIN TOTAL	5	28	26	18	23

Data on additional physical characteristics of these soils, such as permeability and available water capacity, were obtained from soil surveys for counties in Illinois and Wisconsin. These data indicate that, for certain hydrologic soil groups, the soil characteristics can be in a wide range. For example, the Casco-Fox-Ockley soils and Saybrook-Dana-Drummer soils are listed in hydrologic group B. Both have similar permeabilities and available water capacity in the upper layers of the soil. However, Casco-Fox-Ockley soils are developed on sandy and gravelly outwash, and subsoils that are highly permeable, and have little water-retention capacity. Saybrook-Dana-Drummer soils are developed on silty loam, having moderate permeability and high water-storage capacity. These distinctions in soil characteristics have significance in the modeling scheme adopted for this study. Thus, hydrologic soil group B was further subdivided into soils developed on coarse-textured outwash (B1) and on medium- to fine-textured till (B2).

### *Geographic Distribution*

Figure 6 illustrates the significant differences in soil type across the Fox River watershed. Soils in the western part of the watershed predominantly belong in hydrologic groups A and B1. The Mukwonago River, Honey Creek, and Boone Creek watersheds have the greatest percentages of A and B1 soils. Other major tributaries in the western portion of the Fox River watershed, such as White River, Sugar Creek, and Nippersink Creek, have concentrations of A and B1 soils near 50%. Watersheds in the eastern portion of the Fox River watershed (Wind Lake Drainage Canal, Eagle Creek, Squaw Creek, and Poplar Creek) contain predominantly C and D soils.

### **Land Use**

#### *Available Data*

Land-use information for the Illinois portion of the basin was available from two sources: 1) the DENR-IGIS coverage, which is developed from Landsat remote-sensing imagery and uses the USGS Land Use and Land Cover Classification System; and 2) compiled by the Northeastern Illinois Planning Commission (Schaefer and Hey, 1979) in association with the U.S. Environmental Protection Agency's Section 208 hydrologic modeling. The land-use classification systems used in the two sources are not identical but offer similar levels of detail. The DENR-IGIS land-use information was adopted for use in the Illinois portion of the watershed because the soils information was available through the same coverage. The major land uses throughout the Fox River watershed from this coverage are given in table 7.

Wisconsin land use data were obtained along with the soils information from the SEWRPC. A summary of this information is presented in table 8. The classification system varies somewhat from that associated with the Illinois land-use data: the major interpretative

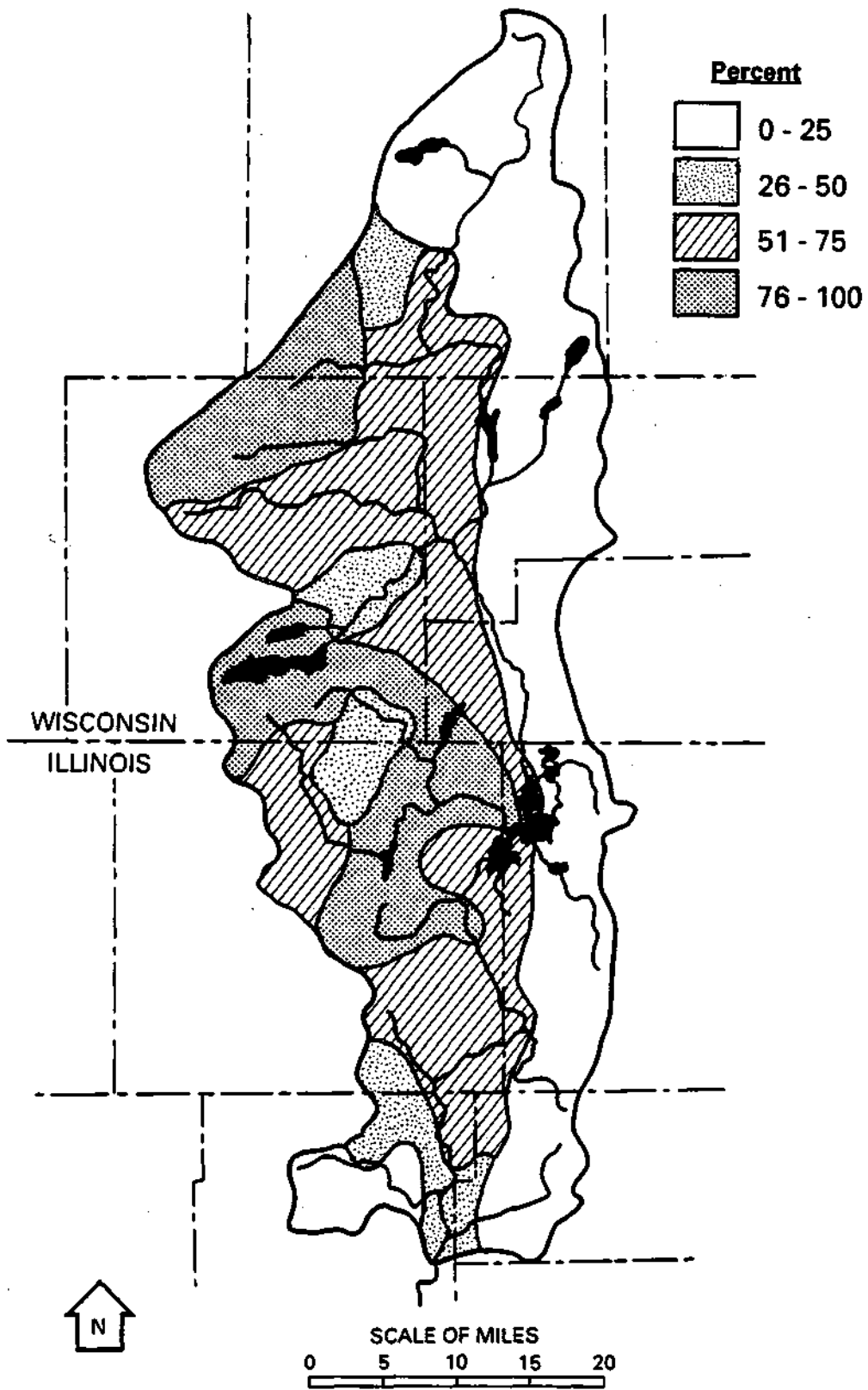


Figure 6. Geographic distribution of soils in the Fox River watershed

**Table 7. Examples of Land Use in the Illinois Portion of the Fox River (percent)**

ILLINOIS TOTAL

Cropland and pasture	60%
Residential	14
Forestland	10
Nonresidential urban	5
Water	4
Wetlands	3
Other land uses	<u>4</u>
	100%

*Totals for Selected Sub-Watersheds*

Nippersink Creek

Cropland and pasture	79%
Forestland	8
Residential	5
Wetlands	3
Other land uses	<u>5</u>
	100%

Boone Creek

Cropland and pasture	59%
Forestland	22
Residential	8
Barren/transitional land	4
Other land uses	<u>7</u>
	100%

Flint Creek

Cropland and pasture	39%
Residential	30
Forestland	11
Nonresidential urban	10
Wetland	3
Barren/transitional	3
Other land uses	<u>4</u>
	100%

Squaw Creek

Cropland and pasture	60%
Residential	13
Forestland	10
Non-residential urban	6
Water	4
Other land uses	<u>7</u>
	100%

Tyler Creek

Cropland and pasture	82%
Residential	6
Forestland	4
Nonresidential urban use	3
Other land uses	<u>5</u>
	100%

Poplar Creek

Cropland and pasture	69%
Residential	16
Nonresidential urban use	5
Barren/transitional	5
Other land uses	<u>5</u>
	100%

**Table 8. Examples of Land Use in the Wisconsin Portion of the Fox River (percent)**

WISCONSIN TOTAL

Row crop	40%
Open space (18% agricultural, 5% wetland)	23
Woodland	10
Hay	9
Residential	8
Water	5
Other land uses	<u>5</u>
	100%

*Totals for Selected Sub-Watersheds*

Fox River above Waukesha

Open space	32%
Residential	20
Row crop	19
Non-residential urban use	6
Woodland	6
Hay	6
Water	4
Other land uses	<u>7</u>
	100%

Wind Lake Drainage Canal

Row crop	44%
Open space	17
Hay	8
Residential	8
Water	7
Woodland	7
Other land uses	<u>9</u>
	100%

Mukwonago River

Row crop	34%
Open space	21
Woodland	20
Hay	10
Residential	5
Water	4
Other land uses	<u>6</u>
	100%

Honey Creek

Row crop	55%
Open space	18
Woodland	11
Hay	7
Residential	3
Water	2
Other land uses	<u>4</u>
	100%

Sugar Creek

Row crop	55%
Open space	16
Woodland	11
Hay	9
Residential	3
Other land uses	<u>6</u>
	100%

difference lies with the category "open space." The 23% land use associated with open space is believed to be a combination of pastureland and wetlands. The breakdown between pasture and wetlands is estimated as 18% and 5%, respectively, and is based on general land-use estimates for the Fox River by Fegeas et al. (1983).

### *Geographic Distribution*

As seen in table 7, there are few changes in the geographic distribution of land use in the Fox River watershed. The predominant land use throughout the watershed is cropland and pastureland accounts for approximately 60% of all land use. Residential and urban land use is greater in Illinois than in Wisconsin, and tends to be concentrated in three areas: the cities of Waukesha and Elgin, and in suburban development along the eastern side of the watershed in Illinois. Most of the urban land is low-density residential development, which has only a small amount of impermeable land surface. Woodlands comprise an average 10% of the watershed, and tend to be interspersed with other land uses. The Mukwonago River and Boone Creek watersheds have over 20% woodland. Water surfaces account for approximately 65 sq mi, or 5% of the watershed. Wetland areas also account for approximately 5% of the watershed, and are more concentrated in its Wisconsin portion.

## **Streamflow**

### *Available Streamflow Information*

Table 9 lists the USGS continuous recording gages that provide discharge information for streams in and adjacent to the Fox River watershed. The location of these gages is shown in figure 7. The streamgages for the Fox River at Wilmot and Nippersink Creek near Spring Grove are of particular interest: when combined they account for approximately 85% of the inflow into the Chain of Lakes. A streamgage on Squaw Creek, the next largest tributary that enters the Chain of Lakes, has recently been added. The Fox River at Algonquin is the nearest USGS gage downstream of the Chain of Lakes. The next USGS gage downstream is at South Elgin, which is the downstream limit of this study. Discharge estimates are also made for McHenry Dam using discharge ratings for the gates and spillway.

Discharge records from six streamgages located outside the limits of study (table 9, figure 7) were also used in the development of the rainfall-runoff model. In addition to the gages described above, five gages along the Chain of Lakes and nearby Fox River provide continuous records of river and lake stage. These gages were not used in the model development.

### *Historical Flooding*

Table 10 lists the 14 greatest peak flows recorded on the Fox River at Algonquin, and a brief description of the type of precipitation or snowmelt event that produced the flooding. Snowmelt is frequently a major cause of flooding events in March or early April. A significant number of these floods follow lesser rain events occurring when the streams are already swollen



**Table 9. List of USGS Streamgages in the Fox River Watershed Area**

<u>Station Name</u>	<u>USGS Gage NO.</u>	<u>Years of Record</u>	<u>Drainage Area (Sq mi)</u>
<i>Continuous Discharge Records for Locations within the Limits of Study</i>			
Fox River at Waukesha, WI	05-543830	(1963-present)	126.
Mukwonago River at Mukwonago, WI	05-544200	(1973-present)	74.1
White River near Burlington, WI	05-545300	(1973-1982)	97.5
Fox River at Wilmot, WI	05-546500	(1939-present)	868.
Squaw Creek at Round Lake, IL	05-547755	(1989-present)	17.2
Nippersink Creek near Spring Grove, IL	05-548280	(1966-present)	192.
Boone Creek near McHenry, IL	05-549000	(1948-1982)	15.5
Flint Creek near Fox River Grove	05-549850	(1989-present)	37.0
Fox River at Algonquin, IL	05-550000	(1915-present)	1403.
Poplar Creek at Elgin, IL	05-550500	(1951-present)	35.2
Fox River at South Elgin, IL	05-551000	(1989-present)	1556.
<i>Continuous Discharge Records for Locations Outside the Limits of Study</i>			
Menomonee River at Menomonee Falls, WI	04-087030	(1979-present)	34.7
Root River Canal near Franklin, WI	04-087233	(1963-present)	57.0
Bark River near Rome, WI	05-426250	(1979-present)	122.
Jackson Creek near Elkhorn, WI	05-431014	(1983-present)	8.9
Des Plaines River at Russell, IL	05-527800	(1967-present)	123.
Ferson Creek near St. Charles, IL	05-551200	(1960-present)	51.7
Blackberry Creek near Yorkville, IL	05-551700	(1960-present)	70.2
<i>Continuous Stage Records along the Chain of Lakes</i>			
Channel Lake near Antioch, IL	05-547000	(1939-present)	--
Fox Lake near Lake Villa, IL	05-547500	(1939-present)	--
Nippersink Lake at Fox Lake, IL	05-548000	(1939-present)	--
Fox River at Johnsburg, IL	05-548500	(1939-present)	1205.
Fox River near McHenry, IL	05-549500	(1941-present)	1250.

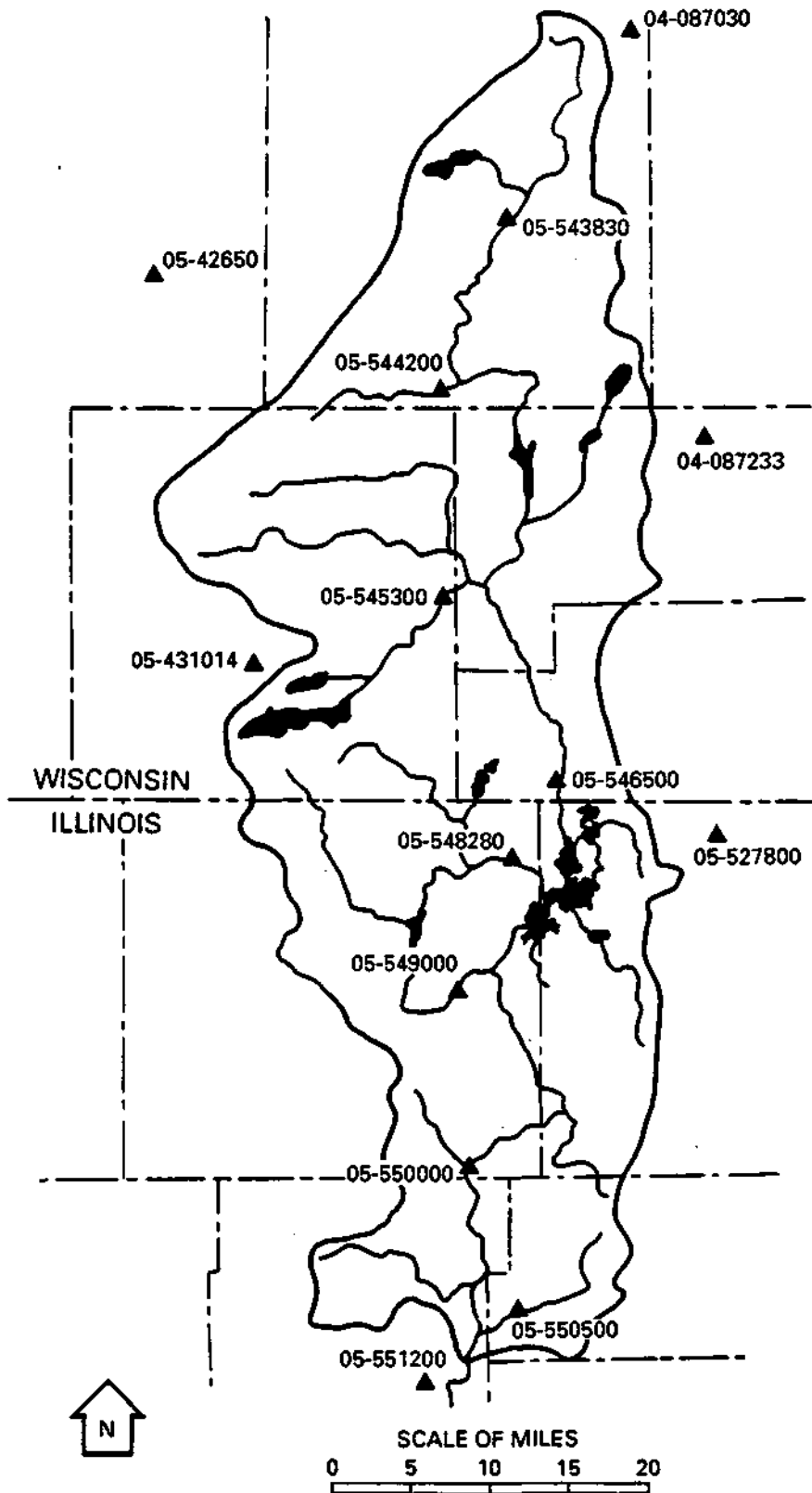


Figure 7. Location of streamgaging stations in and near the Fox River watershed

**Table 10. Major Flood Peaks Recorded at the Fox River at Algonquin, Fox River at Wilmot, and Nippersink Creek near Spring Grove**

<u>Streamgage and Years of Record</u>	<u>Date of Flood Peak</u>	<u>Peak Flow (cfs)</u>	<u>Cause of Flooding</u>
Algonquin (1916-1989)	Apr 6,1960	6610	Snowmelt
	Apr 2,1979	6610	Snowmelt and light rain/ streams swollen by previous snowmelt
	Oct 3,1986	6170	Heavy rain
	Apr 1,1916	5850	Heavy rain
	Mar 6,1918	5750	Snowmelt
	May 4,1973	5730	Moderate rain/streams swollen by previous rains
	July 5,1938	5630	Heavy rain
	Mar 16,1929	5450	Snowmelt
	Mar 12,1974	5310	Snowmelt and light rain/ streams swollen by previous snowmelt
	Feb 10,1938	5160	Snowmelt and light rain/ streams swollen by previous snowmelt
	Apr 11,1983	5150	Moderate rain/streams swollen by previous melt
	May 1,1921	4950	Moderate rain
	Mar 31,1982	4870	Light rain/streams swollen by previous rain
	Mar 21,1919	4800	Heavy rain
	Wilmot (1939-1989)	Mar 31,1960	7520
Apr 23,1973		6530	Moderate rain/streams swollen by previous rains.
Mar 17,1943		5700	Moderate rain on snow
Mar 27,1979		5010	Snowmelt and light rain/ streams swollen by previous snowmelt
Mar 21,1948		5000	Heavy rain
Jan 7,1946		4170	Moderate rain on snow
Mar 27,1962		4060	Snowmelt
Apr 4,1983		4020	Moderate rain/streams swollen by previous melt
Mar 20,1952		4010	Snowmelt and light rain/ streams swollen by previous snowmelt
Mar 10,1974		3985	Snowmelt and light rain/ streams swollen by previous snowmelt
Spring Grove (1960-1989)	Sep 26,1986	2910	Heavy rain
	Feb 20,1971	2430	Moderate rain and snowmelt
	June 12,1967	2120	Heavy rain
	Mar 6,1976	2120	Heavy rain
	May 17,1974	1990	Moderate rain
	Feb 11,1986	1950	Snowmelt
	Mar 21,1979	1820	Snowmelt and light rain
	Apr 4,1983	1820	Heavy rain
	Mar 4,1974	1810	Snowmelt and light rain
	May 3,1973	1610	Moderate rain

**Notes:** Heavy rain = in excess of 2 inches  
Moderate rain = 1 to 2 inches  
Light rain = less than 1 inch

with previous snowmelt. The inadequacy of the Fox River to convey high flows is therefore another major cause of flooding. Heavy rains in the latter part of the spring and summer can also produce major flood events, yet the frequency of this type of flooding is considerably less than the early spring flooding.

Also listed in table 10 are the largest peak flows recorded on both the Fox River at Wilmot and Nippersink Creek at Spring Grove. The events that create the greatest flooding at either Wilmot or Spring Grove are not necessarily those that create the greatest peak at Algonquin. The largest flood peaks at Wilmot occur almost exclusively during March and April. Flood peaks from Nippersink Creek show a greater variety in occurrence. One possible conclusion from these values is that March and April flood events in the Chain of Lakes region originate primarily from the Wisconsin portion of the Fox River watershed. However, flood events in the Chain of Lakes that occur later in spring and in the summer or fall usually require a significant flow contribution from Nippersink Creek and other tributaries that flow directly into the lakes.

It ordinarily takes several days after the rainfall and snowmelt before flood peaks in the Fox River watershed reach the Chain of Lakes region. Figures 8 and 9 illustrate the date of rainfall and the resulting hydrographs for two major historical floods in the region. The sum of flows at the Wilmot and Spring Grove gages approximates the shape of the inflow hydrograph into the Chain of Lakes. In both figures the time to peak for flows entering the Chain of Lakes is three to five days.

An analysis of gaging records from smaller streams in the Fox River region indicate that the magnitude of peak discharges can vary greatly between watersheds of the same size. This difference in peak flow is partially a result of the storage effects of lakes. However, it also appears that watersheds with a high percentage of A and B1 soils have significantly lower flood discharges than other watersheds. Table 11 lists the peak discharges recorded at 14 continuous recording or crest stage gages for locations in and near the Fox River watershed. Gages in watersheds dominated by A and B1 soils include: Mukwonago River, Boone Creek, and Bark River. Differences in period of record make it difficult to directly compare these maximum flows. However, the gages on the three streams listed above have considerably lower flows than the remaining gages.

Table 12 lists the 100-year discharges estimated for several streams in the Fox River watershed various flood insurance studies. These values also illustrate the wide range of flood discharges expected across the watershed, attributed primarily to either lake storage or differences in soil type.

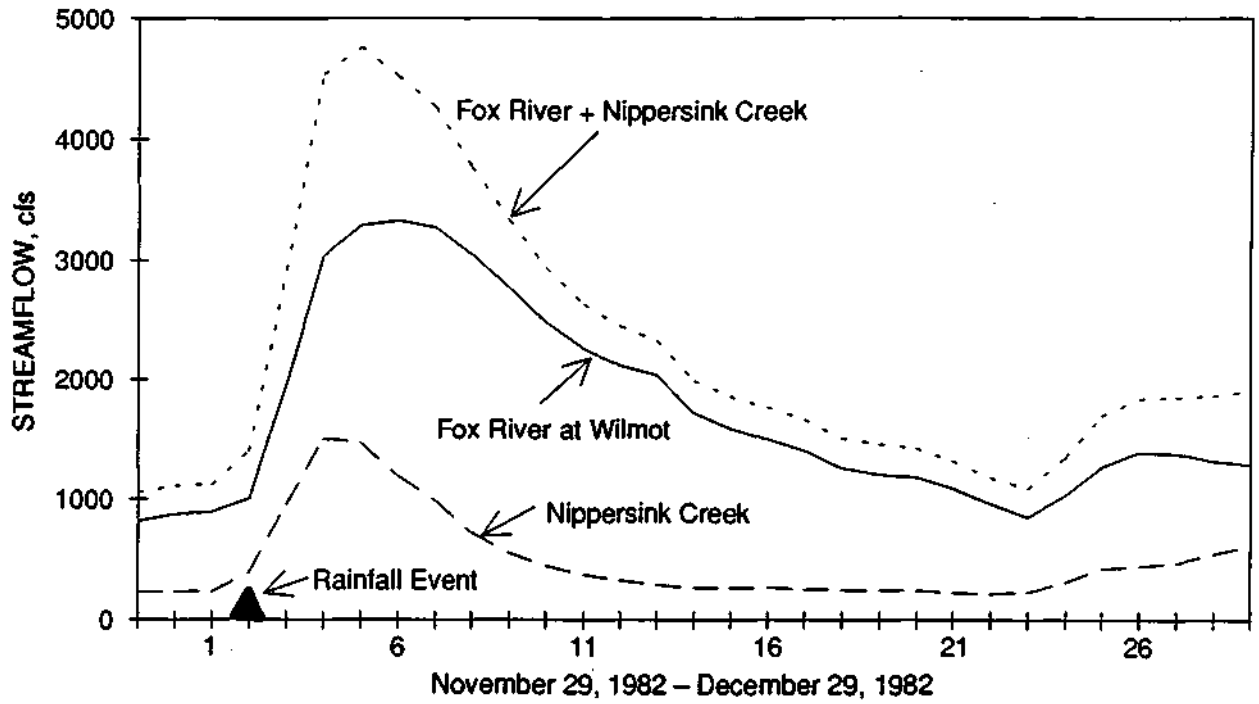


Figure 8. Inflow flood hydrographs for the Chain of Lakes:  
November and December 1982

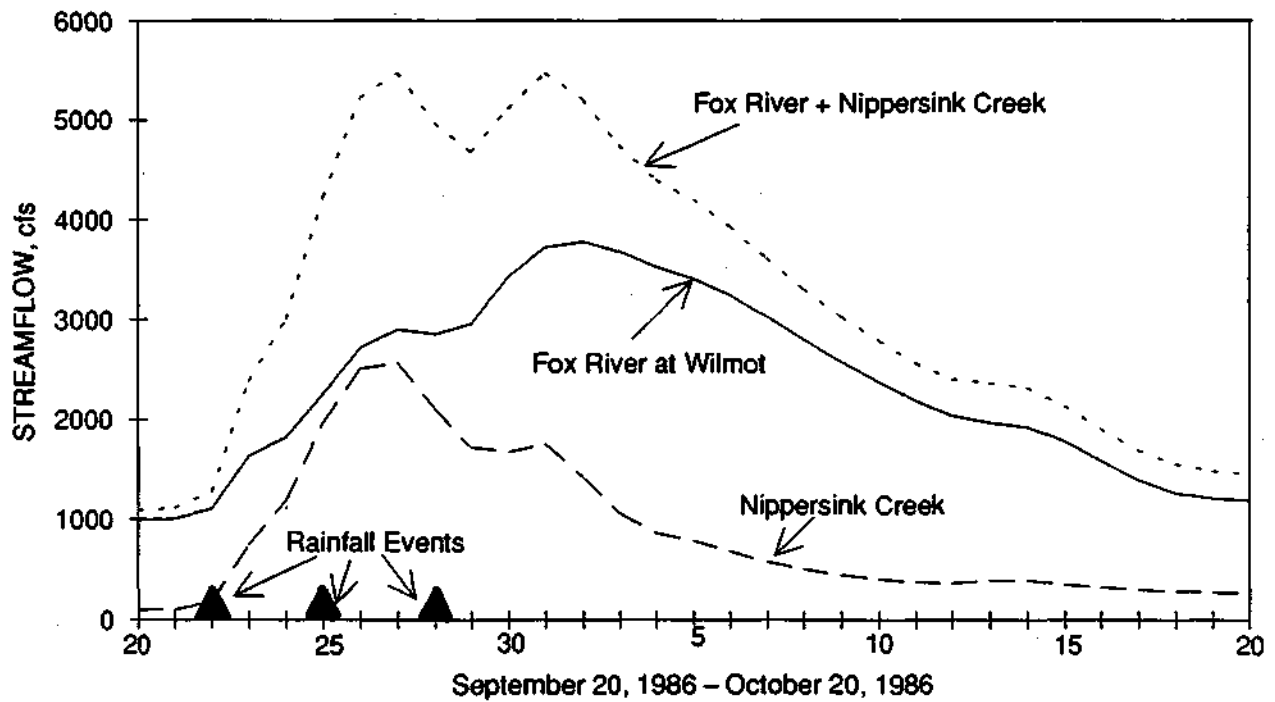


Figure 9. Inflow flood hydrographs for the Chain of Lakes:  
September and October 1986

**Table 11. Maximum Discharges Observed at Gages on Smaller Streams in or near the Fox River watershed**

<u>Streamgage</u>	<u>Years of Record</u>	<u>Drainage Area (sq mi)</u>	<u>Maximum Discharge (cfs)</u>
Bark River near Rome, WI	1979-1989	122.	433
Mukwonago River at Mukwonago, WI	1974-1989	74.1	292
Boone Creek near McHenry, IL	1949-1989	15.5	345
White River near Burlington, WI	1973-1982	110.	1960
Poplar Creek at Elgin, IL	1949-1989	35.2	896
Ferson Creek near St. Charles, IL	1962-1989	51.7	1970
North Br. Nippersink Cr. near Genoa City, WI	1962-1989	13.6	375
Sugar Creek near Elkhorn, WI	1962-1989	6.63	900
Root River Canal near Franklin, WI	1963-1989	57.0	1440
Fox River at Waukesha, WI	1963-1989	127.	2500
Blackberry Creek near Yorkville, IL	1960-1989	70.2	2060
South Br. Kishwaukee River near DeKalb, IL	1979-1989	77.7	3500
Des Plaines River near Russell, IL	1962-1989	123.	2120
Menomonee River at Menomonee Falls, WI	1979-1989	34.7	1440

**Table 12. Estimates of the 100-Year Flood Peak (Q100) from Flood Insurance Studies Conducted for Streams in the Fox River Watershed**

<u>Locations</u>	<u>Drainage Area (sq mi)</u>	<u>Q100 (cfs)</u>
Muskego Lake	34.4	16
Wind Lake	49.1	50
Bohner Lake	4.2	50
Pleasant Lake	24.1	70
Pell Lake	1.5	10
Lake Geneva	31.0	520
Lake Como	13.4	640
Pewaukee Lake	33.8	1043
Bassett Creek	8.8	765
Peterson Creek	12.6	730
Spring Brook	6.8	1230
Wind Lake Canal	98.5	2475
Goose Lake Canal	19.7	1040
Como Creek	16.7	670
E Br Nippersink Creek	16.1	1400
Honey Creek	92.0	2400
N Br Nippersink Creek	45.2	3280
Sugar Creek	58.7	1785
White River	96.3	3970
Deer Creek	8.1	1050
Genessee Creek	23.5	1675
Jericho Creek	16.0	1100
Pebble Creek	18.0	1710
Poplar Creek	24.9	1420
Sussex Creek	15.4	700

## MODEL DEVELOPMENT AND CALIBRATION

### Desired Attributes of the Rainfall-Runoff Model

The Fox River watershed has a hydrologically diverse character, which appears to result from the range and distribution of different soil types, as well as from the distribution of lakes and other sources of detention storage. Diversity complicates the watershed modeling procedure because of difficulties in estimating parameters that express the hydrologic differences. Quite often these parameter-estimation problems force a modeler to treat hydrologically diverse sub-watersheds as one lumped system (James and Burges, 1982). In this study, an attempt was made to develop parameters that maintain much of the hydrologic character in the modeling of each sub-watershed.

Examination of the flow records available in the Fox River watershed indicates that many of the flooding events in the Fox watershed arise from snowmelt events and snowmelt with precipitation. Estimates of flow magnitude are also highly dependent on the antecedent streamflow conditions. Significant increases in spring flow are also observed at times when there is little rainfall or snowmelt but when increased temperatures suggest the occurrence of ground thaw. The ground thaw does not directly result in flood events, but it can create high antecedent streamflow conditions for subsequent rainfall events. The modeling approach should therefore contain methods to adequately deal with snowmelt and frozen-ground hydrologic processes. The concerns with antecedent conditions also suggest that the use of a continuous simulation model is appropriate.

An examination of precipitation and streamflow records also indicates that the flood peaks for the entire watershed generally follow precipitation by five or six days. Ordinarily, for small and medium-sized basins, hourly or sub-hourly differences in precipitation intensity have a significant effect on the timing and magnitude of peak flows. However, since the response for the Fox River watershed is slow, the total flow at the Chain of Lakes should be relatively insensitive to hourly differences in rainfall. Use of daily totals of precipitation produces nearly the same hydrologic response as from the hourly rates. This is an important advantage since the measurement of hourly rainfall in the watershed is sparse, and methods that imitate hourly precipitation using daily rainfall totals have questionable accuracy.

Given the observations listed above, the model developed for the simulation of flows in the Fox River watershed should have the following attributes:

- The use of continuous simulation of streamflow and watershed-moisture conditions is desired. A forecast model requires reliable estimates of antecedent soil moisture, streamflow, and reservoir storage. Event models are not designed to easily generate all these antecedent conditions. With continuous simulation, a model can forecast all situations, not just major flood events.

- Sub-models or model components should provide for differences in soil type and soil moisture, and simulate the hydrologic processes of evapotranspiration, infiltration, snowmelt, percolation of soil water, and changes in percolation due to ground freezing.
- The availability of practical data should be balanced against model complexity and ability to adequately represent the watershed. The model should use parameters that are sufficiently physically based to provide confidence in extrapolating conditions, and take advantage of available land use and soils data, and readily available climatological data. However, given the available data, and cost and time considerations, a homolog approach is recommended, which does not require distributed characteristics for each sub-watershed and the use of a daily time-step.
- The model structure should allow enough flexibility for day-to-day forecasting as well as simulating a long streamflow record. Development of a front-end model that allows the user to update model inputs, such as daily precipitation, is a desired option.

A few continuous simulation models in the public domain satisfy the hydrologic requirements of the modeling procedure, the first two attributes listed above. Of these models, the Hydrologic Simulation Program -- FORTRAN (HSPF), and its progenitor, the Stanford model, are probably best known. These continuous simulation models typically require a detailed database and considerable effort to calibrate and apply. Given the available data and resources, the investigators chose to modify and apply the existing Precipitation Augmentation for Crops Experiment (PACE) continuous simulation model (Durgunoglu et al., 1987), with which they were familiar. Portions of the PACE model were adapted and auxiliary components developed for use in the modeling effort, a model structure that could provide ease of use for forecasting.

### **Model Structure**

A three-step procedure was devised for the modeling of hydrographs for the Fox River and its tributaries. Each procedure is associated with a model component. The components and procedures are listed as follows:

1. *Soil-moisture modeling for land use and soil types.* Apply the soil-moisture component of the PACE model to simulate the hydrologic processes affecting the water budget for each land use and soil combination in the watershed. The soil-moisture modeling will identify the flow path(s) by which excess precipitation will reach the stream: surface runoff, interflow (subsurface storm runoff), or baseflow (subsurface dry-weather flow).
2. *Modeling the response of the watershed hydrographs.* Calibrate the runoff response for gaged sub-watersheds and develop regional parameters for application to all tributaries to the Fox River. The runoff response from each watershed should vary depending upon the flow path by which water reaches the stream.
3. *Routing flows through the stream system.* The sub-watershed hydrographs are routed through the major stream channels in the Fox watershed using a relatively kinematic wave routing method that is calibrated using streamgage records.



A diagram of these three components is provided in figure 10. The modeling procedures associated with each of these three components are explained in detail later in this section.

The resulting model was developed specifically for use with the Fox River watershed. The general modeling approach is applicable to many other watersheds, but such application would require additional parameter development. The temporal resolution of the model should be shortened to hourly or sub-hourly intervals for use in analyzing the flood hydrology of smaller watersheds or ones having faster concentration times.

As previously mentioned, the hydrographs of smaller watersheds within the Fox River watershed may be sensitive to hourly rainfall rates. Thus, the flows predicted from this model on these sub-watersheds using daily data may not accurately estimate flood peaks in all cases. The model procedure developed should be considered applicable to large watersheds that are insensitive to sub-daily fluctuations in rainfall intensity.

### **Component 1: Soil-Moisture Modeling for Land Use and Soil Types**

All watershed models begin with some estimate of the hydrologic budget, where the rainfall is partitioned into infiltration, surface runoff, and possibly other losses. This hydrologic budget is commonly estimated in either a lumped approach, which models only the total watershed response to rainfall, or a distributed approach, which models the response of each small area within the watershed and the effect of its interaction on neighboring areas.

A third common approach, the homolog approach, simulates the hydrologic processes for a discrete number of points. Each of these point-process simulations is considered "typical", or a homolog, of the hydrologic processes that would occur for a given land use and soil condition. A given combination of land uses and soil types could occur in numerous locations in the same watershed, however, the hydrologic response is modeled for this combination only once, and the response is assumed to be independent of geographic situation. Estimates of the hydrologic response from each hydrologic response unit (HRU) are weighted so that an average response for each sub-watershed can be computed.

#### *PACE Soil-Moisture Modeling*

The PACE watershed model is a quasi-distributed parameter model originally developed by the Illinois State Water Survey to analyze changes in soil-moisture distribution, surface runoff, ground-water movement, and evapotranspiration of a watershed that would result from cloud seeding. The acronym "*PACE*" comes from the title of the project for which the model was originally developed: Precipitation Augmentation for Crops Experiment. A description of the components in the PACE watershed model is presented in Durgunoglu et al. (1987). The model is a useful tool for the evaluation of the water budget of agricultural areas in Illinois.

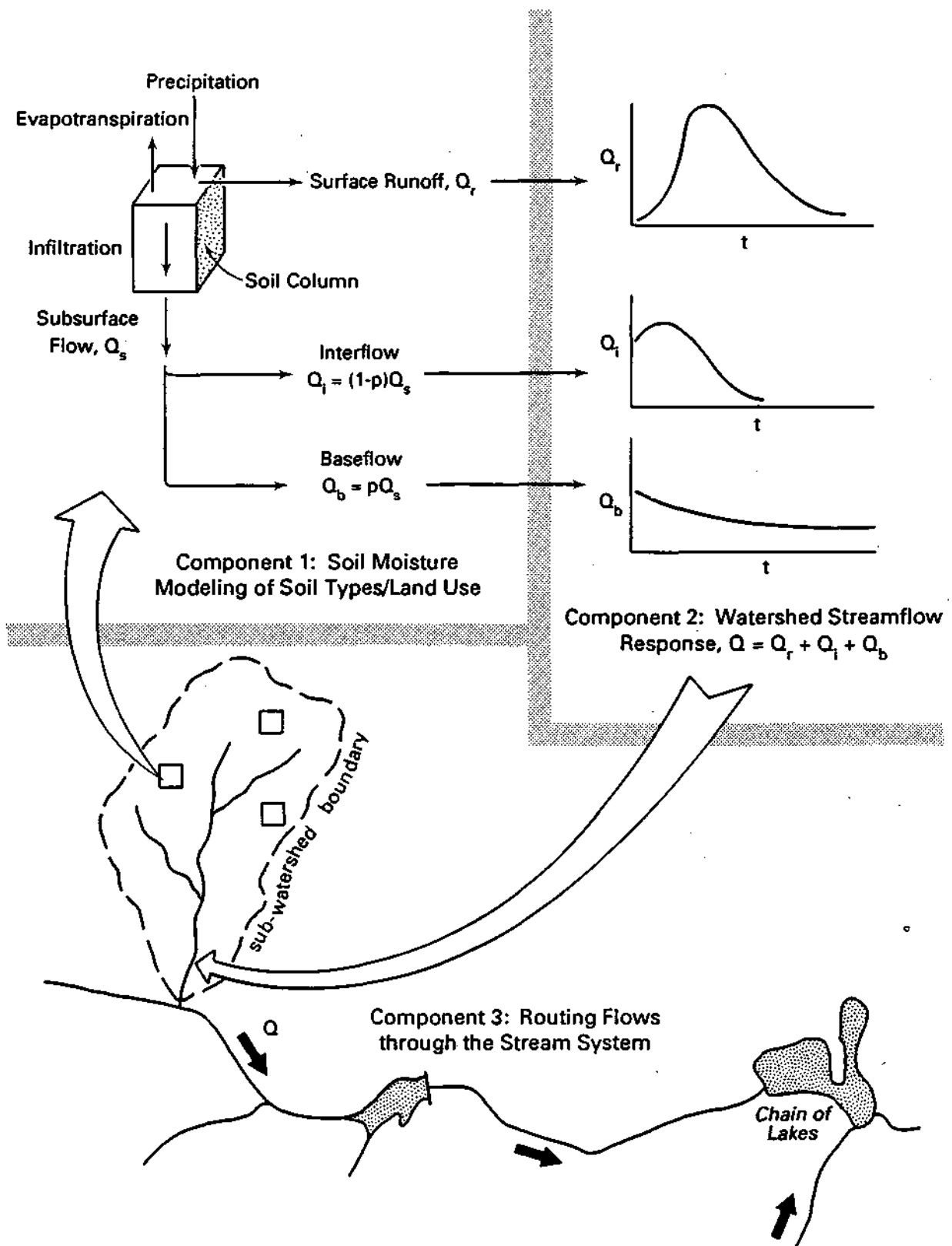


Figure 10. Components of the Fox River Hydrologic Model

The routing of surface runoff and ground-water movement in the PACE model uses finite-difference solutions of equations that require detailed topographic and substrata information for their implementation. The level of detail required for these two components surpasses the resources available for the current study. Thus, only the soil-moisture component of the PACE model is used to compute the daily water budget for typical soils and land use in the Fox River watershed. Instead of using the surface runoff and subsurface flow components of the PACE model to estimate the sub-watershed response, these flow processes are modeled using the empirical hydrograph analysis described in the next section.

Infiltration. The modeling of infiltration in the PACE model is patterned after the U.S. Department of Agriculture CREAMS (Chemicals, Runoff, and Erosion from Agricultural Management Systems) water-budget model. When hourly or sub-hourly precipitation is available, infiltration is modeled using a Green-Ampt procedure. When daily precipitation is used, as in this study, a modification of the SCS Runoff Curve number is used. The standard curve number (CN) is modified on a daily basis so that the CN value used in the estimation of runoff and infiltration is a function of the distribution of soil moisture in the top 2 meters of the soil. The top layers of the soil have the greatest effect on the modified CN value, and lower layers have a successively lesser effect. Daily runoff is predicted from the equation:

$$Q_r = (P - 0.2 SR)^2 / (P + 0.8 SR) \quad (1)$$

where  $Q$  is the daily amount of surface runoff (inches),  $P$  is the daily rainfall (inches), and  $SR$  is the retention variable, which changes under different moisture conditions. The maximum value of  $SR$  ( $SMX$ ) occurs when the soil moisture is at field capacity. The value of  $SMX$  is computed from the  $CN$ , which is a soil-dependent model input, as follows:

$$SMX = (1000/CN1 - 10) \quad (2)$$

The estimation of  $SR$  from  $SMX$  is weighted as a function of the moisture in each of the different soil layers:

$$SR = SMX (1.0 - \sum(W_j(SM_j/UL_j))) \quad (3)$$

where for each soil layer ( $j$ ),  $W_j$  is the weighting factor,  $SM_j$  is the soil-moisture content, and  $UL_j$  is the saturation limit for soil moisture. The weighting factor decreases with depth by a negative exponential function.

The weighting factors ( $W_j$ ), and the maximum  $CN$  value ( $SMX$ ) were calibrated by two methods. The PACE soil-moisture component was originally designed to be calibrated using soil moisture measurements observed over time. In this method, the changing amount of soil moisture is used to identify the infiltration and vertical percolation rates. However, the only soil in the Fox River region where this moisture information is available is the Drummer soil (a typical B2 soil), measured near Waterton in DeKalb County. For B1 and C soils, the model

parameters were calibrated in the "standard" method in which the simulated streamflow is matched to observed streamflow. The Poplar Creek and Boone Creek watersheds were used for calibration. The two calibration procedures result in compatible parameter estimates. Parameters for less prevalent A and D soils were estimated using a combination of SCS procedures and the other calibrated soils as guidelines.

Even with the modifications described above, the curve number method may have some difficulty in calibrating to storm events with dissimilar levels of rainfall intensity (Knapp et al., 1991). In the model calibration, greater emphasis was placed on matching the runoff volume for larger, more intense storm events. The result of this calibration procedure is a bias to overestimate the runoff volume for some small storms, but the overall water yield (annual flow, seasonal flow) is not affected.

*Modifications to the PACE Soil-Moisture Component*

Snow and Snowmelt. Snow simulation and frozen-ground routines were added to the PACE soil-moisture component to allow it to better simulate flow conditions during the winter and early spring. The programming changes resulted in increased model accuracy and improved the ease of model calibration.

The snow simulation routine developed by the U.S. Army Corps of Engineers, Pittsburgh District, is documented in Hoggan et al. (1987). The model assumes that precipitation occurs as snowfall when the daily mean temperature is less than 32° F. The initial density of the fallen snow (the water content in the snow divided by the snow depth) is estimated as 0.10. Over time, freezing and thawing will occur within the snowpack to cause an increase in the density of the snowpack. Snowmelt, the melted water that leaves the snowpack, does not occur until the snowpack is "ripe", i.e., has achieved a density of 0.50. The amount of daily snowmelt (SM) is then estimated by a degree-day algorithm:

$$SM = (c_m + 0.007 P) (T - 32) \quad (4)$$

where P and T are the amount of rain (nonfrozen precipitation) and average air temperature for the day of interest, respectively, and  $c_m$  is the coefficient of snowmelt. The calibrated value for  $c_m$  is 0.07 (inches of melt per degree-day above freezing).

Frozen Ground. The frozen-ground algorithm is an empirical degree-day approach developed using daily soil and air temperatures measured at Dubuque, Iowa and Urbana, Illinois. Conduction from the air to the top soil layer and subsequently to lower soil layers is based on the temperature gradient. Snow cover greatly inhibits the conduction process.

The frozen-ground algorithm affects the water budget as follows. When the temperature of a soil layer is below freezing, the vertical movement of water within the soil is retarded — in effect reducing the soil's hydraulic conductivity. Water that enters the top layers of the soil will freeze and remain until the soil is saturated. When the soil-moisture content exceeds the normal

field capacity and approaches saturation, a high proportion of the rainfall that falls on the soil will result in surface runoff. Later in the spring, when air temperatures rise substantially above freezing for several days, the soil will start to thaw. When a particular soil layer thaws, its water content above the field capacity will drain as subsurface flow. Minor flooding can result from thawing if a sufficient amount of moisture is frozen in the soil.

#### *Implementation of PACE to Land Use and Soil Type Combinations*

In the modeling procedure, each watershed is divided into precipitation-soil-land use divisions (HRUs). A weight assigned to each HRU is equal to the portion of the watershed covered by that particular soil type and land use. When possible, the number of land-use types being modeled was reduced to create a higher degree of parsimony in the modeling procedure. Four land uses were used in the modeling: row crops, grasses, woodlands, and impervious areas. Many other land-use types exist in the watershed, however, most of them represent a smaller portion of the watershed and their hydrologic response can be explained by a combination of the four categories. For example, urban areas are subdivided into impervious area and grassland (lawn and pasture).

Impervious Land Surfaces. The estimation of the amount of impervious area is a matter of particular interest. Aerial photography can accurately estimate a watershed's total amount of impervious area. However, if this amount of impervious area is applied, most rainfall-runoff models will greatly overestimate runoff volumes and peak flows for the watershed (Delleur, 1983; Schaefer and Hey, 1979; Warwick and Tadepalli, 1991). Two primary reasons for this overestimation are given by Warwick and Tadepalli (1991):

- 1) Many of the impervious areas are not hydraulically connected to the storm sewers and channels that convey the storm runoff. For the Fox River watershed, most of the urban area is low-density residential land use, for which the surface is typically around 30 to 40% impervious. However, Schaefer and Hey (1979) indicate that the hydraulically connected impervious areas in such residential areas may be as little as 10 to 20% for sewered areas and less than 2% for nonsewered areas.

- 2) Most models do not account for storage effects in sewers and channels. To account for these, the depression storage on impermeable areas may often be increased to as much as 0.3 to 0.4 inches. [Theoretically, the depression storage for relatively smooth, impermeable surfaces should be less than 0.05 inches.] For the Fox River model, many storage effects throughout the watershed are neglected; thus, the estimate of depression storage on flows from impermeable areas is likely to be great.

Rainfall-runoff models can be calibrated for urban areas by either reducing the estimate of the hydraulically connected impervious area, or by increasing the depression storage amount. The first of these approaches is more common and was used. Residential areas were originally assumed to be 19% impervious. However, for all the sub-watersheds being calibrated, the best agreement between simulated and observed flow was achieved when the percentage of

hydraulically connected impervious area was reduced to a very small amount, generally less than 5%. Residential and urban areas that are not modeled as hydraulically connected impervious areas are modeled as grassland.

As calibrated, the percent of hydraulically-connected impervious area is significantly less than 1% of the total land use for the study area, and is greater than 1% in only eight of the 75 sub-watersheds being modeled. When included in the model, the impervious areas have little total effect on the sub-watershed hydrographs. For model parsimony, the amount of impervious area for all areas was assumed to be zero. Simulation of impervious areas can be restored in the model as the amount of impervious area in the watershed increases, or if additional model development warrants greater detail in sub-watershed modeling. Large water-surface areas are also essentially impervious lands, but their runoff volume is described using lake storage-routing models.

Effect of Land Use and Soil Type on the Water Budget. As modeled, the land-use classification directly affects the estimate of interception and evapotranspiration, which indirectly affects the soil-moisture and subsequent estimates of surface runoff infiltration. An example of the difference in the total water budget (surface runoff versus subsurface flow) between the grass, cropland, and forestland uses is given in table 13. A portion of the subsurface flow given in this table results in storm runoff while the remainder stays in subsurface storage and later results in baseflow (low and medium flow). The variation in total water yield between the land-use types is accounted for by differences in evapotranspiration.

The water-budget modeling is more sensitive to changes in the soil type than to land use. Table 14 provides an example of the differences in the surface runoff and subsurface flow yield based on soil type. Variation in the total water yield is caused by differences in evapotranspiration. Water yield for the B2 and C soils is significantly less than for the other soil types because the soil moisture available for use by plants is greater, and a higher level of evapotranspiration occurs. Surface runoff is significantly less for A and B1 soils than for C and D soils, but subsurface flow is greater.

During storm events, the soil type is again the major influence on whether the excess precipitation becomes surface runoff or subsurface flow. Figure 11 provides a typical example of the differences in surface runoff and subsurface flow for a storm event. In most circumstances, A and B1 soils have small values of surface runoff and large values of subsurface flow. Most of the subsurface flow in these soils results in baseflow rather than storm runoff. Surface runoff is greater in B2 soils and becomes increasingly greater in C and D soils. Approximately half of the subsurface flow in the B2, C, and D soils becomes interflow (i.e., subsurface storm runoff).

The PACE soil-moisture component was originally designed for use on agricultural watersheds. The model's strengths lie in its ability to objectively evaluate the soil-moisture condition, and its effects not only on surface runoff but on the percolation of water that results in subsurface flow. While the model tends to be good at describing the hydrology for these

**Table 13. Example of the Annual Distribution of Surface Runoff and Subsurface Flow (in inches) Estimated by the PACE Soil Moisture Component for Different Land Uses: Soil Types B1 and C**

<i>Soil Type B1</i>			
	<u>Grass</u>	<u>Cropland</u>	<u>Woodland</u>
Surface Runoff	1.7	1.8	<b>1.6</b>
Subsurface Flow	13.7	14.8	12.6
Total Water Yield	15.4	16.6	14.2

<i>Soil Type C</i>			
	<u>Grass</u>	<u>Cropland</u>	<u>Woodland</u>
Surface Runoff	3.3	3.6	3.2
Subsurface Flow	10.3	10.5	8.8
Total Water Yield	13.6	14.1	12.0

**Note:** The Lake Geneva precipitation gage was used for these examples.

**Table 14. Example of the Annual Distribution of Surface Runoff and Subsurface Flow (in inches) Estimated by the PACE Soil-Moisture Component for Different Soil Types**

	<u>A</u>	<u>B1</u>	<u>B2</u>	<u>C</u>	<u>D</u>
Surface Runoff	1.1	<b>1.8</b>	2.3	3.6	4.7
Subsurface Flow	14.6	14.8	11.0	10.5	9.9
Total Water Yield	15.7	16.6	13.3	14.1	14.6

**Note:** The Lake Geneva precipitation gage was used for this example. The land use type used for this example is cropland.

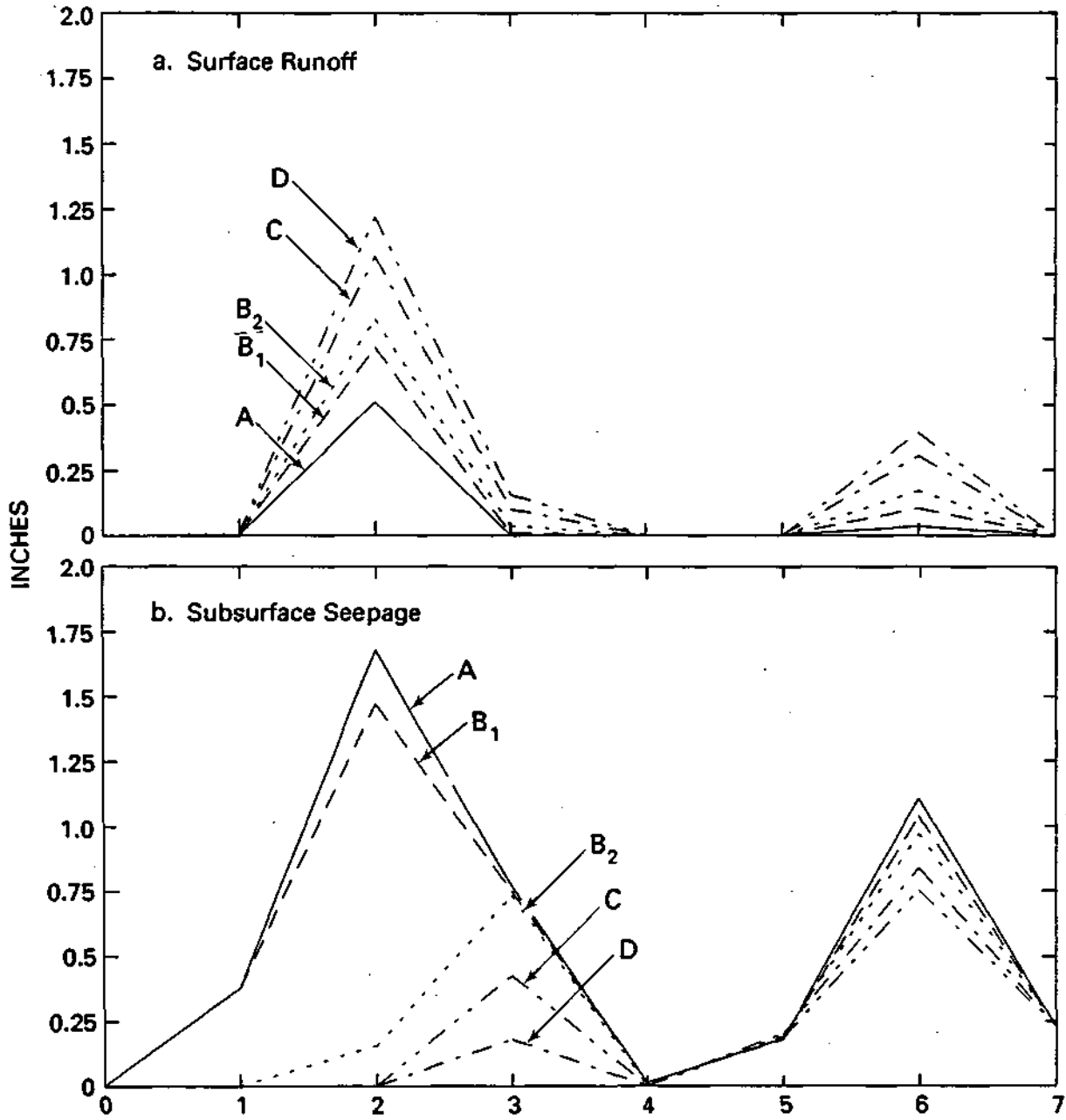


Figure 11. Daily amounts of a) surface runoff, and b) subsurface flow, from soil types A, B1, B2, C, and D: Lake Geneva, September 1986



conditions, it is less accurate when applied to urban and forested areas. Modeling of forest hydrology is limited because it does not account for the uptake of water from strata below the 2-meter thick modeled soil layer. The modeling of forests therefore turns into a condition similar to the agricultural/crop simulation.

#### *Separation of Subsurface Flow into Interflow and Baseflow*

As shown in figure 10, the subsurface flow estimated by the soil-moisture model is subdivided into two flow paths: baseflow and interflow. The portion of the subsurface flow that enters the baseflow is designated by the parameter  $p$ , where  $Q_b = p Q_s$ . The amount of the interflow is computed as  $Q_i = (1-p) Q_s$ . The value of the parameter  $p$  is estimated using the composite of soil types in a watershed, and ranges from 0.45 in watersheds comprised of C and D type soils to 0.90 in watersheds comprised mainly of A and B1 type soils. Estimation of the parameter  $p$  is described later in the section: "Modeling Watershed Hydrograph Response."

#### *Soil-Moisture Modeling Output*

The PACE soil-moisture component estimates the daily volume of excess water that leaves the soil column, which must follow one of two outflow paths: 1) surface runoff; or 2) subsurface flow into shallow ground water, which is further subdivided into interflow and baseflow. Additional information can be output for any of the hydrologic processes simulated by the component, such as: 3) total moisture in any of various soil layers; 4) daily snowmelt; 5) snow cover (the equivalent amount of water in the snowpack); and 6) daily potential and actual evapotranspiration.

Table 15 provides an example of the output using the PACE soil-moisture component for three different periods. Of particular interest is the distribution of the surface runoff and subsurface flow for different runoff events. During snowmelt events, a major portion of the water the soil column as subsurface flow.

## **Component 2: Modeling Watershed Hydrograph Response**

#### *Variations in Hydrologic Response to Storm Rainfall*

Directly after a rainfall event, water can reach the stream by two primary flow paths: surface runoff and interflow (figure 10). Interflow is the lateral movement of water through the soil or its substrata, primarily as part of the overall storm runoff. This lateral movement can occur rapidly, and the current understanding of the interflow process attributes much of the flow to macropores. Water in the soil after a storm may also be directly recharged to the shallow ground-water reservoir, and its discharge to the stream is usually sufficiently slow so that this water can no longer be associated with the storm. This ground-water flow, called baseflow, is a primary factor in maintaining streamflow during dry periods.

**Table 15. Example of PACE Model Output**

<u>Description of Parameters</u>													
	(1)	(2)	(4)	(5)	(6)	(7)	(8)	(9)	(10)	(11)	(12)	(13)	(14)
	(1) Mean daily air temperature, °F (2) Precipitation, inches (3) Evapotranspiration, inches (not listed for winter months) (4) Surface runoff, inches (5) Subsurface flow, inches (6) Total snow, water equivalent in inches (winter months only) (7) Depth of snowpack, inches (winter months only) (8) Snowmelt, inches (winter months only) (9) Soil moisture in top 20 inches, inches (10) Soil moisture from the 20 to 80 inch depth, inches (11) Soil temperature at the 2 inch depth, °F (winter months only) (12) Soil temperature at the 4 inch depth, °F (winter months only) (13) Soil temperature at the 8 inch depth, °F (winter months only) (14) Soil temperature at the 16 inch depth, °F (winter months only)												
Parameters													
Date	(1)	(2)	(4)	(5)	(6)	(7)	(8)	(9)	(10)	(11)	(12)	(13)	(14)
21-Feb-74	37	018	012	0.00	6.29	12.57	0107	618	14.94	27.5	26.7	27.0	28.8
22-Feb-74	33	1.75	0.29	0.00	7.60	22.98	0.00	6.31	14.94	27.6	27.1	27.4	29.0
23-Feb-74	18	0.00	0.00	0.00	7.60	22.98	0.00	6.31	14.94	25.6	26.6	27.5	29.1
24-Feb-74	14	0.00	0.00	0.00	7.60	22.98	0.00	6.31	1454	23.9	25.8	27.4	29.5
25-Feb-74	17	0.00	0.00	0.00	7.60	22.98	0.00	6.31	14.94	23.2	25.2	27.2	29.3
26-Feb-74	24	0.00	0.00	0.00	7.60	22.98	0.00	6.31	1454	23.5	25.2	27.1	29.3
27-Feb-74	37	0.00	0.00	0.00	7.59	1518	0.01	6.31	1453	26.0	26.0	27.5	29.4
28-Feb-74	41	0.00	0.00	0.50	6.95	1351	0.63	6.33	15.00	28.0	27.0	27.6	29.4
1-Mar-74	33	0.00	0.00	0.03	6.88	13.78	0.07	6.37	15.00	28.1	27.6	27.5	29.6
2-Mar-74	44	0.00	0.00	0.84	6.04	1210	0.54	6.36	15.00	30.1	28.6	28.4	30.0
3-Mar-74	57	0.00	0.00	1.50	4.59	8.60	1.75	6.13	15.00	33.3	30.4	29.2	30.1
4-Mar-74	39	0.73	0.73	0.45	3.77	7.54	0.53	6.20	15.00	32.8	31.0	29.5	30.4
5-Mar-74	43	0.00	0.00	0.76	3.00	6.00	0.77	6.13	15.00	33.5	31.6	30.4	30.5
6-Mar-74	45	0.00	0.00	1.18	2.09	4.18	0.91	5.82	15.00	34.4	32.4	31.0	31.1
7-Mar-74	43	0.00	0.00	0.73	1.32	2.64	0.77	5.80	15.00	34.8	32.9	31.5	31.5
8-Mar-74	38	0.26	0.15	0.48	0.89	1.78	0.43	5.86	15.00	34.5	33.2	31.9	31.9
9-Mar-74	46	0.27	0.00	2.30	0.00	0.00	0.89	4.70	15.00	35.6	33.8	32.4	32.3
10-Mar-74	35	0.00	0.00	0.00	0.00	0.00	0.00	4.69	15.00	35.6	33.8	32.4	32.3
11-Mar-74	33	0.20	0.00	0.02	0.15	1.08	0.00	4.71	15.00	35.6	33.8	32.4	32.3
12-Mar-74	37	0.01	0.00	0.01	0.15	0.66	0.00	4.68	15.00	35.6	33.8	32.4	32.3
13-Mar-74	29	0.00	0.00	0.00	0.15	0.66	0.00	4.66	15.00	35.6	33.8	32.4	32.3

Date	(1)	(2)	(3)	(4)	(5)	(9)	(10)
6-Jun-74	72	010	010	0.00	0.00	4.08	14.63
7-Jun-74	69	0.22	0.09	0.00	0.00	4.23	14.61
8-Jun-74	67	0.00	0.13	0.00	0.00	4.11	14.59
9-Jun-74	67	1.96	0.13	0.41	0.52	4.61	15.00
10-Jun-74	66	0.33	0.10	0.00	0.12	4.64	15.00
11-Jun-74	58	0.39	0.12	0.00	0.29	4.62	15.00
12-Jun-74	60	0.00	0.18	0.00	0.00	4.44	15.00
13-Jun-74	64	0.07	0.14	0.00	0.00	4.38	15.00
13-Aug-74	70	0.00	0.18	0.00	0.00	2.14	11.90
14-Aug-74	67	0.00	0.22	0.00	0.00	2.04	11.84
15-Aug-74	73	0.00	0.18	0.00	0.00	1.97	11.79
16-Aug-74	74	1.50	0.16	0.00	0.00	3.36	11.80
17-Aug-74	70	0.00	0.21	0.00	0.00	3.25	11.78
18-Aug-74	71	0.00	0.27	0.00	0.00	3.07	11.74
19-Aug-74	77	0.00	0.29	0.00	0.00	2.88	11.70
20-Aug-74	77	0.00	0.17	0.00	0.00	2.78	11.70
21-Aug-74	77	0.00	0.21	0.00	0.00	2.65	11.69

The amount of water associated with each flow path varies between storms, and is dependent upon factors such as soil moisture, intensity of rain, and whether the water source is rainfall, snowmelt, or thawing of the soil. The storm hydrograph for a watershed is therefore not constant, and varies depending upon the type of storm event occurring. This approach differs from a standard unit hydrograph approach since the source or flow path of the excess precipitation is considered. The output from the PACE soil-moisture component is used to provide the amount of water in the flow paths, which is then used to explain the hydrologic response for storm events.

The streamflow for each sub-watershed is modeled by three elements, each representing different flow paths: 1) the surface runoff hydrograph, which is a linear regression model that estimates surface runoff; 2) the interflow hydrograph; and 3) the baseflow hydrograph, which is computed from the total storage of the shallow ground water and its slow release to the stream. These three hydrograph types are illustrated in figure 10. Parameters for the surface runoff and interflow hydrographs are calibrated using the linear regression procedure described below.

#### *Regression Analysis*

The watershed response is determined so that the storm hydrograph changes depending on the seasonality and antecedent conditions of the storm event. The regression analysis is used to develop the relationship between the hydrologic parameters present in the PACE soil-moisture component and the observed hydrograph for each sub-watershed.

The relationship between the parameters simulated by the PACE soil-moisture component and the associated observed streamflow from gaged sub-watersheds was investigated using simple linear regression analysis. The parameters in the following chart were used as variables in the regression analysis procedure. All variables except the daily precipitation and streamflow are estimated from the PACE soil-moisture component.

Dependent variable:	Recorded daily streamflow = $Q(t)$
Independent variables:	Recorded daily precipitation = $P(t)$
	Previous daily streamflow = $Q(t-1)$
	Surface runoff for the current day and four previous days = $Q_r(t), Q_r(t-1), Q_r(t-2), Q_r(t-3), Q_r(t-4)$
	Subsurface flow for the current day and four previous days = $Q_s(t), Q_s(t-1), Q_s(t-2), Q_s(t-3), Q_s(t-4)$
	Snowmelt = $SM(t)$
	Snow cover = $SC(t)$
	Soil moisture in the top 0.5 meters = $SW1(t)$
	Soil moisture in the top 2 meters = $SW2(t)$
Evapotranspiration = $ET(t)$	
Potential ET = $PET(t)$	

A separate regression analysis was performed using the average daily streamflow records from six continuous recording streamgages located in or near the Fox River watershed (table 16). Two streamgages located in the Fox River watershed were not used in the regression analysis because their flow is largely influenced by lake storage: White River near Burlington and Mukwonago River at Mukwonago.

For each gaging station record, a set of runoff events was chosen from which to estimate the regression coefficients. These events included a wide range of runoff conditions, such as runoff resulting from summer storms and spring snowmelt. Only isolated storm events were used in the computation of the regression coefficients. Runoff events from multiple storms were not used.

A stepwise regression procedure was followed to identify which independent variables could best explain the variation in the observed runoff hydrographs. Depending on the watershed, different independent variables displayed the greatest correlation to the streamflow amount. But, in general, the streamflow was most closely related to the previous day's streamflow, as well as the surface runoff and subsurface flow parameters produced by the PACE soil-moisture component. It is logical that the surface runoff and subsurface flow parameters should have the greatest correlation because, as the soil-moisture component is formulated, these parameters provide the two hydrologic flow paths that directly result in streamflow.

Regression coefficients were computed using a short list of independent parameters having the greatest correlation. Coefficients (table 17) were calibrated for each of the seven streamgage records using the regression analysis. The regression procedure can explain more than 70% of the variance in the daily values of the observed storm hydrographs at each gage.

*Using Regression Coefficients to Estimate Watershed Hydrographs*

The coefficients from the regression analysis can be used to estimate daily runoff using the following equation:

$$\begin{aligned}
 Q(t) = & c_1 Q(t-1) + c_2 Q_r(t) + c_3 Q_r(t-1) + c_4 Q_r(t-2) + c_5 Q_r(t-3) \\
 & + c_6 Q_r(t-4) + c_7 Q_s(t) + c_8 Q_s(t-1) + c_9 Q_s(t-2)
 \end{aligned} \tag{5}$$

where the streamflow estimates, surface runoff, and subsurface flow are all given in inches. The flow estimates are converted to an average daily discharge rate in cubic feet per second (cfs) by multiplying  $Q(t)$  by the constant 26.93 and the drainage area of the watershed in sq mi.

The estimation of the total storm runoff for any sub-watershed, given by equation 5, can be interpreted as the addition of two hydrographs, the first related to surface runoff and the second related to subsurface flow (or more precisely the interflow):

**Table 16. Streamgauge Records Used in Hydrograph Regression Analysis**

<u>Gaging Stations</u>	<u>Drainage Area (sq mi)</u>	<u>Years of Record</u>	<u>Channel Slope (ft/mi)</u>	<u>Channel Length (mi)</u>
Jackson Creek near Elkhorn, WI	9.0	1983-1987	18.8	4.2
Boone Creek near McHenry, IL	15.5	1973-1982	7.5	7.6
Menomonee River at Menomonee Falls, WI	34.7	1979-1987	6.7	8.0
Poplar Creek at Elgin, IL	35.2	1973-1987	9.1	16.4
Ferson Creek near St. Charles, IL	51.7	1973-1987	13.3	13.4
Root River Canal near Franklin, WI	57.0	1973-1987	6.3	18.8
Fox River at Waukesha, WI	126.0	1973-1987	4.0	21.8

**Table 17. Calibrated Coefficients of Surface Runoff from Sub-Watersheds**

	<u>(1)</u>	<u>(2)</u>	<u>(3)</u>	<u>(4)</u>	<u>(5)</u>	<u>(6)</u>	<u>(7)</u>
$Q(t-1)$	0.30	0.30	0.30	0.30	0.30	0.30	0.40
$Q_r(t)$	0.53	0.22	0.31	0.32	0.27	0.25	0.14
$Q_r(t-1)$	0.09	0.21	0.15	0.19	0.19	0.22	0.18
$Q_r(t-2)$	0.00	0.03	0.10	0.15	0.13	0.12	0.17
$Q_r(t-3)$	0.00	0.04	0.05	0.08	0.05	0.04	0.18
$Q_r(t-4)$	0.00	0.00	0.01	0.02	0.00	0.02	0.12
$Q_s(t)$	0.10	0.06	0.12	0.25	0.10	0.18	0.14
$Q_s(t-1)$	0.07	0.02	0.02	0.03	0.06	0.08	0.20
$Q_s(t-2)$	0.01	0.01	0.01	0.00	0.00	0.01	0.05

**Notes:** (1) = Jackson Creek, (2) = Boone Creek, (3) = Menomonee Falls, (4) = Poplar Creek, (5) = Ferson Creek, (6) = Root River Canal, and (7) = Fox River at Waukesha

$$Q_r^*(t) = c_1 Q_r^*(t-1) + c_2 Q_r(t) + c_3 Q_r(t-1) + c_4 Q_r(t-2) + c_5 Q_r(t-3) + c_6 Q_r(t-4) \quad (6)$$

and

$$Q_i(t) = c_1 Q_i(t-1) + c_7 Q_s(t) + c_8 Q_s(t-1) + c_9 Q_s(t-2) \quad (7)$$

where  $Q_r^*(t)$  and  $Q_i(t)$  indicate the surface runoff and interflow hydrographs, respectively.

Example for Computing the Surface Runoff Hydrograph. The ordinates of the hydrographs are directly related to the regression coefficients, but in a complicated manner because of the effect of the serial correlation coefficient,  $c$ . Assume, for example, that the following coefficients are estimated by the regression procedure and that the surface runoff for an isolated storm (day  $t$ ) is equal to 1 inch:

$$c_1 = 0.3 \text{ (serial coefficient)}$$

$$c_2 = 1.0$$

$$c_7 = P$$

$$\text{all other coefficients} = 0.0$$

Also assume that the antecedent surface runoff,  $Q_r^*(t-1)$ , equals zero. The surface runoff hydrograph for the five days after the storm event (day  $t$ ) is estimated from equation 6 as follows:

$$Q_r^*(t) = 0.3 (0) + 1.0 (1) = 1.0 \text{ inch}$$

$$Q_r^*(t+1) = 0.3 (1.0) + 1.0 (0) = 0.3 \text{ inch}$$

$$Q_r^*(t+2) = 0.3 (0.3) + 1.0 (0) = 0.09 \text{ inch}$$

$$Q_r^*(t+3) = 0.3 (0.09) + 1.0 (0) = 0.027 \text{ inch}$$

$$Q_r^*(t+4) = 0.3 (0.027) + 1.0 (0) = 0.0081 \text{ inch}$$

Relating Coefficients to Total Storm Volume. In the above example, the volume of flow for the surface runoff hydrograph for the five days is 1.4251 inches. An expansion of the series for an infinite number of days indicates that the volume of flow eventually approaches 1.428571 inches, which is the inverse of 0.7, or  $1/(1-c_1)$ . To maintain mass balance, 1 inch of surface runoff should produce 1 inch of volume in the hydrograph. For this to occur in the above example, the coefficient  $c_2$  would instead have to equal  $1-c_1$ , or 0.7.

For the general case, the total volume under the surface runoff hydrograph can be estimated from the following equation:

$$\text{Volume (surface runoff)} = Q_r^*(c_6 + c_5 + c_4 + c_3 + c_2) / (1-c_1) \quad (8)$$

In the same manner, the volume of the interflow hydrograph can be shown to be:

$$\text{Volume (interflow)} = p Q_s (c_9 + c_8 + c_7) / (1-c_1) \quad (9)$$

To maintain mass balance, the summation of all coefficients related to surface runoff ( $c_6 + c_5 + c_4 + c_3 + c_2$ ) must equal  $(1-c_1)$ . In similar fashion, for the volume of the interflow hydrograph to add up to  $Q$ , the summation of the coefficients related to interflow ( $c_7 + c_8 + c_9$ ) must equal  $p(1-c_1)$ .

#### *Regionalization of Hydrograph Response*

An examination of table 17 indicates that the calibrated coefficients are variable from one watershed to another. Two trends are evident in the calibrated parameters:

- 1) The coefficients related to the subsurface flow parameters have greater magnitude on watersheds whose average soil permeability is less (for example, the Poplar Creek, Root River Canal, and Fox River at Waukesha watersheds). These watersheds typically have small amounts of subsurface flow; yet, as the coefficients suggest, a greater portion of the available sub-surface flow becomes part of the storm runoff.
- 2) The time of concentration of the surface runoff is considerably less from the smaller watersheds than from the large watersheds.

These trends are further examined in following paragraphs.

Subsurface Flow. The portion of the subsurface flow,  $Q_s$ , which goes directly to the baseflow algorithm is computed as a function of the types of soils in the watershed. If the lower layers of the soil are highly permeable (greater than 2 inches per hour), then most of the subsurface flow from the soil column is expected to enter the shallow ground water and is slowly released to the stream as baseflow. If the substrata is of lower permeability, then a significant portion of the subsurface flow is expected to move laterally into the streams as part of the overall storm runoff. The portion of the subsurface flow entering the baseflow is estimated as an empirical function of the percentage of soils in the watershed having a high permeability in the soil substrata. This empirical relationship is:

$$p = 0.140 AB + 0.45 \quad \text{if } AB \leq 0.5 \quad (10)$$

and

$$p = 0.885 AB + 0.078 \quad \text{if } AB > 0.5 \quad (11)$$

where  $p$  is the portion of subsurface flow used as input into the baseflow algorithm, and  $AB$  is the portion of soils in the watershed that belong to hydrologic groups A and B1. These equations are graphed in figure 12.

The value of  $p$  is greatest for watersheds with the most permeable soils, where most of the subsurface flow becomes baseflow. Thus, hydrographs from permeable watersheds generally have lower peak discharge and less total volume than those from less permeable watersheds.

The remaining water that originates from subsurface flow becomes interflow. The regression procedure indicates that much of the runoff from interflow occurs the same day as the storm event, and the amount of interflow is reduced to near zero by the third day after the storm. For use in estimating regional conditions, the coefficients  $c_7$ ,  $c_8$ , and  $c_9$  in equation 7 are estimated as  $0.40p$ ,  $0.20p$ , and  $0.10p$ , respectively.

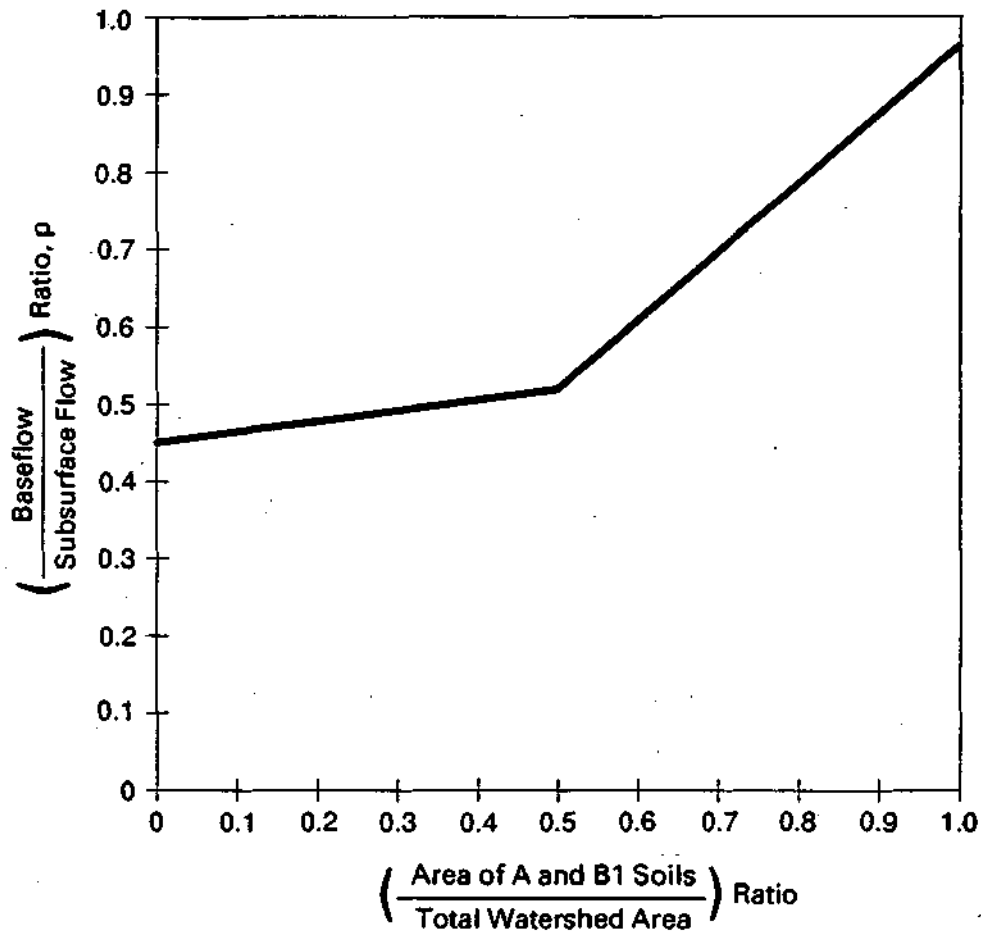


**Figure 12. Portion of computed subsurface flow resulting in baseflow**

Surface Runoff. The time of concentration of the surface runoff is primarily a function of watershed size. An examination of the coefficients in table 17 indicates, for example, that most of the surface runoff from Jackson Creek results in streamflow the same day as the storm. For the Fox River at Waukesha, however, a considerable amount of storm runoff occurs 3 or 4 days after the storm. The regional approach relates the time of concentration to the watershed's total drainage area.

The relationship of the time of concentration to other watershed characteristics such as channel slope and stream length was also examined. In previous regional flood studies, these watershed characteristics have been significant factors in determining flood peak and hydrograph shape (Singh, 1981; Curtis, 1977). However in this analysis, no statistically significant correlation to these additional watershed characteristics was found.

For the regional application, the shape of the surface runoff hydrograph is assumed to follow a Poisson probability distribution. The mean occurrence rate of the Poisson distribution,  $X$ , is estimated from the drainage area (DA) of the sub-watershed as follows:



$$= 0.0124 (DA) + 0.38 \quad (12)$$

The surface-runoff coefficients can be estimated using equation 12 and the following adaptations of the Poisson distribution function:

$$c_2 = e^{-\lambda}$$

$$c_3 = \lambda e^{-\lambda}$$

$$c_4 = \lambda^2 e^{-\lambda} / 2$$

$$c_5 = \lambda^3 e^{-\lambda} / 6$$

$$c_6 = \lambda^4 e^{-\lambda} / 24$$

The effect of the drainage area and the variable  $\lambda$  on the surface-runoff coefficients is illustrated in figure 13.

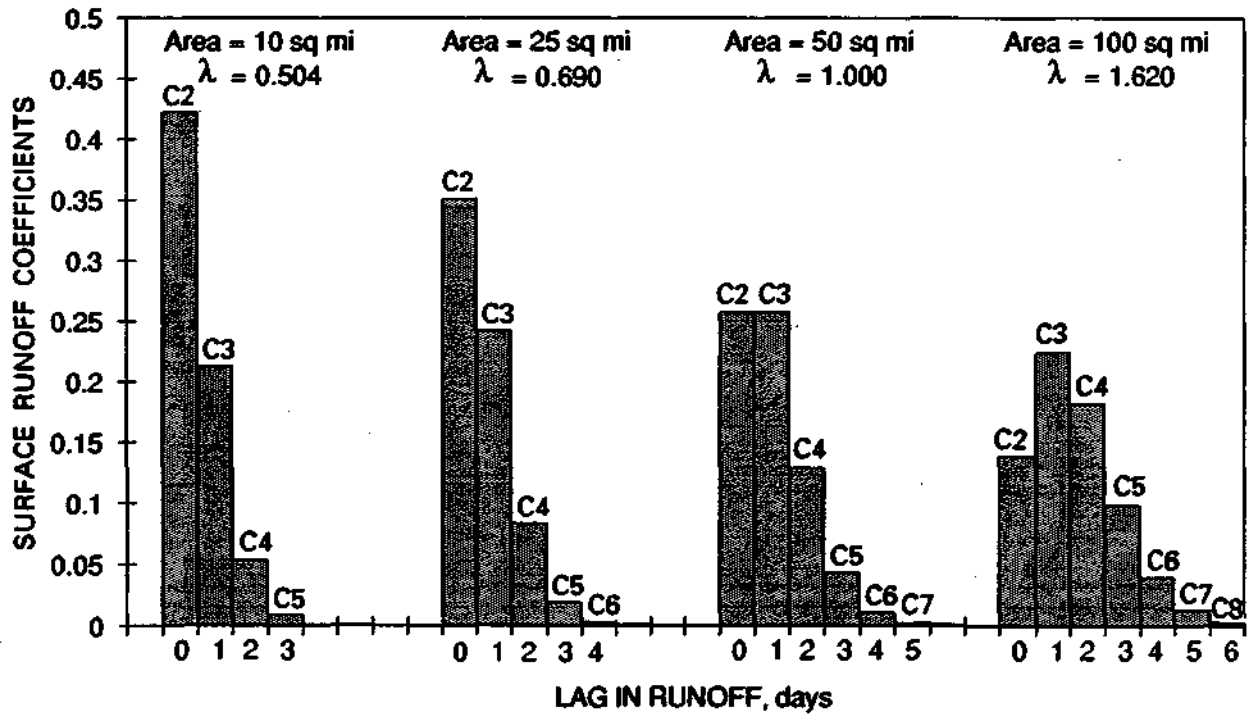


Figure 13. Relationship between watershed drainage area and surface runoff hydrographs

The surface-runoff coefficients, as shown in figure 13, provide a hydrograph shape for the streamflow that originates as surface runoff. This type of daily hydrograph is analogous to the unit hydrograph for a watershed but differs in two major aspects:

- 1) Unit hydrographs are computed for runoff from rainfall falling within a short, compact storm period. In contrast, the daily hydrographs are computed for rainfall occurring over an entire day and assume no knowledge about that day's temporal distribution of rainfall. Thus, the daily hydrographs tend to be broader and have lower peaks than the unit hydrographs, which are not appropriate when using daily rainfall data.
- 2) The daily hydrographs, estimated using equation 12, does not include the influence of the interflow hydrograph, which can be a major source of storm runoff. The effect of interflow is especially great during the first few days after a storm in watersheds having permeable soils.

Equation 12 is an empirical function of the daily hydrologic response displayed by the six calibrated watersheds in the Fox River watershed. The equation provides an effective daily response for these and other watersheds in the Fox River basin that are believed to behave in a similar fashion. The equation should not be applied to other major watersheds without additional analysis.

#### *Estimation of Baseflow*

The baseflow for each watershed is modeled by an exponential decay, single storage reservoir, where the outflow on day  $t$ ,  $Q_b(t)$ , is a function of the accumulated storage of subsurface water,  $GW(t)$ :

$$Q_b(t) = k GW(t) \quad (13)$$

The storage is computed as:

$$GW(t) = GW(t-1) - Q_b(t-1) + p Q_s(t) \quad (14)$$

where  $p$  is the portion of the subsurface flow,  $Q_s$ , that is used as input to the baseflow model.

The value of the parameter  $k$  and initial conditions of the value  $GW$  are calibrated for each watershed. Following a one-year warm-up period, the baseflow model becomes insensitive to the initial estimates of  $GW$ , thereby indicating model stability. The calibrated value of  $k$  was similar for most calibrations, and for the regional analysis was assumed to be a constant,  $k = 0.002$ . The initial value for the storage,  $GW$ , was assumed to be 5 inches over the entire watershed. An entire year of simulation may be needed before the model converges to an appropriate value of  $GW$ .

### *Simulation of Sub-Watershed Hydrographs*

The Fox River watershed is divided into 75 sub-watersheds (table 18) for which daily streamflow is simulated for the period 1973-1987. The proportion of soil types and land use types in each watershed is given in table 19. Also shown is the precipitation gage used in the simulation analysis for each watershed. Table 20 identifies the hydrograph coefficients developed for each watershed using equation 12.

While the regional hydrographs are generally applicable throughout the Fox River watershed, they may not account for local differences in storage and channel slope for individual watersheds. Use of the hydrographs for flood studies to determine flooding on small to medium watersheds may therefore produce variable results. The model is also not designed to use hourly rainfall intensities, to which flood hydrographs on smaller watersheds are sensitive.

### *Comparison of Simulated and Observed Hydrographs for Sub-Watersheds*

Figures 14-19 provide typical examples of the simulated (estimated) versus the historical (observed) daily streamflows at three gaged watersheds (Poplar Creek, Boone Creek, and Root River Canal). The Root River Canal outside of the Fox River watershed is included for descriptive purposes. The regional coefficients are used to develop the estimates of the storm runoff response shown in these figures.

The comparisons of estimated and observed flows in these figures are provided not only to display the model's general accuracy, but also to indicate examples of difficulties for which the model does not replicate the watershed hydrology. The following four observations are noted in comparing the observed and estimated hydrographs:

- 1) The accuracy of the simulation of the sub-watershed storm runoff is variable. The volume of runoff and peak flow resulting from storm events is, on average, satisfactorily estimated. However, there exist numerous events that are either overestimated or underestimated. To a great extent this variability occurs because, for these small watersheds, the model uses precipitation measured at a single raingage to represent the average precipitation over the watershed. The inadequate rainfall information provided by a single gage, a common problem in rainfall-runoff modeling, is the greatest source of model error (Schilling and Fuchs, 1986). An example of a precipitation gage that grossly misrepresents the total watershed rainfall follows:

Example: On June 9, 1979 the following 24-hour totals of precipitation (inches) were measured:

Elgin	4.56	McHenry	1.03
Barrington	2.90	Aurora	0.94
Antioch	1.98	Wheaton	0.56
Marengo	1.10	Lake Geneva	0.52
Chicago O'Hare	1.07	Burlington	0.38

The rainfall measured at Elgin is significantly greater than that measured at the other raingages in the area. As a result, the streamflow for Poplar Creek (for which the model uses the Elgin raingage) is greatly overestimated (figure 15).

**Table 18. Sub-Watersheds in the Fox River Basin**

WISCONSIN

Identification Cede	Drainage Area fsa mi)	Description of Watershed
F1	39.6	Upper Fox River #1
F2	9.9	Upper Fox River #2
F3	26.1	Poplar Creek
F4	23.0	Pewaukee Lake
F5	25.5	Fox River lateral inflow #1
F6	20.3	Pebble Creek
F7	24.3	Genessee Creek
F8	16.3	Pebble Brook
F9	37.6	Fox River lateral inflow #2
M1	25.6	Eagle Springs Lake
M2	16.8	Jericho Creek
M3	9.7	Lake Beulah
M4	15.6	Mukwonago River
F10	16.4	Fox River lateral inflow #3
F11	13.1	Fox River lateral inflow #4
F12	22.5	Lake Tichigan lateral inflow
W1	31.7	n Muskego Lake
W2	13.8	Wind Lake inflows
W3	23.1	Goose Lake Canal
W4	18.7	Wind Lake Canal lateral inflow
F13	13.2	Eagle Creek
F14	14.5	Fox River lateral inflow #5
H1	25.5	Honey Creek watershed #1
H2	14.1	Honey Creek watershed #2
H3	22.1	Honey Creek watershed #3
H4	21.6	Honey Creek watershed #4
H5	30.4	Sugar Creek watershed #1
H6	18.0	Sugar Creek watershed #2
H7	15.0	Sugar Creek watershed #3
H8	20.0	Lake Geneva
H9	6.4	Lake Como
H10	19.6	White River lateral inflow #1
H12	32.1	Ore Creek/Ivanhoe Creek
H11	23.0	White River lateral inflow #2
F15	22.0	Hoosier Creek
F16	23.1	Fox River lateral inflow #6
F17	25.1	Peterson Creek/New Munster Creek
F18	26.4	Fox River lateral inflow #7

**Table 18. Concluded***ILLINOIS*

Identification Code	Drainage Area (sq mi)	Description of Watershed
N1	8.0	Upper Nippersink Creek
N2	10.4	Alden Creek
N3	9.9	Nippersink Creek lateral inflow #1
N5	18.4	Slough Creek
N6	18.4	Silver Creek
N4	14.4	VanderKarr Creek
N7	15.8	Wonder Lake lateral inflow
N8	20.6	Nippersink Creek lateral inflow #2
N9	18.8	North Branch Nippersink Creek
N11	12.7	East Branch North Branch Nippersink Creek
N12	12.9	North Branch lateral inflow
N13	12.8	Elizabeth Lake Drain
N14	6.7	Nippersink Creek lateral inflow #3
N15	9.5	Nippersink Creek lateral inflow #4
I1A	15.2	Trevor Creek
I1B	15.2	Trevor Creek
I2A	13.7	Sequoit Creek
I2B	13.7	Sequoit Creek
I3A	46.5	Squaw Creek
I3B	46.5	Squaw Creek
I4	35.7	Chain of Lakes lateral inflow
I5A	10.6	Lily Lake Drain/Bradenburg Lake area
I5B	10.6	Lily Lake Drain/Bradenburg Lake area
I6	12.7	Dutch Creek
I7	23.3	Boone Creek
I8	8.9	Fox River lateral inflow #8
I9	15.0	Sleepy Hollow Creek
I10	26.3	Fox River lateral inflow #9
I11	12.4	Cotton Creek/Mutton Creek
I12	11.5	Slocum Lake Drain
I13	36.8	Flint Creek
I14	23.2	Fox River lateral inflow #10
I15	25.8	Spring Creek
I16	27.2	Crystal Creek
I17	43.5	Jelkes Creek and Fox River lateral inflow
I18	40.0	Tyler Creek
I19	44.3	Poplar Creek

**Table 19. Land Use and Soil Type Combinations for Each Watershed  
(by fraction of the watershed)**

Land Use Type	Watersheds											
	<b>F1</b>	F2	<b>F3</b>	F4	F5	F6	F7	F8	F9	M1	M2	<b>M3</b>
(1)	0.000	0.000	0.000	0.000	0.000	0.000	0.033	0.000	0.000	0.079	0.000	0.094
(2)	0.000	0.000	0.000	0.000	0.000	0.000	0.035	0.000	0.000	0.070	0.000	0.074
(3)	0.000	0.000	0.000	0.000	0.000	0.000	0.000	0.000	0.000	0.037	0.000	0.042
(4)	0.000	0.000	0.000	0.000	0.048	0.000	0.091	0.000	0.268	0.269	0.430	0.285
(5)	0.000	0.000	0.000	0.000	0.080	0.000	0.089	0.000	0.272	0.289	0.298	0.218
(6)	0.000	0.000	0.000	0.000	0.000	0.000	0.020	0.000	0.060	0.140	0.160	0.126
(7)	0.211	0.121	0.151	0.392	0.183	0.282	0.236	0.345	0.000	0.000	0.000	0.000
(8)	0.218	0.103	0.126	0.328	0.315	0.340	0.227	0.214	0.000	0.000	0.000	0.000
(9)	0.038	0.019	0.024	0.055	0.020	0.054	0.052	0.076	0.000	0.000	0.000	0.000
(10)	0.128	0.235	0.203	0.048	0.060	0.045	0.020	0.048	0.049	0.013	0.019	0.036
(11)	0.133	0.196	0.153	0.051	0.098	0.059	0.026	0.028	0.052	0.016	0.024	0.025
(12)	0.022	0.038	0.031	0.000	0.000	0.000	0.000	0.011	0.011	0.000	0.000	0.016
(13)	0.112	0.138	0.160	0.065	0.073	0.090	0.074	0.148	0.120	0.039	0.028	0.039
(14)	0.117	0.127	0.127	0.061	0.123	0.113	0.097	0.095	0.139	0.031	0.041	0.028
(15)	0.021	0.023	0.025	0.000	0.000	0.017	0.000	0.035	0.029	0.017	0.000	0.017

	Watersheds											
	<b>M4</b>	F10	F11	F12	W1	W2	<b>W3</b>	<b>W4</b>	F13	F14	<b>H1</b>	<b>H2</b>
(1)	0.107	0.000	0.000	0.020	0.000	0.000	0.000	0.000	0.000	0.040	0.030	0.014
(2)	0.046	0.000	0.000	0.028	0.000	0.000	0.000	0.000	0.000	0.036	0.056	0.034
(3)	0.038	0.000	0.000	0.000	0.000	0.000	0.000	0.000	0.000	0.014	0.000	0.000
(4)	0.179	0.242	0.191	0.102	0.000	0.000	0.000	0.029	0.000	0.254	0.174	0.188
(5)	0.113	0.287	0.247	0.158	0.000	0.000	0.000	0.063	0.000	0.235	0.406	0.425
(6)	0.073	0.059	0.049	0.027	0.000	0.000	0.000	0.000	0.000	0.093	0.072	0.079
(7)	0.120	0.000	0.000	0.045	0.100	0.029	0.030	0.000	0.022	0.000	0.000	0.000
(8)	0.075	0.000	0.000	0.067	0.105	0.036	0.118	0.000	0.073	0.000	0.000	0.000
(9)	0.049	0.000	0.000	0.014	0.016	0.000	0.000	0.000	0.000	0.000	0.000	0.000
(10)	0.014	0.053	0.111	0.137	0.217	0.182	0.112	0.193	0.144	0.052	0.011	0.019
(11)	0.017	0.061	0.133	0.179	0.270	0.205	0.334	0.347	0.420	0.061	0.037	0.065
(12)	0.000	0.013	0.027	0.035	0.035	0.029	0.034	0.040	0.049	0.020	0.000	0.000
(13)	0.093	0.113	0.104	0.059	0.104	0.271	0.095	0.117	0.070	0.083	0.046	0.045
(14)	0.043	0.144	0.116	0.110	0.135	0.213	0.251	0.188	0.200	0.080	0.145	0.112
(15)	0.033	0.028	0.022	0.019	0.018	0.035	0.026	0.023	0.022	0.032	0.023	0.019

**Table 19. Continued**

Land Use Type	Watersheds											
	H3	H4	H5	H6	H7	H8	H9	H10	H12	H11	F15	F16
(1)	0.000	0.000	0.000	0.022	0.000	0.020	0.010	0.027	0.034	0.075	0.000	0.032
(2)	0.016	0.025	0.000	0.032	0.021	0.018	0.000	0.034	0.026	0.079	0.013	0.037
(3)	0.000	0.000	0.000	0.000	0.000	0.000	0.000	0.000	0.007	0.016	0.000	0.000
(4)	0.165	0.235	0.097	0.214	0.221	0.461	0.390	0.156	0.079	0.148	0.000	0.205
(5)	0.380	0.406	0.353	0.235	0.308	0.190	0.108	0.178	0.160	0.154	0.000	0.261
(6)	0.067	0.079	0.056	0.055	0.066	0.144	0.270	0.042	0.025	0.044	0.000	0.069
(7)	0.000	0.000	0.013	0.051	0.044	0.000	0.000	0.082	0.108	0.086	0.050	0.000
(8)	0.000	0.000	0.056	0.055	0.063	0.000	0.000	0.074	0.189	0.094	0.107	0.000
(9)	0.000	0.000	0.000	0.013	0.013	0.000	0.000	0.044	0.033	0.020	0.014	0.000
(10)	0.024	0.024	0.026	0.029	0.027	0.034	0.026	0.030	0.029	0.014	0.107	0.049
(11)	0.067	0.043	0.098	0.046	0.042	0.018	0.000	0.052	0.072	0.018	0.303	0.066
(12)	0.000	0.000	0.015	0.000	0.000	0.010	0.025	0.000	0.009	0.000	0.035	0.017
(13)	0.079	0.064	0.053	0.100	0.070	0.051	0.087	0.118	0.077	0.110	0.092	0.097
(14)	0.173	0.104	0.201	0.122	0.103	0.034	0.024	0.132	0.140	0.117	0.249	0.132
(15)	0.029	0.020	0.032	0.026	0.022	0.020	0.060	0.031	0.012	0.025	0.030	0.035

	Watersheds											
	F17	F18	N1	N2	N3	N5	N6	N4	N7	N8	N9	N11
(1)	0.000	0.020	0.000	0.000	0.000	0.000	0.000	0.000	0.000	0.000	0.012	0.023
(2)	0.021	0.016	0.000	0.000	0.000	0.000	0.000	0.000	0.000	0.000	0.037	0.019
(3)	0.000	0.000	0.000	0.000	0.000	0.000	0.000	0.000	0.000	0.000	0.000	0.000
(4)	0.065	0.222	0.011	0.048	0.011	0.032	0.194	0.010	0.164	0.036	0.034	0.364
(5)	0.113	0.257	0.619	0.649	0.619	0.540	0.535	0.463	0.495	0.619	0.103	0.269
(6)	0.011	0.059	0.037	0.058	0.037	0.013	0.021	0.000	0.104	0.088	0.000	0.040
(7)	0.035	0.000	0.000	0.000	0.000	0.022	0.056	0.012	0.000	0.000	0.138	0.000
(8)	0.065	0.000	0.314	0.134	0.314	0.383	0.160	0.515	0.000	0.149	0.379	0.000
(9)	0.000	0.000	0.019	0.011	0.019	0.010	0.000	0.000	0.000	0.020	0.033	0.000
(10)	0.134	0.072	0.000	0.000	0.000	0.000	0.000	0.000	0.000	0.000	0.026	0.027
(11)	0.225	0.084	0.000	0.000	0.000	0.000	0.000	0.000	0.000	0.000	0.076	0.022
(12)	0.023	0.019	0.000	0.000	0.000	0.000	0.000	0.000	0.000	0.000	0.000	0.000
(13)	0.104	0.110	0.000	0.000	0.000	0.000	0.000	0.000	0.051	0.000	0.041	0.128
(14)	0.187	0.113	0.000	0.100	0.000	0.000	0.034	0.000	0.154	0.078	0.111	0.108
(15)	0.017	0.028	0.000	0.000	0.000	0.000	0.000	0.000	0.032	0.010	0.010	0.000

**Table 19. Concluded**

Land-Use Type	Watersheds											
	N12	N13	N14	N15	I1A I1b	I2A I2B	I3A I3B	I4	I5A I5B	I6	I7	I8
(1)	0.000	0.000	0.000	0.000	0.000	0.000	0.000	0.000	0.000	0.000	0.000	0.000
(2)	0.000	0.000	0.000	0.000	0.000	0.000	0.000	0.000	0.000	0.000	0.000	0.000
(3)	0.000	0.000	0.000	0.000	0.000	0.000	0.000	0.000	0.000	0.000	0.000	0.000
(4)	0.104	0.106	0.156	0.156	0.000	0.027	0.000	0.252	0.282	0.080	0.150	0.358
(5)	0.534	0.584	0.625	0.625	0.000	0.047	0.000	0.106	0.280	0.443	0.475	0.572
(6)	0.042	0.148	0.145	0.145	0.000	0.000	0.000	0.136	0.037	0.019	0.175	0.000
(7)	0.047	0.000	0.000	0.000	0.046	0.080	0.031	0.027	0.056	0.000	0.028	0.012
(8)	0.241	0.000	0.000	0.000	0.072	0.137	0.081	0.011	0.062	0.000	0.089	0.019
(9)	0.019	0.000	0.000	0.000	0.000	0.000	0.013	0.014	0.000	0.000	0.033	0.000
(10)	0.000	0.000	0.000	0.000	0.037	0.239	0.171	0.160	0.000	0.000	0.000	0.000
(11)	0.000	0.000	0.000	0.000	0.058	0.395	0.452	0.068	0.000	0.000	0.000	0.000
(12)	0.000	0.000	0.000	0.000	0.000	0.014	0.072	0.086	0.000	0.000	0.000	0.000
(13)	0.000	0.020	0.012	0.012	0.307	0.023	0.044	0.071	0.133	0.068	0.000	0.015
(14)	0.013	0.113	0.050	0.050	0.434	0.038	0.117	0.030	0.132	0.374	0.039	0.024
(15)	0.000	0.029	0.012	0.012	0.046	0.000	0.019	0.039	0.018	0.016	0.011	0.000

	Watersheds										
	I9	I10	I11	I12	I13	I14	I15	I16	I17	I18	I19
(1)	0.000	0.000	0.000	0.000	0.000	0.000	0.000	0.000	0.000	0.000	0.000
(2)	0.000	0.000	0.000	0.000	0.000	0.000	0.000	0.000	0.000	0.000	0.000
(3)	0.000	0.000	0.000	0.000	0.000	0.000	0.000	0.000	0.000	0.000	0.000
(4)	0.127	0.270	0.014	0.013	0.015	0.270	0.107	0.263	0.175	0.022	0.025
(5)	0.352	0.332	0.092	0.021	0.015	0.332	0.249	0.406	0.150	0.134	0.065
(6)	0.118	0.105	0.000	0.000	0.000	0.105	0.084	0.000	0.040	0.000	0.000
(7)	0.021	0.020	0.040	0.142	0.118	0.020	0.044	0.075	0.291	0.106	0.000
(8)	0.058	0.032	0.239	0.169	0.095	0.032	0.102	0.117	0.249	0.634	0.020
(9)	0.020	0.000	0.012	0.063	0.027	0.000	0.034	0.000	0.068	0.030	0.000
(10)	0.000	0.032	0.041	0.174	0.326	0.032	0.081	0.055	0.014	0.000	0.236
(11)	0.000	0.040	0.248	0.208	0.261	0.040	0.186	0.084	0.000	0.000	0.594
(12)	0.000	0.013	0.012	0.078	0.073	0.013	0.063	0.000	0.000	0.000	0.020
(13)	0.065	0.060	0.041	0.050	0.035	0.060	0.012	0.000	0.013	0.010	0.011
(14)	0.179	0.073	0.249	0.060	0.035	0.073	0.028	0.000	0.000	0.064	0.029
(15)	0.060	0.023	0.012	0.022	0.000	0.023	0.010	0.000	0.000	0.000	0.000

Notes: (1) = Grass, Soil A; (2) = Crop, Soil A; (3) = Woodland, Soil A; (4) = Grass, Soil B1; (5) = Crop, Soil B1; (6) = Woodland, Soil B1; (7) = Grass, Soil B2; (8) = Crop, Soil B2; (9) = Woodland, Soil B2; (10) = Grass, Soil C; (11) = Crop, Soil C; (12) = Woodland, Soil C; (13) = Grass, Soil D; (14) = Crop, Soil D; (15) = Woodland, Soil D



**Table 20. Hydrograph Parameters for Sub-Watersheds**

Water- shed	Parameter									
	(1)	(2)	(3)	(4)	(5)	(6)	(7)	(8)	(9)	(10)
F1	1.0	0.550	0.293	0.255	0.111	0.032	0.007	0.220	0.110	0.055
F2	1.0	0.550	0.423	0.213	0.054	0.009	0.001	0.220	0.110	0.055
F3	1.0	0.550	0.346	0.244	0.086	0.020	0.004	0.220	0.110	0.055
F4	1.0	0.550	0.359	0.240	0.080	0.018	0.003	0.220	0.110	0.055
F5	1.0	0.550	0.349	0.243	0.085	0.020	0.003	0.220	0.110	0.055
F6	1.0	0.550	0.372	0.235	0.074	0.016	0.002	0.220	0.110	0.055
F7	1.0	0.550	0.354	0.241	0.082	0.019	0.003	0.220	0.110	0.055
F8	1.0	0.550	0.391	0.228	0.066	0.013	0.002	0.220	0.110	0.055
F9	1.0	0.391	0.300	0.254	0.108	0.030	0.006	0.157	0.078	0.039
M1	1.0	0.140	0.349	0.243	0.085	0.020	0.003	0.056	0.028	0.014
M2	1.0	0.136	0.389	0.229	0.067	0.013	0.002	0.055	0.027	0.014
M3	1.0	0.180	0.424	0.212	0.053	0.009	0.001	0.072	0.036	0.018
M4	1.0	0.448	0.395	0.226	0.065	0.012	0.002	0.179	0.090	0.045
F10	1.0	0.402	0.391	0.228	0.066	0.013	0.002	0.161	0.080	0.040
F11	1.0	0.549	0.407	0.221	0.060	0.011	0.001	0.220	0.110	0.055
F12	1.0	0.550	0.362	0.239	0.079	0.017	0.003	0.220	0.110	0.055
W1	1.0	0.550	0.323	0.250	0.097	0.025	0.005	0.220	0.110	0.055
W2	1.0	0.550	0.403	0.222	0.061	0.011	0.002	0.220	0.110	0.055
W3	1.0	0.550	0.359	0.240	0.080	0.018	0.003	0.220	0.110	0.055
W4	1.0	0.550	0.380	0.232	0.071	0.014	0.002	0.220	0.110	0.055
F13	1.0	0.550	0.395	0.226	0.065	0.012	0.002	0.220	0.110	0.055
F14	1.0	0.328	0.400	0.224	0.063	0.012	0.002	0.131	0.066	0.033
H1	1.0	0.269	0.348	0.243	0.085	0.020	0.003	0.108	0.054	0.027
H2	1.0	0.267	0.402	0.223	0.062	0.011	0.002	0.107	0.053	0.027
H3	1.0	0.367	0.364	0.238	0.078	0.017	0.003	0.147	0.073	0.037
H4	1.0	0.263	0.366	0.237	0.077	0.017	0.003	0.105	0.053	0.026
H5	1.0	0.474	0.337	0.246	0.090	0.022	0.004	0.190	0.095	0.047
H6	1.0	0.428	0.383	0.231	0.069	0.014	0.002	0.171	0.086	0.043
H7	1.0	0.377	0.398	0.225	0.063	0.012	0.002	0.151	0.075	0.038
H8	1.0	0.185	0.374	0.235	0.074	0.015	0.002	0.074	0.037	0.019
H9	1.0	0.234	0.442	0.203	0.047	0.007	0.001	0.094	0.047	0.023
H10	1.0	0.549	0.374	0.234	0.073	0.015	0.002	0.220	0.110	0.055
H12	1.0	0.549	0.322	0.250	0.097	0.025	0.005	0.220	0.110	0.055
H11	1.0	0.377	0.354	0.241	0.082	0.019	0.003	0.151	0.075	0.038
F15	1.0	0.550	0.364	0.238	0.078	0.017	0.003	0.220	0.110	0.055
F16	1.0	0.388	0.359	0.240	0.080	0.018	0.003	0.155	0.078	0.039
F17	1.0	0.550	0.351	0.242	0.084	0.019	0.003	0.220	0.110	0.055
F18	1.0	0.414	0.324	0.250	0.096	0.025	0.005	0.166	0.083	0.041

**Table 20. Concluded**

Water-shed	Parameter									
	(1)	(2)	(3)	(4)	(5)	(6)	(7)	(8)	(9)	(10)
N1	1.0	0.332	0.433	0.208	0.050	0.008	0.001	0.133	0.066	0.033
N2	1.0	0.254	0.421	0.214	0.055	0.009	0.001	0.102	0.051	0.025
N3	1.0	0.332	0.423	0.213	0.054	0.009	0.001	0.133	0.066	0.033
N5	1.0	0.405	0.381	0.232	0.070	0.014	0.002	0.162	0.081	0.040
N6	1.0	0.259	0.381	0.232	0.070	0.014	0.002	0.103	0.052	0.026
N4	1.0	0.549	0.400	0.224	0.062	0.012	0.002	0.220	0.110	0.055
N7	1.0	0.247	0.394	0.227	0.065	0.013	0.002	0.099	0.049	0.025
N8	1.0	0.265	0.371	0.236	0.075	0.016	0.003	0.106	0.053	0.026
N9	1.0	0.550	0.355	0.247	0.091	0.022	0.004	0.220	0.110	0.055
N11	1.0	0.290	0.409	0.220	0.059	0.011	0.001	0.116	0.058	0.029
N12	1.0	0.320	0.408	0.220	0.059	0.011	0.001	0.128	0.064	0.032
N13	0.0	0.000	0.000	0.000	0.000	0.000	0.000	0.000	0.000	0.000
N14	1.0	0.103	0.441	0.204	0.047	0.007	0.001	0.041	0.021	0.010
N15	1.0	0.103	0.426	0.212	0.053	0.009	0.001	0.041	0.021	0.010
I1A	0.0	0.000	0.000	0.000	0.000	0.000	0.000	0.000	0.000	0.000
I1B	1.0	0.550	0.396	0.225	0.064	0.012	0.002	0.220	0.110	0.055
I2A	0.0	0.000	0.000	0.000	0.000	0.000	0.000	0.000	0.000	0.000
I2B	1.0	0.550	0.404	0.222	0.061	0.011	0.002	0.220	0.110	0.055
I3A	1.0	0.550	0.269	0.257	0.123	0.039	0.009	0.220	0.110	0.055
I3B	1.0	0.550	0.269	0.257	0.123	0.039	0.009	0.220	0.110	0.055
I4	1.0	0.549	0.307	0.253	0.104	0.029	0.006	0.220	0.110	0.055
I5A	1.0	0.392	0.420	0.215	0.055	0.009	0.001	0.157	0.078	0.039
I5B	0.0	0.000	0.000	0.000	0.000	0.000	0.000	0.000	0.000	0.000
I6	1.0	0.443	0.409	0.220	0.059	0.011	0.001	0.177	0.089	0.044
I7	1.0	0.214	0.359	0.240	0.080	0.018	0.003	0.086	0.043	0.021
I8	1.0	0.099	0.429	0.210	0.052	0.008	0.001	0.040	0.020	0.010
I9	1.0	0.394	0.397	0.225	0.064	0.012	0.002	0.158	0.079	0.039
I10	1.0	0.297	0.345	0.244	0.086	0.020	0.004	0.119	0.059	0.030
I11	1.0	0.550	0.410	0.219	0.058	0.010	0.001	0.220	0.110	0.055
I12	0.0	0.000	0.000	0.000	0.000	0.000	0.000	0.000	0.000	0.000
I13	1.0	0.550	0.303	0.254	0.106	0.030	0.006	0.220	0.110	0.055
I14	1.0	0.297	0.359	0.240	0.080	0.018	0.003	0.119	0.059	0.030
I15	1.0	0.549	0.348	0.243	0.085	0.020	0.003	0.220	0.110	0.055
I16	1.0	0.330	0.342	0.245	0.088	0.021	0.004	0.132	0.066	0.033
I17	1.0	0.549	0.279	0.257	0.118	0.036	0.008	0.220	0.110	0.055
I18	1.0	0.550	0.292	0.255	0.112	0.033	0.007	0.220	0.110	0.055
I19	1.0	0.550	0.276	0.257	0.119	0.037	0.009	0.220	0.110	0.055

Notes: (1) = Portion of surface flow going to storm runoff (always equal to 1 unless the streamflow from the subwatershed is modeled entirely as baseflow).

(2) = Portion of subsurface flow going to storm runoff (1 - p);

The remaining parameters are coefficients defined in equation 5:

(3) =  $c_2$ ; (4) =  $c_3$ ; (5) =  $c_4$ ; (6) =  $c_5$ ; (7) =  $c_6$ ; (8) =  $c_7$ ; (9) =  $c_8$ ; (10) =  $c_9$ .

The coefficient  $c$  in equation 5 is a constant, equal to 0.3.

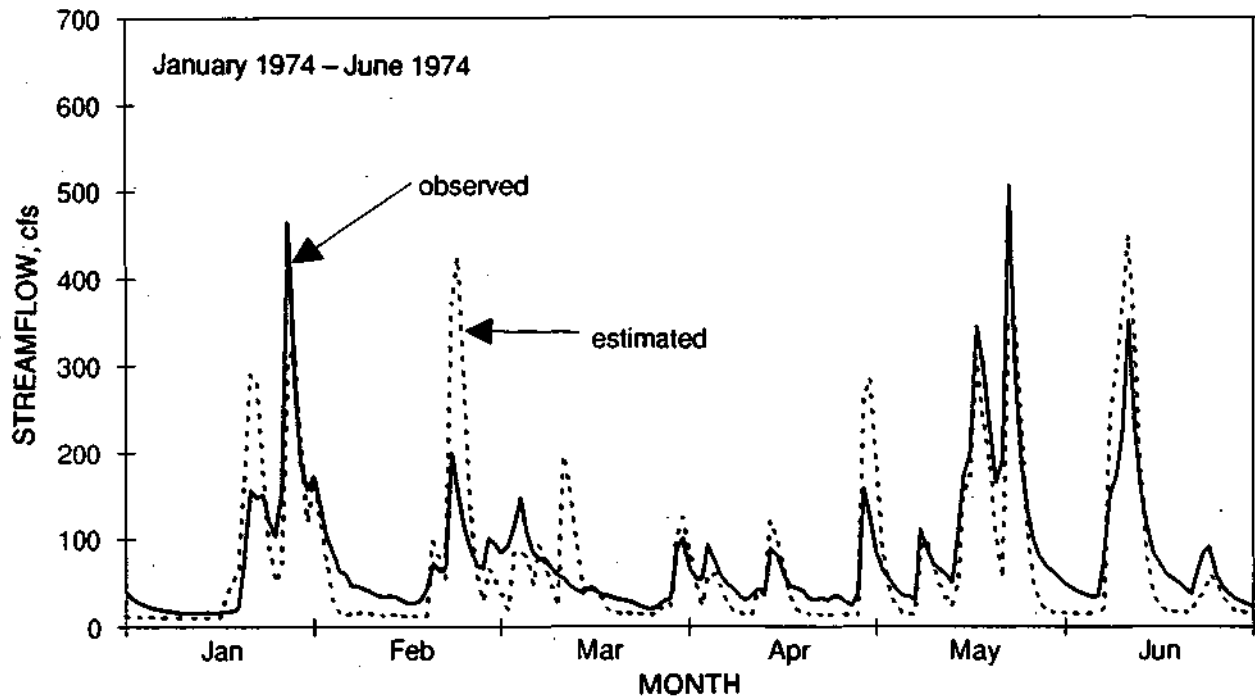


Figure 14. Observed versus estimated flow: Poplar Creek, 1974

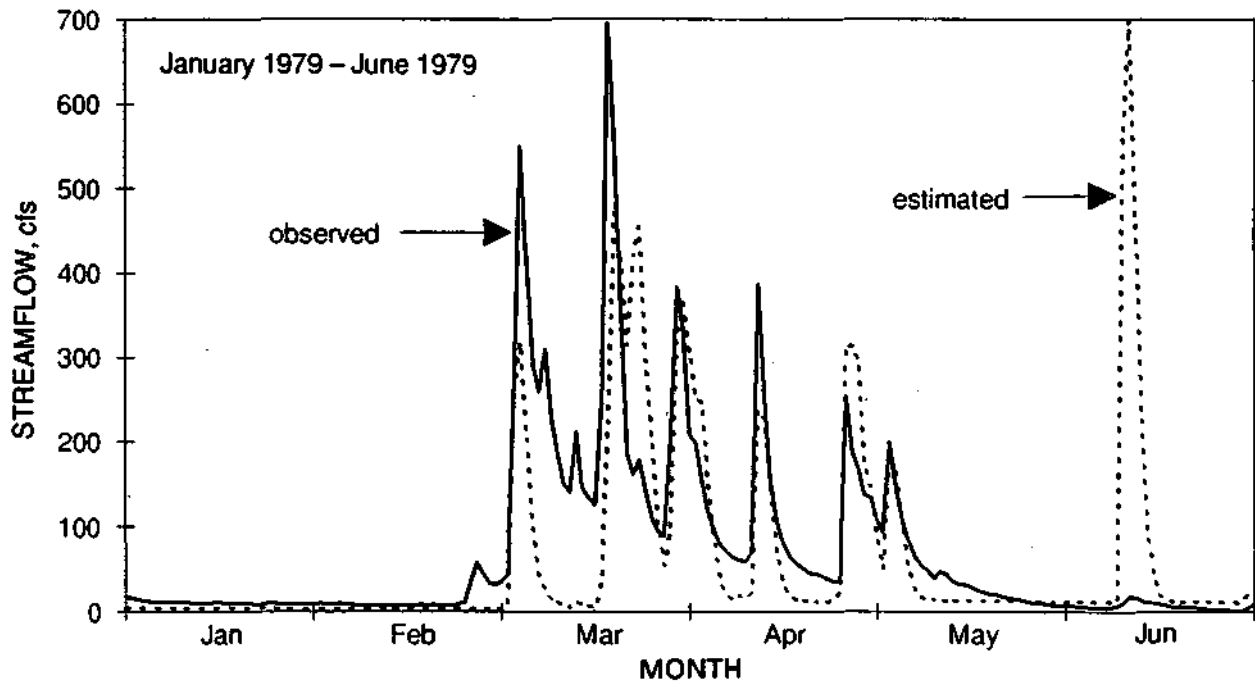


Figure 15. Observed versus estimated flow: Poplar Creek, 1979

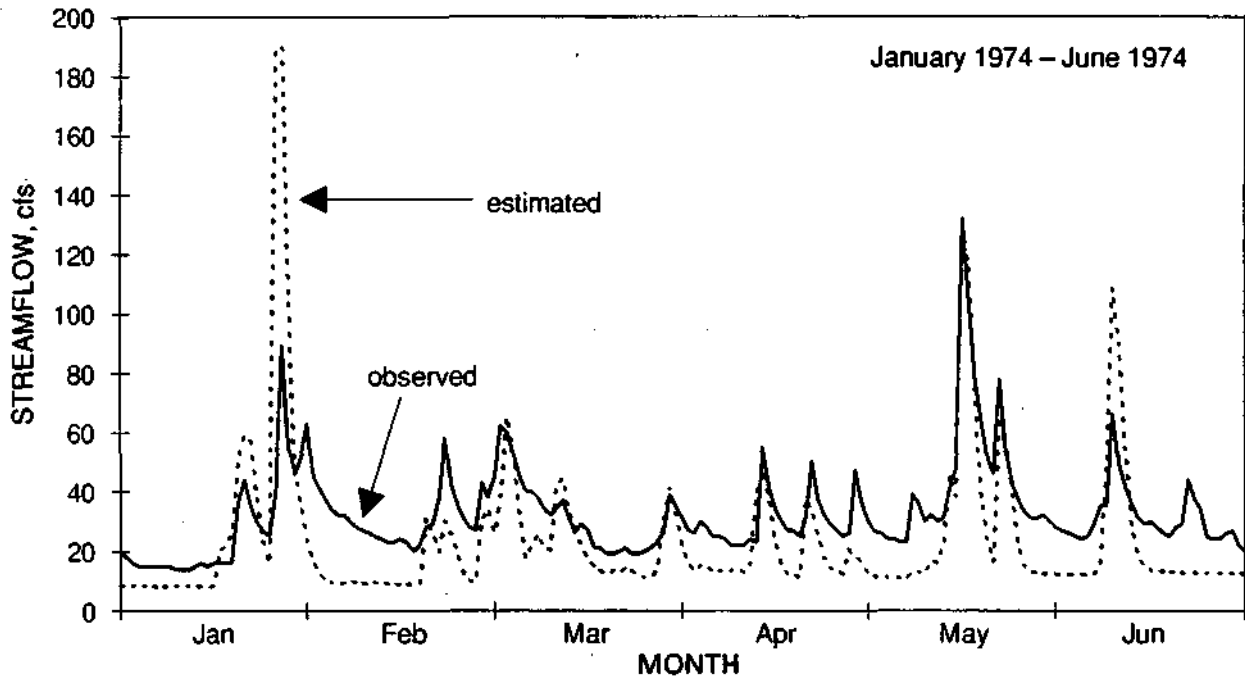


Figure 16. Observed versus estimated flow: Boone Creek, 1974

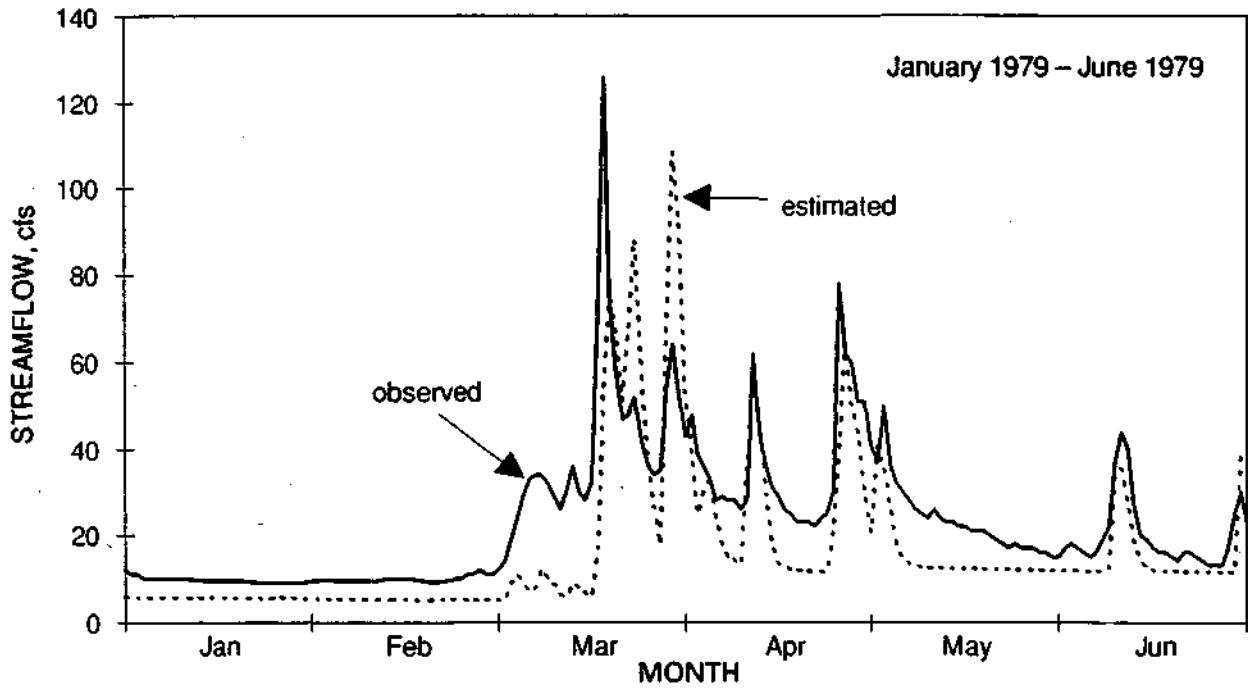


Figure 17. Observed versus estimated flow: Boone Creek, 1979

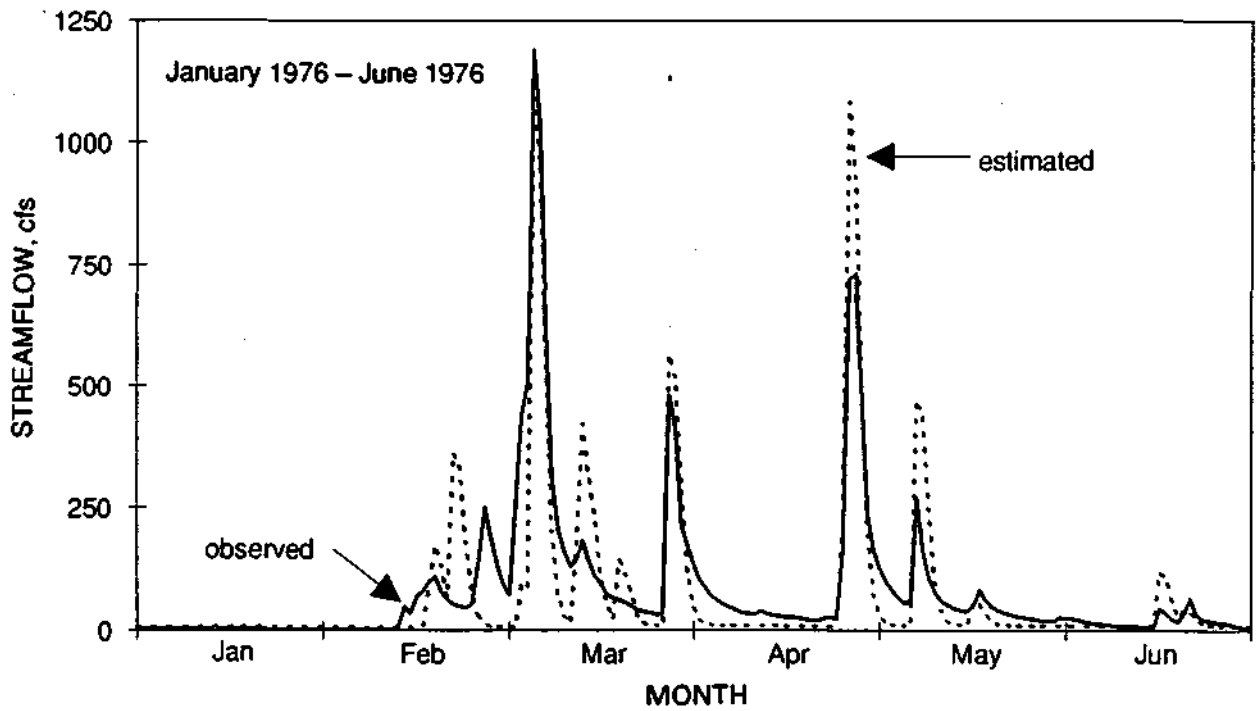


Figure 18. Observed versus estimated flow: Root River Canal, 1976

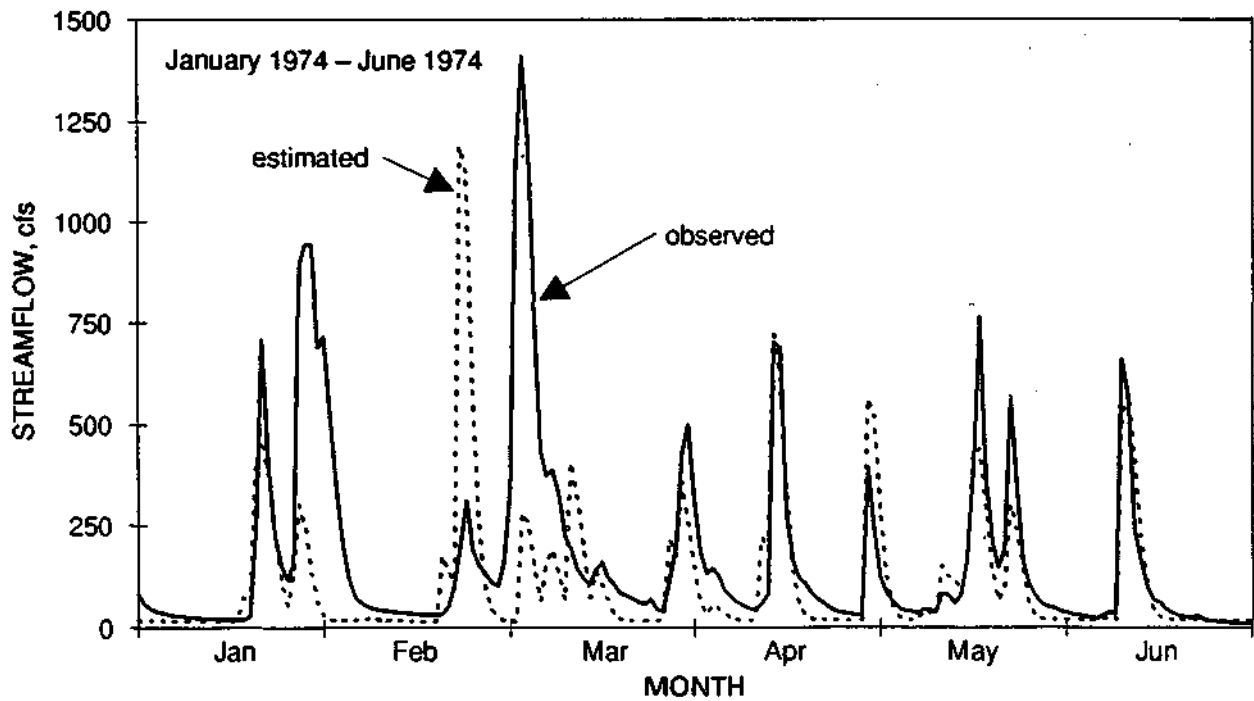


Figure 19. Observed versus estimated flow: Root River Canal, 1974

- 2) Streamflow is usually underestimated during the transition between storm runoff and baseflow conditions. This underestimation typically occurs for several weeks after the recession of the estimated storm runoff, and can be seen in most of the figures. For most watersheds, the baseflow amount during long dry periods is accurately estimated. However, for Boone Creek (figures 16 and 17) the baseflow is underestimated.
- 3) During the winter, precipitation can occur as either rain or snow. The mean average temperature for the day is used by the model to indicate the type of precipitation. Under these circumstances, a snowfall may be interpreted by the model as a rainfall event, and vice versa. The February 22, 1974 storm, shown by the Root River Canal hydrograph (figure 19), illustrates one of these occurrences. The mean temperature for this day is approximately 35°F, therefore the 2-inch precipitation event is modeled as rainfall and a large flood event is simulated. In reality, almost all of the precipitation was snowfall, which did not melt until early March.
- 4) The model generally reproduces the annual series of peak daily flows. The storms that create the annual peak flows for the simulated record are generally, but not always, the same storms that produced the observed peak flows. Table 21 compares the ranked annual peak flows for three watersheds: Poplar Creek, Boone Creek, and Root River Canal. For the Poplar Creek and Root River Canal watersheds, the ranked series of estimated peak flows is similar to the observed series. For the Boone Creek watershed, the estimated values are most often greater than the observed values.

**Table 21. Annual Peak Flow Series (cfs) for Selected Sub-Watersheds**

<i>Poplar Creek (1973-1987)</i>		<i>Boone Creek (1973-1982)</i>		<i>Root River Canal (1973-1987)</i>	
Observed	Estimated	Observed	Estimated	Observed	Estimated
718	753	142	190	1410	1446
696	646	132	155	1190	1327
661	645	126	133	1120	1185
581	635	120	115	1040	1142
562	618	101	108	1020	1090
526	614	89	105	925	1043
523	563	71	91	899	960
506	477	49	84	837	875
467	448	46	79	734	798
453	441	32	40	706	766
364	350			645	717
316	339			569	652
255	312			426	468
180	237			416	424
96	202			84	369

### *Estimation of Six-Hour Hydrograph Values*

A parsing routing was developed to transform the daily runoff hydrographs produced for each of the sub-watersheds into six-hour runoff rates used by the channel and reservoir-routing models. Parsing of daily flows is needed because the daily time-step is too large for application of the Muskingun-Cunge channel routing, described later.

The following procedure parses the daily runoff into five instantaneous runoff rates, which correspond to hours 0, 6, 12, 18, and 24 for each day. The resulting six-hour rates form a continuous hydrograph having piecewise linear segments.

Step 1: Initially, the parsing routing assumes that the flow rate at hour 0 of day  $i$  (equal to hour 24 of day  $i-1$ ) is equal to the midpoint of the average flows for days  $i$  and  $i-1$ . Likewise, the rate at hour 24 of day  $i$  (hour 0 of day  $i+1$ ) is equal to the midpoint of the average flows for days  $i$  and  $i+1$ . The flow rates occurring at hours 6, 12, and 18 for day  $i$  are computed such that mass is conserved. However, the procedure by which the flow rates at hours 6, 12, and 18 are computed differs, depending on whether the daily streamflow values are rising, falling, at a peak, or at a minimum value.

Step 2: If the daily hydrograph is rising (or falling), then the computed six-hour values will strictly increase (or decrease) with time.

Step 3: When a maximum daily value (peak flow) occurs, the time and magnitude of the peak six-hour flow is fixed. The peak flow rate is normally set equal to 120% of the daily flow value. The peak can be set lower than 120% of the daily average in order to conserve mass, but is never greater than this amount. The 1.2:1 ratio that relates the peak instantaneous rate and the maximum daily value was determined through an examination of observed peak flows for the streamgages presented in table 16. The ratio is only appropriate for use with streams in the Fox River watershed having drainage areas less than 100 sq mi.

Step 4: If mass cannot be conserved for a given day, then the flow rates at hours 0, 24, or both are adjusted. If the hour 0 rate is adjusted, this affects the mass balance estimated for the previous day (day  $i-1$ ), which therefore requires recomputing all of the six-hour rates for day  $i-1$ . In this recomputation, the flow rate at hour 0 of day  $i-1$  remains fixed, so that day  $i-2$  is not affected.

A sample output of the estimation of six-hour flows from daily flows is shown (figure 20). This figure illustrates the six-hour values that might be computed under conditions when the daily hydrograph is rising (day 3), falling (day 1, days 5-10), at a peak (day 4), and a minimum (day 2). Note that the flow at hour 24 on day 2 is adjusted to conserve mass for that day.

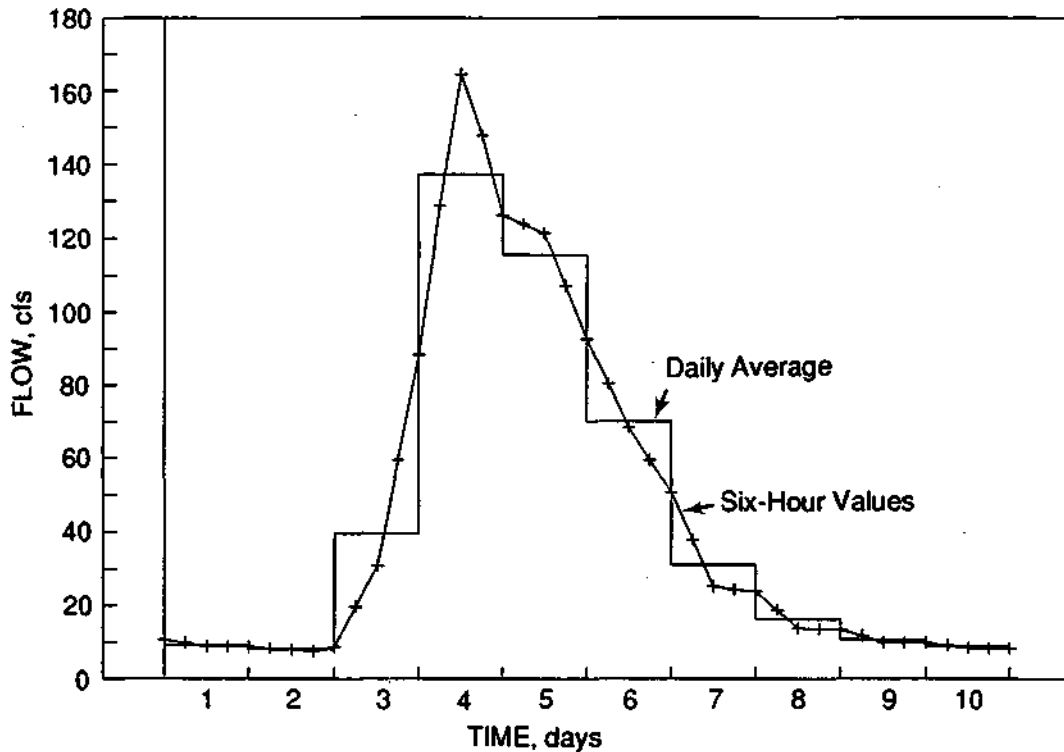


Figure 20. Example of the estimation of six-hour streamflows from daily values

### Component 3: Channel and Reservoir Routing

The flow routing encompasses two distinct types of routing problems: 1) in the main channels and tributaries and 2) through the lakes and reservoirs. Generally, these problems require different models for channel routing and for reservoir routing. As such, the section on flow routing model development is subdivided under these two headings.

Hydrological storage-routing models were selected for both the channel-and reservoir-routing applications. This was partially due to the lack of detailed cross-sectional data that would be required for a more sophisticated model, such as a full dynamic-wave model. Hydrological storage routing models are relatively easy to apply yet retain parameters and/or relations characteristic of the system's physiographic properties. A limitation of these models is that they cannot simulate backwater effects.



### Channel Routing

Channel routing is performed using the Muskingum-Cunge method. This method, and its applicability to channel-routing problems, has been extensively discussed by numerous researchers (Ponce et al., 1978; Koussis, 1980; and Younkin and Merkel, 1988). According to the *HEC-1 Users Manual* U.S. Army Corps of Engineers, (1990), the advantages of the Muskingum-Cunge method over other hydrological techniques are: 1) the model has physically based parameters, 2) the method compares well with results obtained using the full unsteady flow equations, and 3) the solution is independent of the user-selected computation interval.

The channel-routing model uses the variable parameter version of the Muskingum-Cunge method as formulated by Ponce and Yevjevich (1978). This method differs from the classical Muskingum-Cunge method in which the routing parameters are constants based on a representative value of channel discharge. The variable parameter method defines the routing parameters as functions of channel discharge, which are recomputed for each time-step of the simulation prior to discharge routing. The variable parameter method was chosen due to the wide range of discharges experienced during continuous simulation studies. An overview of the method is presented, but the interested reader is referred to the original work by Ponce and Yevjevich. For clarity, the Muskingum method discussion is followed by that of the Muskingum-Cunge method.

The Muskingum method is a hydrological storage-routing method that uses the storage equation, a form of the conservation of mass equation, and a discharge-storage relationship. The storage equation is:

$$I - O = dS/dt \quad (15)$$

where I is inflow, O is outflow, and dS/dt is the change in storage, S, over time, t. Equation 15 can be written in discrete form for a small time interval,  $\Delta t$ , by using average values for inflow, outflow, and storage, as:

$$(I_1 + I_2)/2 - (O_1 + O_2)/2 = (S_2 - S_1)/\Delta t \quad (16)$$

where subscripts 1 and 2 refer to the time step's beginning and end, respectively. In the Muskingum method, storage is related to discharge by:

$$S = K[XI + (1 - X)O] \quad (17)$$

where K is a storage coefficient with dimensions of time and X is a dimensionless weighting coefficient. Substituting equation 17 into equation 16 and solving for  $O_2$  yields:

$$O_2 = C_1 I_2 + C_2 I_1 + C_3 O_1 \quad (18)$$

where the coefficients are:

$$C_0 = K - KX + \Delta t/2 \quad (19)$$

$$C_1 = -(KX - \Delta t/2) / C_0 \quad (20)$$

$$C_2 = (KX + \Delta t/2) / C_0 \quad (21)$$

and

$$C_3 = (K - KX - \Delta t/2) / C_0 \quad (22)$$

In the Muskingum method, the routing parameters K and X are determined empirically from measured inflow-outflow hydrographs. Statistical methods or a trial-and-error graphical fitting technique are commonly used.

To apply equation 18 to channel-routing problems, it is written for each reach length (distance step) where inflow enters at the upstream boundary, outflow exits at the downstream boundary, and storage is contained within the reach. Lateral inflow can be incorporated into equation 18 through inclusion of a fourth term,  $C_4$ , on the right-hand side.  $C_4$  is given by:

$$C_4 = 0.5 (q_1 + q_2) \Delta x \Delta t / C_0 \quad (23)$$

where  $q_1$  is the unit width lateral inflow at time  $t_1$ ,  $q_2$  is the unit width lateral inflow at time  $t_2$ , and  $\Delta x$  is the reach length.

Cunge (1969), in a study of the Muskingum method, derived expressions for K and X based on the channel's physiographic properties. He showed that the Muskingum form of the routing equation (equation 18) had a physical basis through the difference scheme used to calculate  $O_2$ . Cunge's (1969) work has become known as the Muskingum-Cunge method, in which measured inflow-outflow hydrographs are not required to fit the routing parameters, as in the Muskingum method. The routing parameters are calculated from channel properties through the following relations:

$$K = \Delta x / c \quad (24)$$

and

$$X = 0.5 - (1 - q / S_0 c \Delta x) \quad (25)$$

where  $c$  is the flood wave celerity,  $q$  is the unit width channel discharge, and  $S_0$  is the channel bed slope. Equations 26 and 27 compute  $c$  and  $q$  as follows:

$$c = dQ / dA \quad (26)$$

and

$$q = Q / B \quad (27)$$

where  $Q$  is the channel discharge,  $A$  is the flow area, and  $B$  is the top width. Although measured inflow-outflow hydrographs are not required for the Muskingum-Cunge method, it is recommended that  $c$  be calculated from measured flow data if it is available.

The routing parameters, K and X, are usually assumed to be constants, which are evaluated for a reference discharge. This discharge should represent an average value for the reach, usually the midpoint between the base flow rate and peak flow rate. The assumption of constant routing parameters, however, produces results that are dependent on the chosen reference discharge. Ponce and Yevjevich (1978) reported that a high reference discharge resulted in a faster travel time and less subsidence than a low reference discharge. Since discharge can vary significantly during flood wave passage, they investigated the use of variable routing parameters. For each time-step prior to discharge routing, Ponce and Yevjevich recalculated q and c, and subsequently K and X. The variable parameter method was found to be sufficiently accurate in reproducing flood waves. Additionally, this method could reproduce nonlinear characteristics in the outflow hydrograph, such as a steeper rising limb and a more gradual recession.

In the variable parameter method, the routing parameters are recomputed for each time-step based on the average discharge during that time-step. Ponce and Yevjevich (1978) presented three methods of increasing complexity for computing a time-step's average discharge: a two-point method, a three-point method, and an iterative four-point method. The two-point method was found to result in a loss of mass. The three-point and iterative four-point methods were satisfactory in conserving mass and produced similar routing results. The three-point method was chosen for this study since it is less complex. Referring to equation 16, the three-point method computes the average discharge occurring over  $\Delta t$  from the previous time-step's inflow,  $I_1$ , the current time-step's inflow,  $I_2$ , and the previous time-step's outflow,  $O_1$ .

#### *Reservoir Routing*

The reservoir-routing component uses the Modified Puls method. This common routing technique is thoroughly described in a number of hydrology textbooks. An overview of the Modified Puls method is presented below.

Equation 16 is rewritten such that the two unknown terms,  $S_2$  and  $O_2$ , are contained on the left-hand side, and the remaining terms are known and written on the right-hand side:

$$2S_2 / \Delta t + O_2 = I_1 + I_2 + 2S_1 / \Delta t - O_1 \quad (28)$$

Since there are two unknowns and only one equation, a second relation is required to solve equation 28. This relation is developed by assuming that both storage and outflow are single-valued functions of stage. For reservoir-routing applications, this assumption is generally reasonable. The stage-storage relation can be determined from topographic maps and the stage-discharge relation can be developed from the outlet works' hydraulic properties. Using the stage-storage and stage-discharge relations, a routing curve is developed, which relates the left-hand side of equation 28 to discharge ( $2S_2 / \Delta t + O_2$  versus  $O$ ). The routing curve is the second

relation used to solve equation 28. For each time-step, the value of the left-hand side of equation 28 is determined. The routing curve is then used to find  $O_2$ .

The accuracy of the Modified Puls method is dependent on the validity of its routing curve. Assumptions inherent in the development of the routing curve are that the reservoir's water surface is level and that the routing curve is invariant throughout the analysis. As previously stated, these assumptions are usually valid for reservoirs that have uncontrolled spillways and that are large in comparison to the inflows and outflows. Automatic gate structures cannot be modeled using the Modified Puls method since the routing curve would change during each time-step.

#### *Application to the Fox River Upstream of Wilmot*

Channel-Routing Model. The channel-routing model was applied to the reach of the Fox River beginning approximately 6 river miles upstream of Waukesha and ending at the USGS gaging station at Wilmot. Major tributaries entering along this reach were also modeled. The tributaries included in this study were: Honey Creek, Sugar Creek, White River, Wind Lake Drainage Canal, and Mukwonago River.

To apply the channel routing model, the main stem Fox River was separated into 13 subreaches. North of Tichigan Lake, the average subreach length is approximately 4.5 miles; south of Tichigan Lake, the subreach length is approximately 3.1 miles. Major tributaries had similar subreach lengths of approximately 3 miles each. This resulted in Honey Creek having seven subreaches, Sugar Creek having four, White River having three, Wind Lake Drainage Canal having two, and Mukwonago River having two. Figure 21 is a schematic diagram showing the channel subreach locations.

Physiographic channel properties were ascertained from a number of sources. USGS flow-rating data for the Fox River at Waukesha and Wilmot for Nippersink Creek at Spring Grove were used to develop conveyance, stage and discharge relations. Federal Emergency Management Agency (FEMA) flood insurance studies (1986) supplied cross-section and roughness information. USGS 15-minute and 7.5-minute topographic maps were used to determine floodplain and channel bottom slopes, floodplain widths, and reach storage. A Land Use Plan map prepared for the SEWRPC provided land use and additional reach storage information. The *Fox River Basin Streamflow Assessment Model: Hydrologic Analysis* report (Knapp, 1988) provided flow and physiographic information.

Many subreaches were found to have similar physiographic properties. Those subreaches exhibiting similar properties were grouped to form six reach types. Table 22 lists these types and the associated subreaches. Routing parameter-discharge relations (equations 24 and 25) developed for each reach type were also used for every subreach within a given type. Individual routing-parameter relations were not developed since all of the reaches were adequately described by one of the six types.

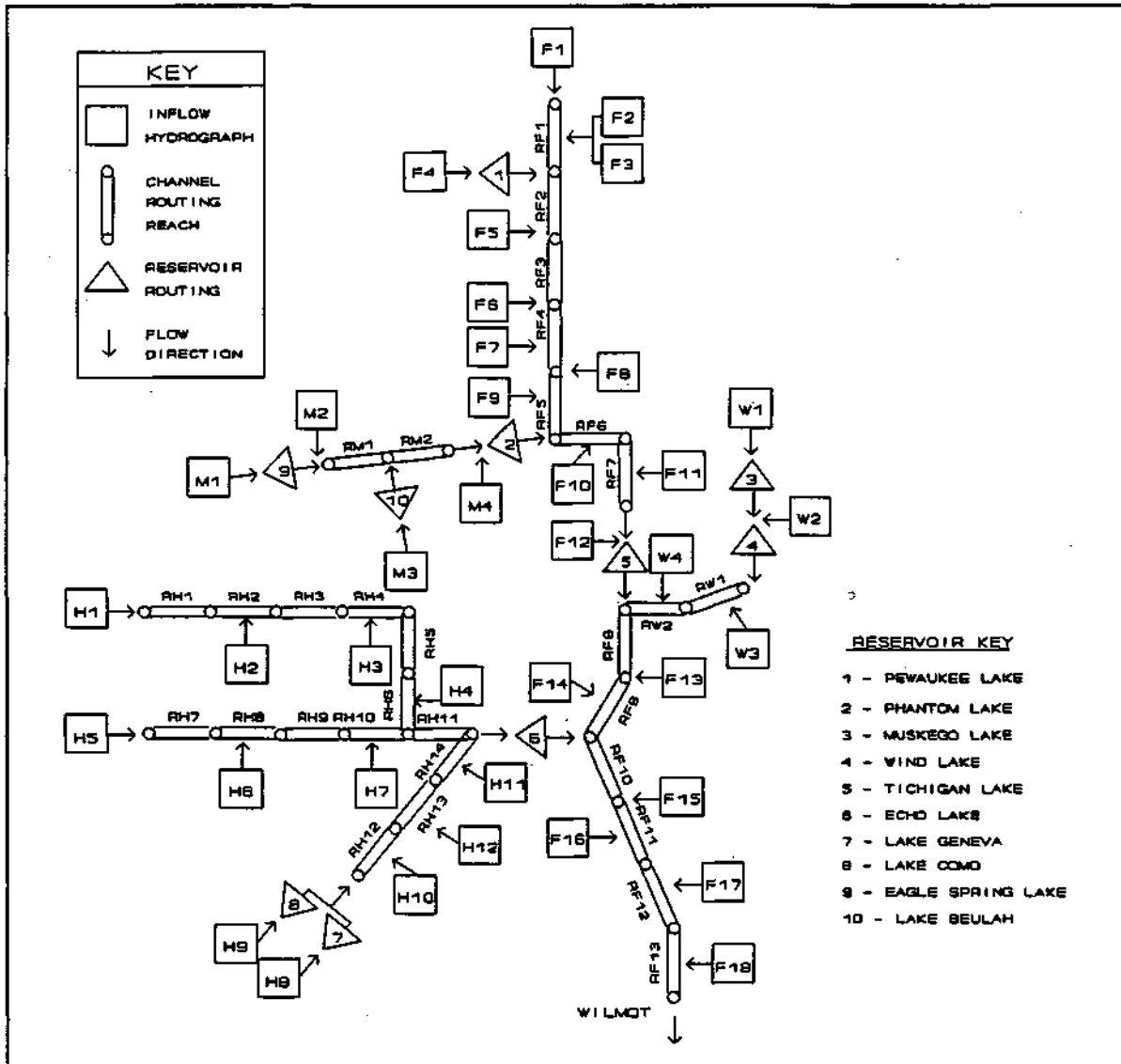


Figure 21. Schematic diagram of routing elements for the Fox River upstream of Wilmot

Table 22. Routing Parameter Reach Types

Reach Type	Subreach Numbers
Northern Fox	RF1-RF4
Mukwonago Swamp	RF5-RF6
Middle Fox	RF7-RF9
Southern Fox	RF10-RF13
Greek (generic)	RM1, RW1-RW2, RH1-RH2, RH4-RH10, RH13-RH14
Swampy Creek	RM2, RH3, RH11-RH12

USGS flow-rating data and FEMA flood insurance studies were used to develop the routing parameter-discharge relations. Both sources of information were needed since the rating data did not contain hydraulic information (discharge, depth, top width, or area) for locations having floodplains. This was true for all of the studied gaging stations and is partially due to the required placement of streamgages near control points such as bridges. Figures 22, 23, and 24 show cross sections located downstream (approximately 0.26 miles), near, and upstream (approximately 0.3 miles) of the USGS gage on Nippersink Creek near Spring Grove. The cross sections located upstream and downstream of the gage contain a widened area occurring above 755 feet mean sea level elevation, which is not evident in the cross section near the gage. Figure 25 shows the depth versus cross-sectional area relations for the USGS rating data and for the cross section located upstream of the gage (number 7.63). Discharge and area relations for the USGS rating data and cross section 7.63 are shown in figure 26. This figure was developed by noting that no significant lateral inflows enter Nippersink Creek between these two locations and by assuming steady-state flow conditions, uniform water depth, and small head losses.

As seen in figure 26, the discharge versus cross-sectional area curve is dependent on the presence of floodplains. The derivative of this curve,  $dQ/dA$ , is the flood wave celerity,  $c$  (equation 26), which is used in the calculation of both  $K$  and  $X$ . Top width, also affected by the presence of floodplains, should be representative of the subreach length since the unit width channel discharge,  $q$  (equation 27), is computed from it and then used calculate  $X$ .

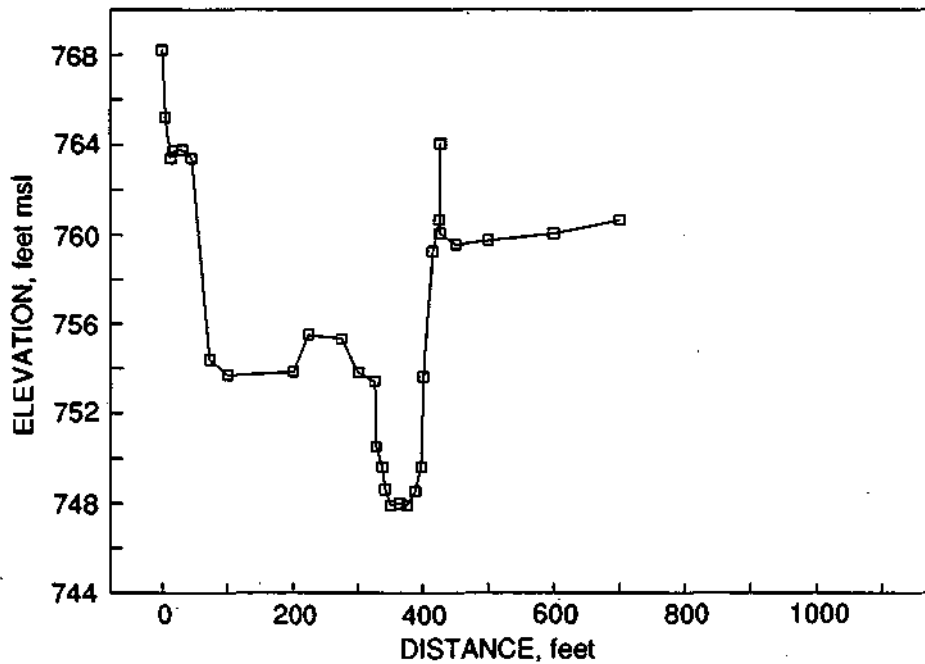


Figure 22. Cross section of Nippersink Creek downstream of the Spring Grove gage

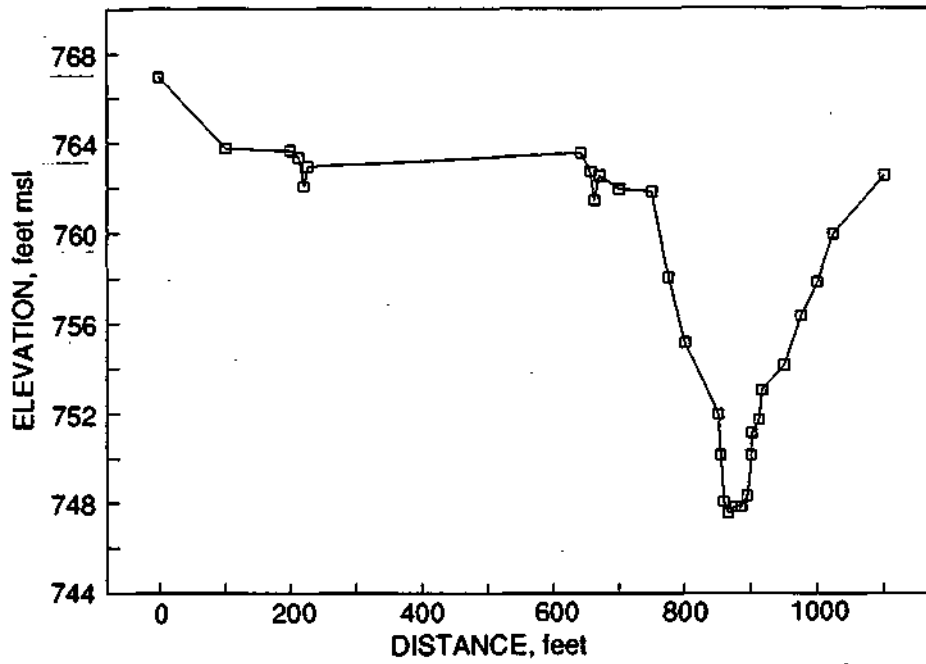


Figure 23. Cross section of Nippersink Creek near the Spring Grove gage

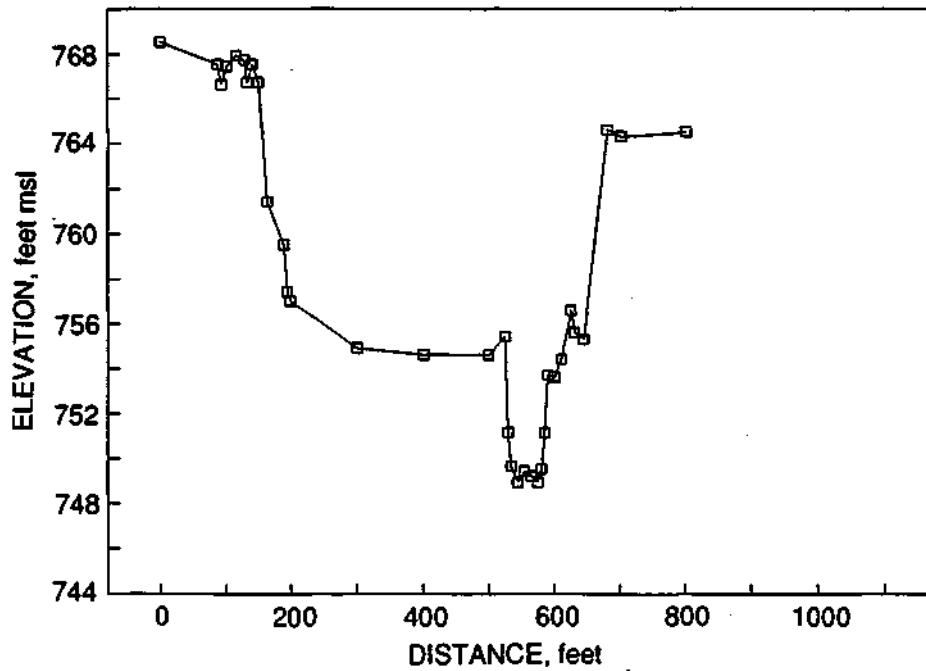


Figure 24. Cross section of Nippersink Creek upstream of the Spring Grove gage

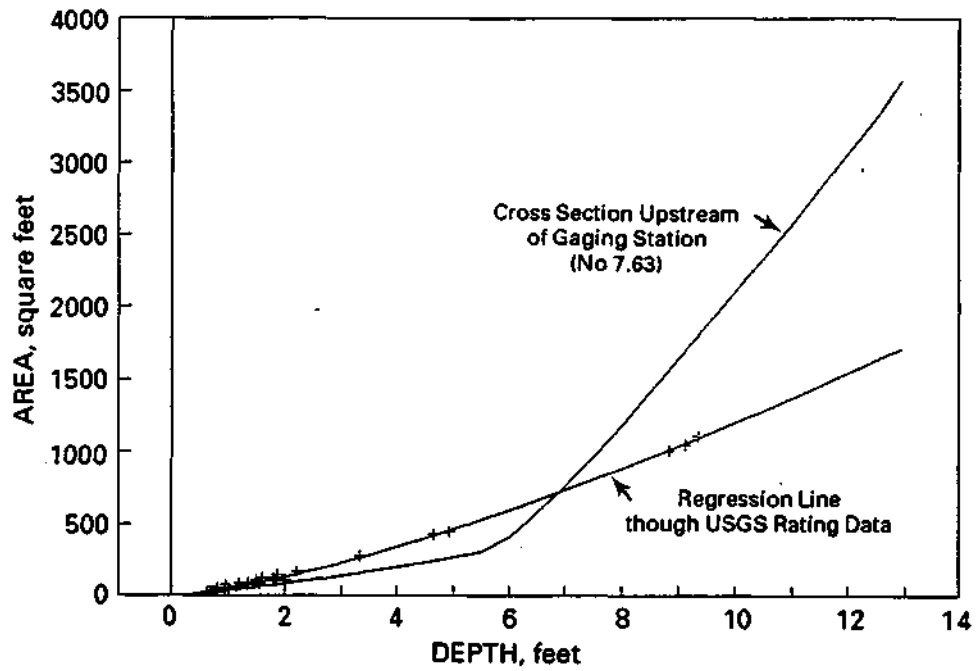


Figure 25. Depth of flow versus cross-sectional area for Nippersink Creek

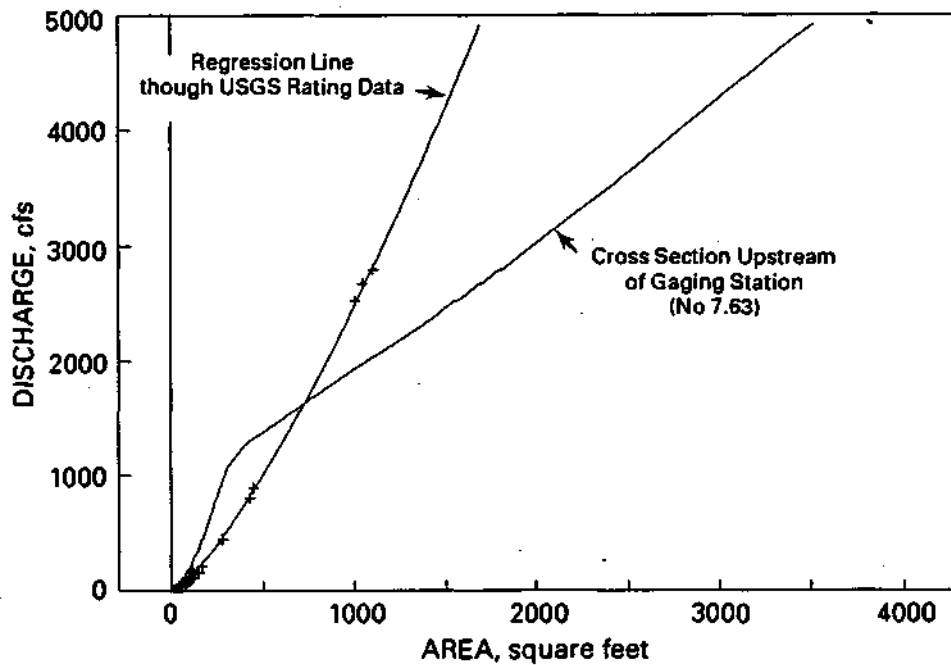


Figure 26. Cross-sectional area versus discharge for Nippersink Creek



The routing parameter-discharge relations were initially developed to cover the entire range of possible flows, from low channel flow to high floodplain flow. Trends were evident in the routing parameter-discharge relations, were not constant. Separate trends were evident for channel flows, for low floodplain flows, and for high floodplain flows. Generally, K increased with increasing discharge and X decreased.

Previous studies have cautioned that the routing-parameter relations be no more than mildly variable with discharge to ensure accurate routing results. A sensitivity analysis was performed on the Fox River relations using the inflow hydrograph data. Accuracy criteria developed by Ponce and Theurer (1982), as well as mass conservation checks, were used to evaluate the results. The Fox River relations, as initially formulated, were found to be too variable. Generally, mass was not conserved and the routing results had questionable accuracy.

To ensure conservation of mass and accuracy, each routing-parameter relation was formulated to be mildly variable with discharge. It was assumed that certain reach types would have routing parameter-discharge relations characteristic of channel to low floodplain flows and that other reach types would have relations characteristic of low to high floodplain flows. The Northern Fox, Middle Fox, Southern Fox, and Creek types were assumed to have channel and low floodplain flow relations. Mukwonago Swamp and Swampy Creek were assumed to have low to high floodplain flow relations. Subreaches within the Mukwonago Swamp and Swampy Creek types generally have flat-bottom slopes and wide overbank areas with numerous depressions and marsh-type vegetation. The Swampy Creek reach type was also used to model Honey Lake since this lake has little storage and could not be adequately modeled by the reservoir routing routine. Table 23 lists the routing-parameter relations. Figures 27 and 28 show these relations graphically.

As seen in figure 28, X can acquire negative values during high discharge conditions. Currently, there is discrepancy in the literature as to whether X can be less than zero. Ponce and Theurer (1982) have argued that X can be less than zero, as long as equation 25 is satisfied, and have cited other researchers who have used negative values for X (Ponce and Theurer, 1982; Kundewicz, 1980). It should be noted, however, that figure 28 was plotted

**Table 23. Fox River Routing Parameter Relations**

<b>Reach Type</b>	<b>K</b>	<b>X</b>
<b>Northern Fox</b>	$0.001q_{ave} + 9.0$	$-0.0001q_{ave} + 0.2$
<b>Mukwonago Swamp</b>	$0.0001q_{ave} + 24.0$	$-0.00001q_{ave} + 0.1$
<b>Middle Fox</b>	$0.001q_{ave} + 12.0$	$-0.0001q_{ave} + 0.1$
<b>Southern Fox</b>	$0.0005q_{ave} + 9.0$	0.1
<b>Creek</b>	$0.002q_{ave} + 12.0$	$-0.0001q_{ave} + 0.2$
<b>Swampy Creek</b>	$0.001q_{ave} + 18.0$	$-0.00005q_{ave} + 0.1$

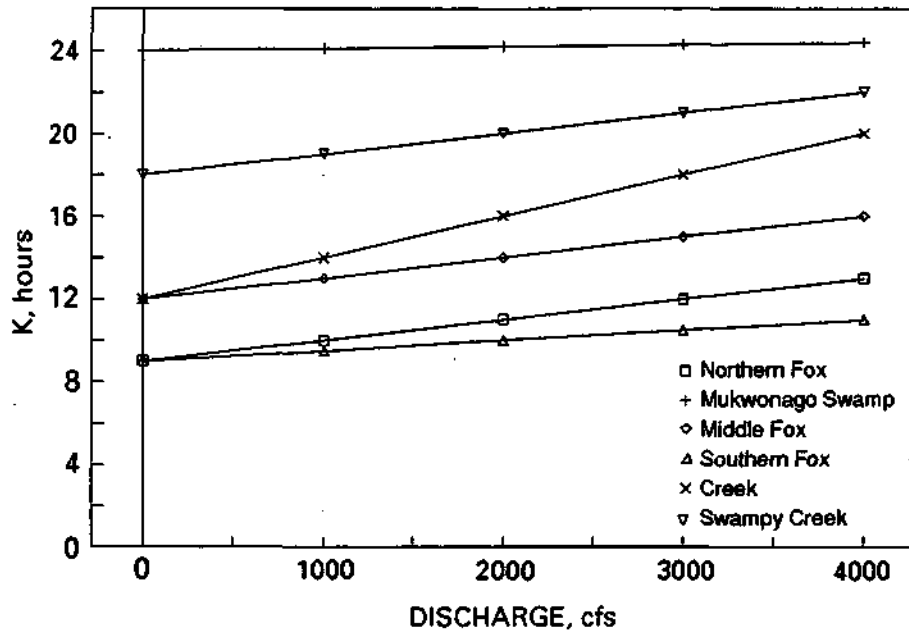


Figure 27. Relationship between Muskingum E and discharge

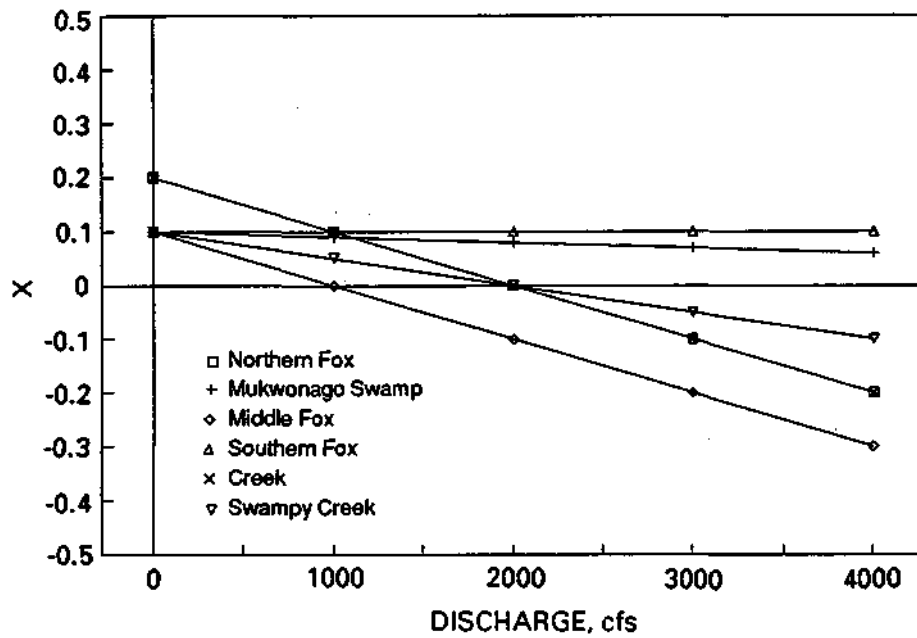


Figure 28. Relationship between Muskingum X and discharge

using a range of discharges between 0 and 4,000 cfs, and that many of the reach types (Northern Fox, Middle Fox, Creek, and Swampy Creek) rarely, if ever, experience discharges as high as 4,000 cfs.

A six-hour time-step was selected as the routing interval. This was felt to give adequate resolution because: 1) tests using a smaller (two-hour) time-step showed little difference in channel-routing results, 2) the rainfall-runoff model which generated the inflow hydrographs used a daily time-step, 3) the models were calibrated using daily flow data, and 4) there was not sufficient data available on the channel's hydraulic properties to justify using a more refined time-step. A parsing algorithm, described earlier, was used to parse the daily inflow hydrograph data into six-hour values. This routine was formulated such that conservation of mass was ensured and that the resulting six-hour values would be representative of expected conditions.

Reservoir-Routing' Model. The reservoir-routing model was applied to ten reservoirs that lie north of Wilmot in the Fox River tributary basin: 1) Pewaukee Lake, 2) Phantom Lake, 3) Muskego Lake, 4) Wind Lake, 5) Tichigan Lake, 6) Echo Lake, 7) Lake Geneva, 8) Lake Como, 9) Eagle Spring Lake, and 10) Lake Beulah. Figure 21 shows the reservoir locations.

Discharge-stage-storage relations for each reservoir were supplied by the SEWRPC. Precipitation gages used to estimate rainfall over the lake surface are listed in table 24. Lake surface evaporation was estimated from potential evapotranspiration estimates produced by the PACE soil-moisture component. All of the climatic data used to estimate lake surface evaporation were measured at Rockford, Illinois, with the exception of temperature data, which used the local information. Table 24 also lists the temperature gage locations.

A six-hour time-step was used in the reservoir routing to conform with the channel-routing model. The daily inflow hydrographs were parsed into six-hour values using the parsing algorithm described earlier. The daily volumes of rainfall and evaporation occurring on the lake surface were assumed to be uniformly distributed over each six-hour increment.

**Table 24. Climatic Data Used in Reservoir Routing**

<u>Reservoir</u>	<u>Raingage</u>	<u>Temperature Gage</u>
Pewaukee	Waukesha	Waukesha
Phantom	Eagle	Antioch
Muskego	Waukesha	Waukesha
Wind	Union Grove	Antioch
Tichigan	Burlington	Burlington
Echo	Burlington	Burlington
Geneva	Lake Geneva	Lake Geneva
Como	Lake Geneva	Lake Geneva
Beulah	Eagle	Antioch
Eagle Spring	Eagle	Antioch

*Application to Nippersink Creek*

Channel-Routing Model. The channel-routing model was applied to the reach of Nippersink Creek beginning at its mouth at Fox Lake and extending upstream to approximately two river miles south of its intersection with the Illinois-Wisconsin border. The North Branch Nippersink Creek and Silver Creek were also routed.

To apply the channel-routing model, the main stem of Nippersink Creek was separated into eight subreaches. The North Branch Nippersink Creek was separated into four subreaches and Silver Creek was represented by one subreach. Each subreach was approximately two miles long. Figure 29 shows the channel subreaches and the inflow hydrograph locations.

Physiographic channel properties were ascertained from a number of sources. USGS flow-rating data for Nippersink Creek at Spring Grove were used to develop conveyance, stage, and discharge relations. The FEMA flood insurance study for Spring Grove supplied cross-section and roughness information. USGS 7.5-minute topographic maps were used to determine floodplain and channel bottom slopes, floodplain widths, and reach storage, and flow and physiographic information was taken from Knapp (1988).

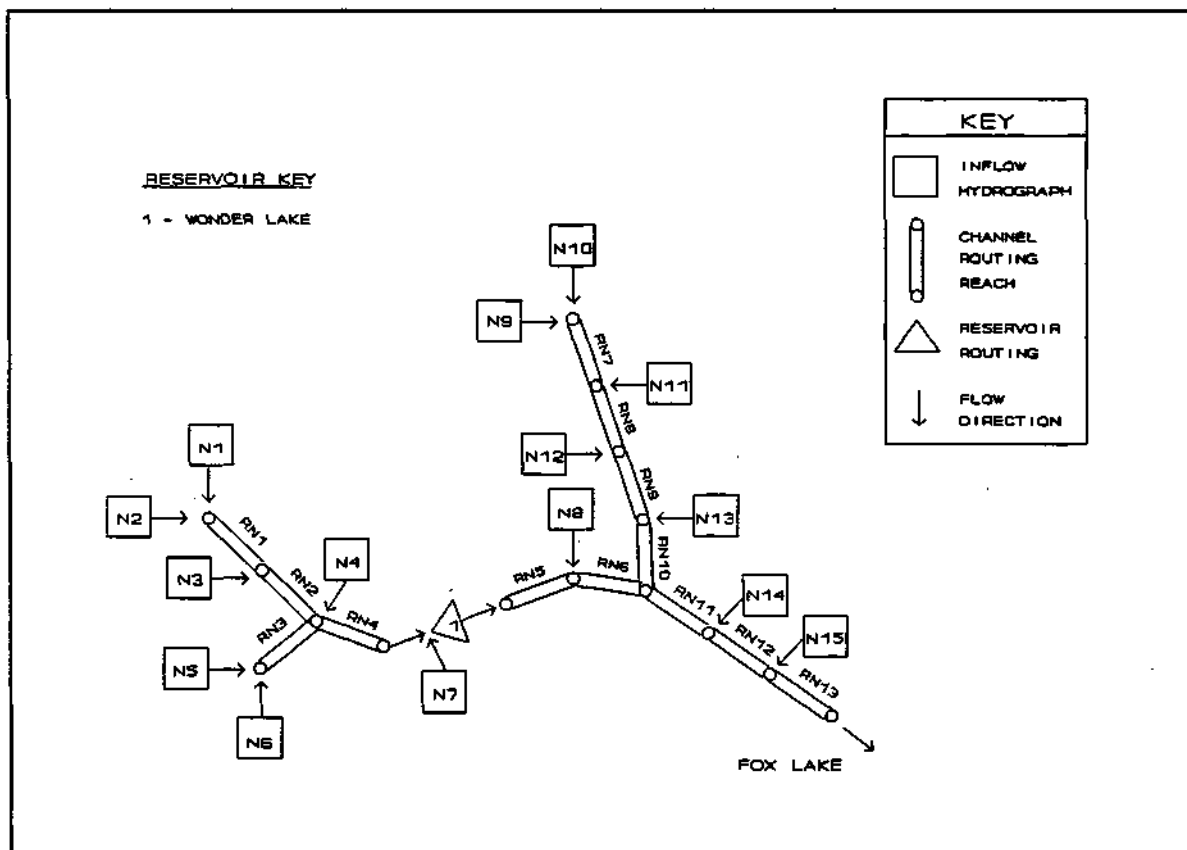


Figure 29. Schematic diagram of routing elements for Nippersink Creek

The subreaches were grouped under two reach categories based on their physiographic properties. Routing parameter-discharge relations (equations 24 and 25,) were developed for each category following the procedure presented in the Fox River section of the report. The routing parameter relations are given in table 25. A six-hour routing-time interval was used.

Reservoir Routing Model. Wonder Lake was routed using the reservoir-routing model with a six-hour time interval. Figure 29 shows the location of Wonder Lake. Discharge-stage-storage relations for Wonder Lake were obtained from the Dam Safety Inspection Report (U.S. Army Corps of Engineers, 1978). Precipitation data were taken from the gage at McHenry. Lake surface evaporation was estimated using estimates of potential evapotranspiration produced by the PACE component. Temperature data were obtained from Antioch. Other climatic data were obtained from Rockford, Illinois.

Twin Lakes (Elizabeth Lake and Lake Marie) provides an additional source of storage in the watershed. The streamflow in Elizabeth Lake Drain, which is the outflow from Twin Lakes to the North Branch Nippersink Creek, is not controlled by a dam but instead passes through a wetland area. Accurate discharge-stage-storage data are not available for this outflow. Previous hydrologic analysis of Elizabeth Lake Drain by the U.S. Army Corps of Engineers (FEMA, 1986) indicates that maximum discharges from Elizabeth Lake are very small -- and estimates that the 100-year discharge from the 13.4-square-mile watershed is 117 cfs. Outflow from this watershed is simulated by having all surface and subsurface runoff used as input into the baseflow algorithm in the hydrograph response component of the model. This modeling technique produces a comparatively uniform flow from the watershed, having low peak discharges during flood events.

*Application to the Fox River from Wilmot to South Elgin*

FEQ Channel-Routing Model. A dynamic-wave model (FEQ) has been developed under a separate study to simulate the hydraulics of the Fox River from Wilmot to South Elgin. The streamflow hydrographs developed in this report will be used with the FEQ model, in a subsequent study, to determine flow stages and discharges along the Chain of Lakes and Fox River. The locations of the FEQ routing reaches and the sub-watersheds being analyzed in this report are shown in figure 30. The development of the FEQ Fox River application is described in *Investigation for Flood Control - Fox River Project FEQ Model - Lake, McHenry, and Kane Counties* (Illinois Department of Transportation, Division of Water Resources, January 1991).

**Table 25. Nippersink Creek Routing Parameter Relations**

<u>Reach Type</u>	<u>K</u>	<u>X</u>
Nippersink Creek	$0.001 q_{ave} + 9.0$	$-0.0001 q_{ave} + 0.1$
Nippersink Detain	$0.0001 q_{ave} + 14.0$	$-0.00005 q_{ave} + 0.1$

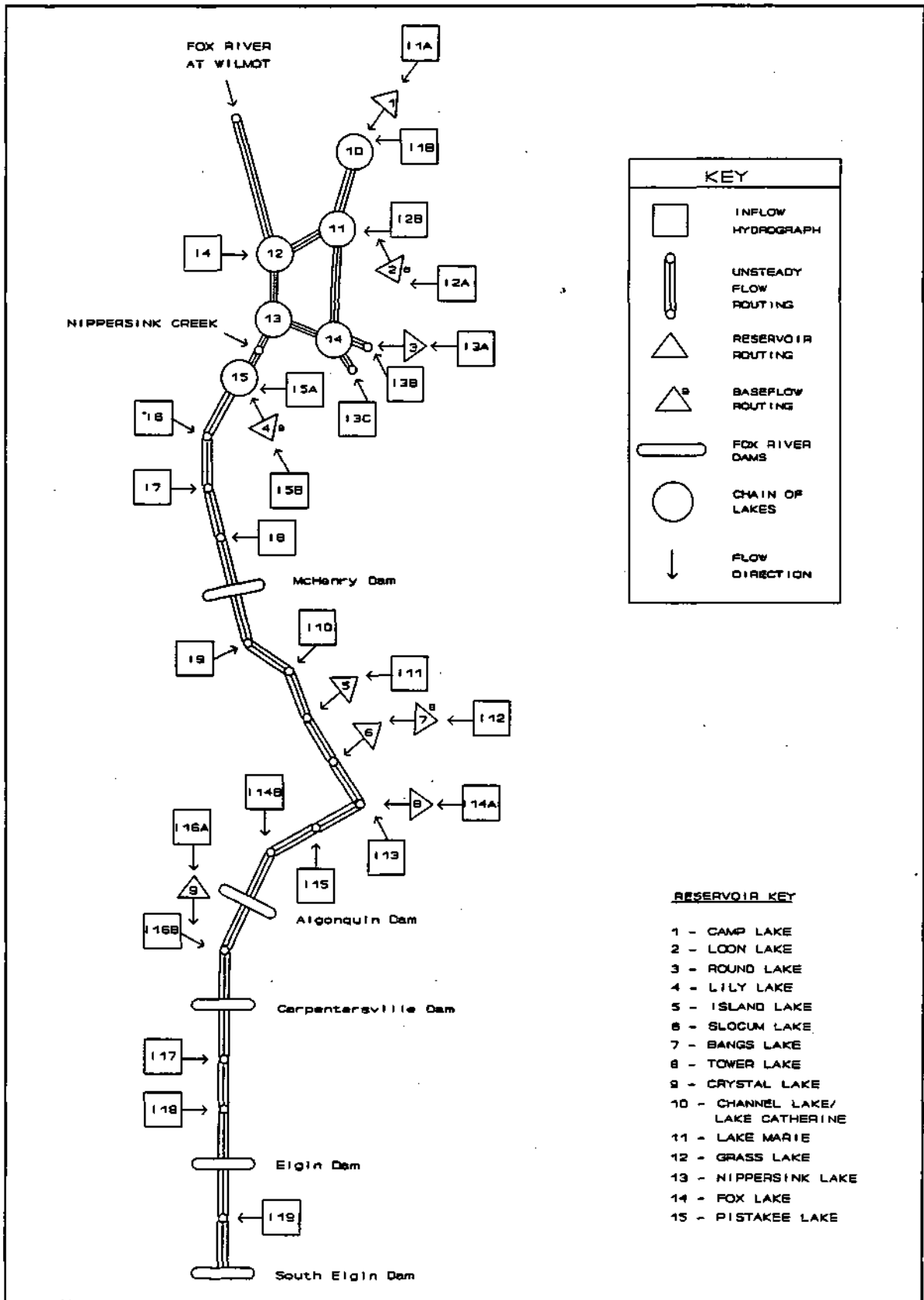


Figure 30. Schematic diagram of routing elements for the Fox River between Wilmot and South Elgin

Reservoir Routing Model. The reservoir routing model was applied to six reservoirs with known discharge-stage-storage relations: Camp Lake, Round Lake, Island Lake, Slocum Lake, Tower Lake, and Crystal Lake. Outflow from three other lakes — Loon Lake, Lily Lake, and Bangs Lake — is expected to be strongly influenced by subsurface drainage, with very low peak discharges. Discharge from these lakes should be similar to the outflow predicted by the baseflow algorithm described earlier in the modeling of hydrograph response. The outflow from these lakes was simulated by having all surface and subsurface runoff in their watershed used as input into the baseflow algorithm of the model. Figure 30 shows the reservoir locations.

## ANALYSIS OF MODELING RESULTS

The effectiveness of the modeling effort to predict inflows to the Fox Chain of Lakes is evaluated by examining the relationship between the observed and estimated flow at two gages: the Fox River at Wilmot and Nippersink Creek near Spring Grove. Comparisons are provided for the period of calibration (1974-1987), and for sets of other years that were simulated after the calibration, and are used for model validation.

The following discussions compare the simulated (estimated) and historical (observed) flow records in four separate categories: 1) annual flows over the period of simulation; 2) average monthly flow over the simulated record; 3) daily flows; and 4) the annual series of peak flows. Various figures presented in the discussion provide the reader with visual comparisons of the simulated and historical flow records. The reader can view a graph of the estimated and observed flow records for the period 1974-1987 by executing the set of computer programs provided on the floppy diskette, which accompanies this report.

### **Comparison of Observed and Estimated Streamflow Records**

#### *Annual Flows*

Table 26 shows the observed and estimated annual flows for the Wilmot, and Spring Grove gages for calendar years 1974-1990. The 1973 year was also simulated but is not listed in the compilation because that year was a "warm-up" period for the model, during which the simulated low and medium flows converged toward the historical record.

The annual estimated flows at both stations generally compare favorably with the annual observed flows. The simulated record tends to be less variable, underestimating the average flow in wet years and overestimating the average flow in dry years. The streamflow during the driest year, 1977, is noticeably underestimated at both gages. But the simulated record for two dry years in the validation period, 1988 and 1989, are reasonably close to the observed totals. The average flow for the 14-year calibration period is underestimated by 32 cfs (4.6%) for the Wilmot gage and overestimated by 3 cfs (1.8%) for the Spring Grove gage. The difference between the average estimated and observed flows for all 19 years is slightly less for the Wilmot gage. The average simulated flow for the watershed is directly associated with the water yield originally estimated in the model's soil-moisture component. There was no adjustment of these parameters to reduce the gap between the estimated and observed average flows at the Wilmot and Spring Grove gages.



**Table 26. Average Annual Flows for the Fox River and Nippersink Creek:  
Observed versus Estimated Flow**

Calibration Years <sup>1</sup>	Fox River at Wilmot		Nippersink Creek near Spring Grove	
	Observed	Estimated	Observed	Estimated
1974	973	864	258	212
1975	626	618	148	164
1976	527	643	123	151
1977	283	392	57	103
1978	684	687	118	174
1979	841	822	210	221
1980	565	624	144	154
1981	574	544	133	120
1982	852	790	208	194
1983	808	612	193	156
1984	756	720	159	180
1985	777	722	184	176
1986	921	737	245	208
1987	642	611	143	158
<b>Validation Years</b>				
1960	----	627	----	----
1961	----	848	----	----
1971	----	----	130	153
1972 <sup>b</sup>	----	----	229	235
1988	464	524	108	123
1989	377	355	72	90
1990 <sup>b</sup>	736	709	181	149
<b>AVERAGE (calibrated years)</b>				
	702	670	166	169
<b>AVERAGE (all years)</b>				
	671	655	160	164

**Notes:** <sup>a</sup>Average flows are computed by calendar year, January to December.

<sup>b</sup>The 1972 and 1990 flow records are compared only for the period January 1 to September 30.

### *Average Monthly Flows*

Average flows for each month during the period 1974-1987 are given in table 27 for the simulated and historical flow records at the Wilmot and Spring Grove gages. The estimated and observed monthly flows for the Wilmot gage are similar, with the greatest variation occurring in February and May, for which the estimated flow record underestimates the historical record. For the Spring Grove gage, the model overestimates flows in the summer months, especially during July and August of 1978, when several large flow events are simulated as a result of heavy rainfall at the McHenry raingage. In addition, the model overestimates summer low flows.

### *Daily Flows*

Daily values of simulated and historical flows for the Fox River at Wilmot are compared for two six-month periods (figures 31 and 32). Simulated and historical daily flows for Nippersink Creek near Spring Grove are compared in figures 33 and 34. The reader can obtain additional visual comparisons by executing the computer programs that are provided on the floppy diskette, which accompanies this report.

Two systematic differences between the simulated and historical flows can be seen in figures 31-34. First, following a storm event, the simulated flow recesses more quickly to low and medium flows than does the historical flow. The slow recession exhibited by the observed flows may be due in part to the large storage of water in streams and wetlands following a storm event, which is released during the hydrograph recession. The effects of the storage on

**Table 27. Average Monthly Flow for the Fox River and Nippersink Creek: Observed versus Estimated Flow, Calendar Years 1974-1987**

Month	Fox River at Wilmot		Nippersink Creek near Spring Grove	
	Observed	Estimated	Observed	Estimated
January	445	422	116	97
February	646	511	162	142
March	1385	1315	313	365
April	1333	1304	302	274
May	844	703	185	164
June	565	475	136	135
July	468	529	112	157
August	458	516	108	140
Septem'ber	463	479	128	132
October	520	477	124	110
November	602	583	133	149
December	692	693	173	166
Annual Average	702	670	166	169

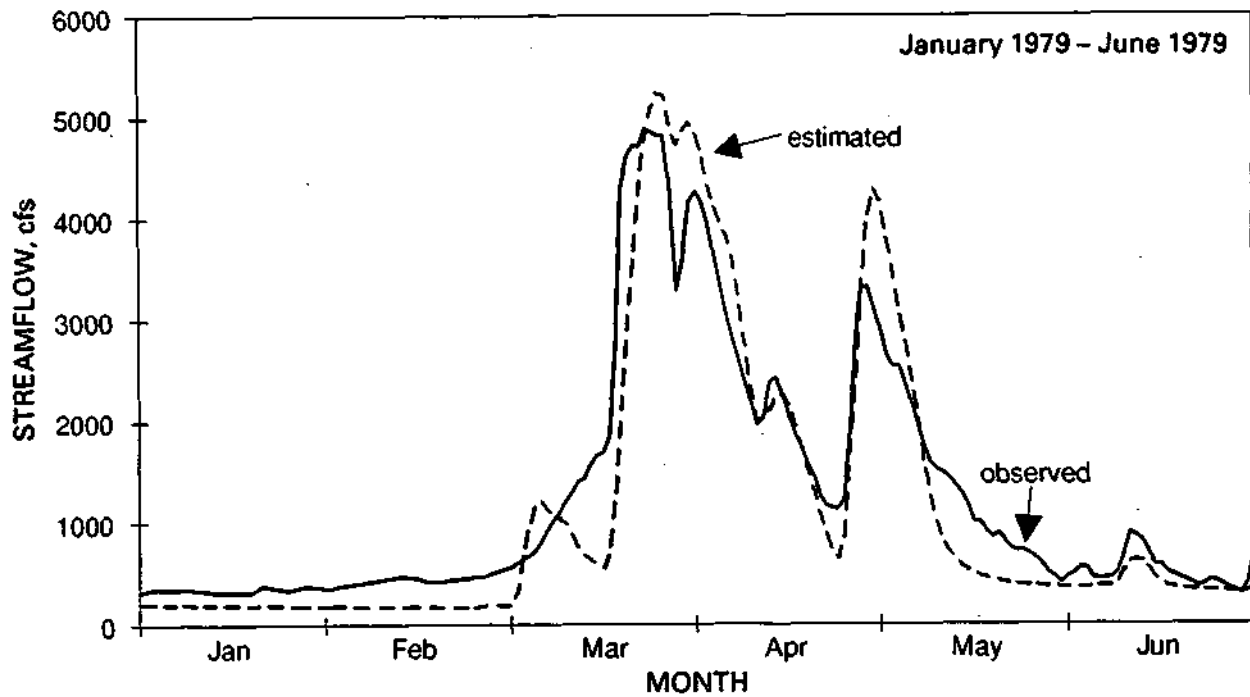


Figure 31. Observed versus estimated flow: Fox River at Wilmot, 1979

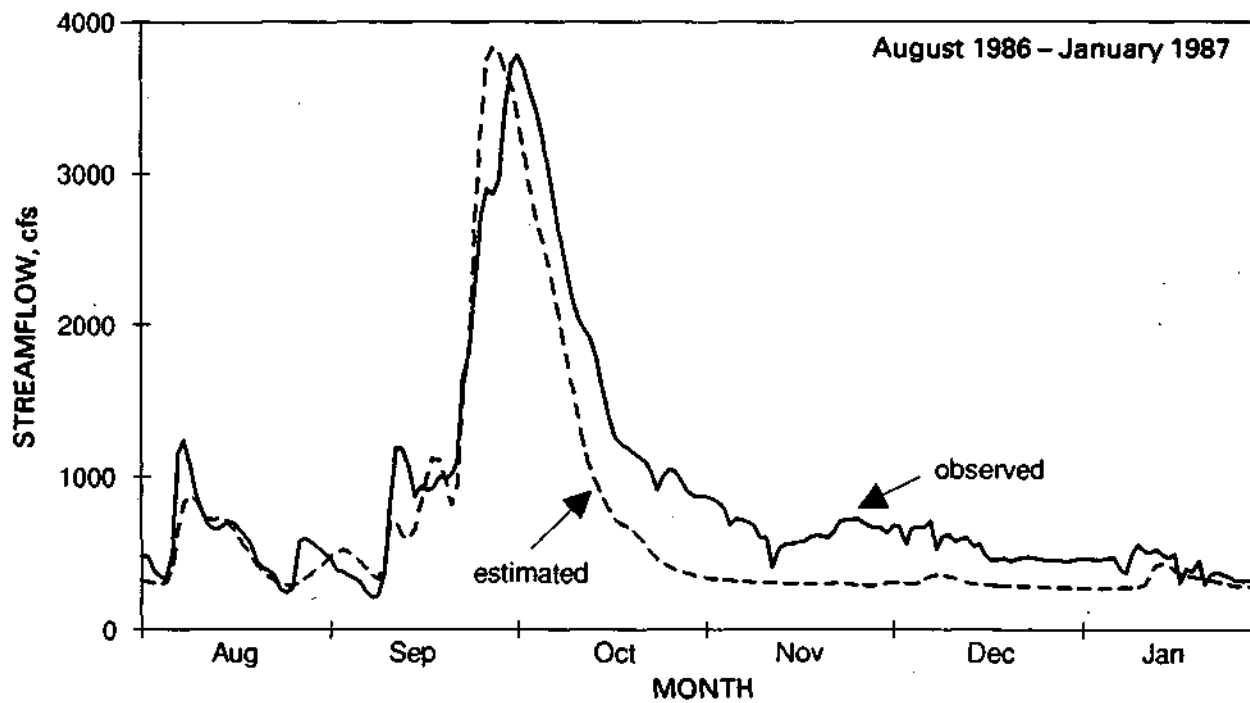


Figure 32. Observed versus estimated flow: Fox River at Wilmot, 1986

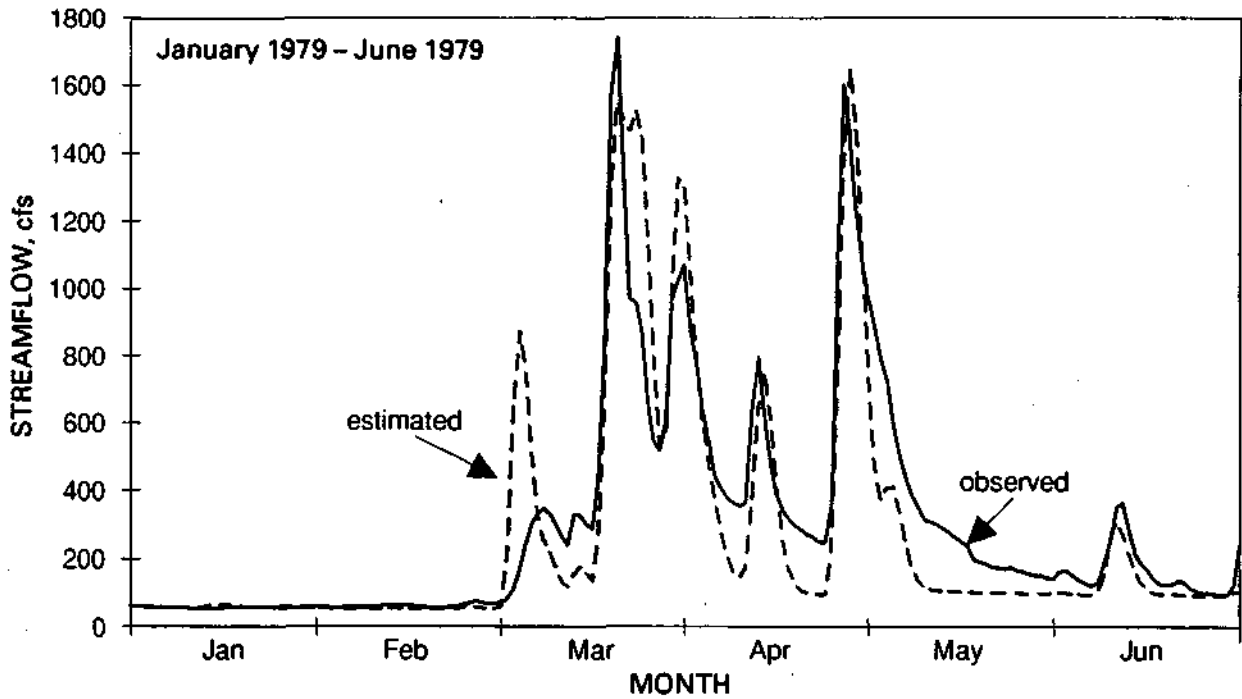


Figure 33. Observed versus estimated flow: Nippersink Creek near Spring Grove, 1979

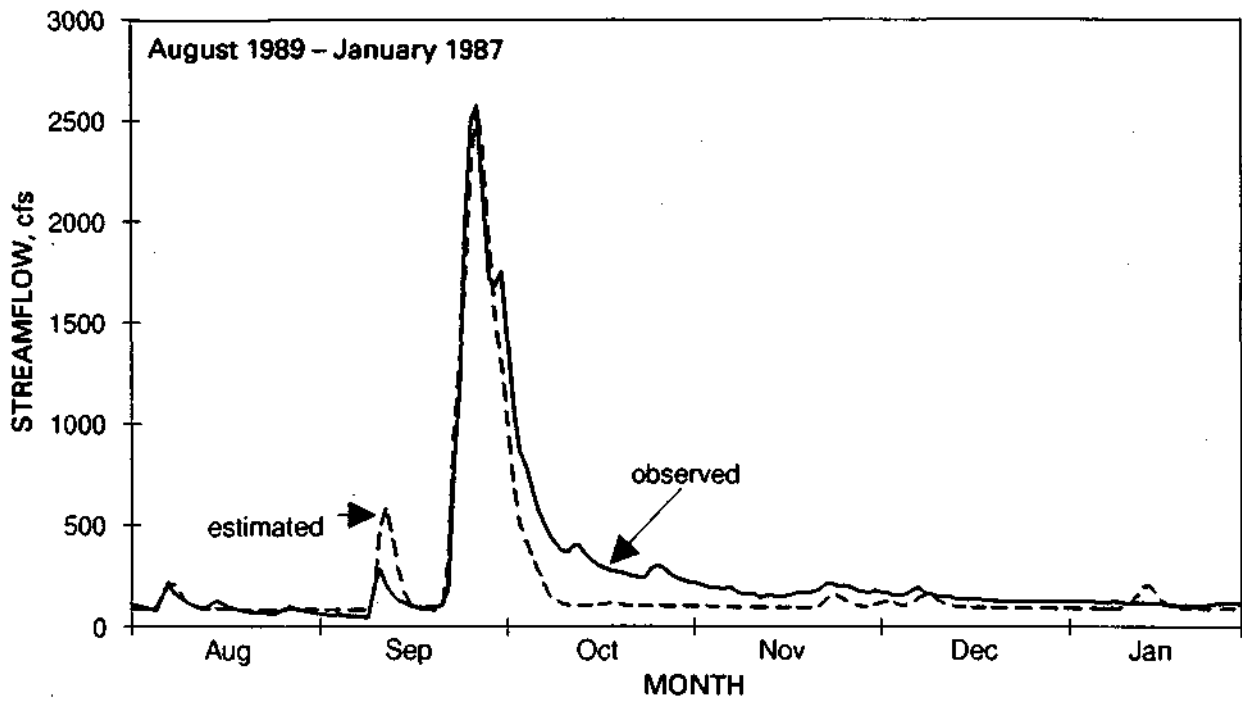


Figure 34. Observed versus estimated flow: Nippersink Creek near Spring Grove, 1986

streamflows could be modeled more effectively by using either an unsteady flow-routing model, which requires an extensive modeling effort, or by adding conceptual, linear storage-routing elements.

The second major difference between the observed and historical storms occurs during summer low flow periods. During dry periods, the historical flows have a tendency to diminish more quickly than the simulated flows. This high rate of recession in the observed flows may be caused by the effect of high evapotranspiration rates on reducing the delivery of baseflow to streams. A more complex baseflow component is needed to more accurately simulate low flow conditions.

The two systematic differences between estimated and simulated streamflow, just described, are also evident in the frequency distribution of daily flows (also termed the flow duration curve), shown in figures 35 and 36. As demonstrated in these figures, the model tends to underestimate medium flows and overestimate low flows.

Errors in Estimating Daily Flows. Model error is defined as the difference between the observed streamflow and the model-estimated streamflow. A statistical summary of the model error for the Spring Grove and Wilmot gages is given in table 28. The model's tendency to underestimate medium flows is indicated by the positive bias shown for these flows. In a similar manner, the model bias identifies the tendency to overestimate low flows. The absolute error is the average difference between observed and estimated flows while the standard error indicates the variability of these differences. On any one simulated day, the probability that the model error is less than the standard error is approximately 68%. Though the absolute values of the model error increase for high flows and flood flows, the ratio between the error and the observed flow (given by the percentage error statistics) indicate that the simulated flows are generally more accurate when estimating flood flows.

The error statistics given for the period of model validation are similar to those during the calibration period for all flow categories except the low flows. The low flows that were observed in the years 1988-1989 are significantly lower than those experienced during the calibration period, 1974-1987, and the model insufficiency during low flow periods is accentuated. The error for all flows during the validation period is larger than that shown during the calibration period only because of the large number of low flow days.

#### *Annual Maximum Flows*

Table 29 lists the estimated and observed maximum 1-day and 7-day flows for the Fox River at Wilmot for each year simulated. The maximum 7-day flow is presented as an indicator of the total runoff volume associated with the annual flood. Table 30 presents the same maximum flow information for Nippersink Creek near Spring Grove, except that a 5-day period is used to indicate the runoff volume of the flood.

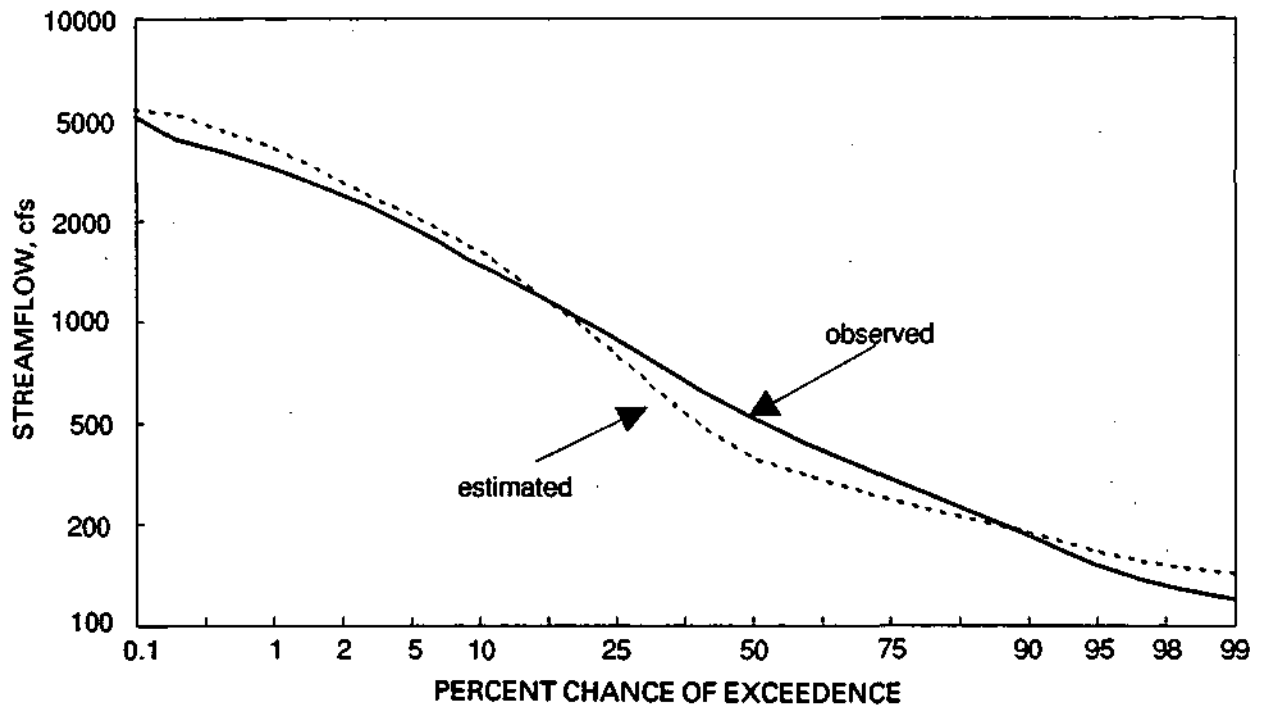


Figure 35. Frequency of daily flows: Fox River at Wilmot

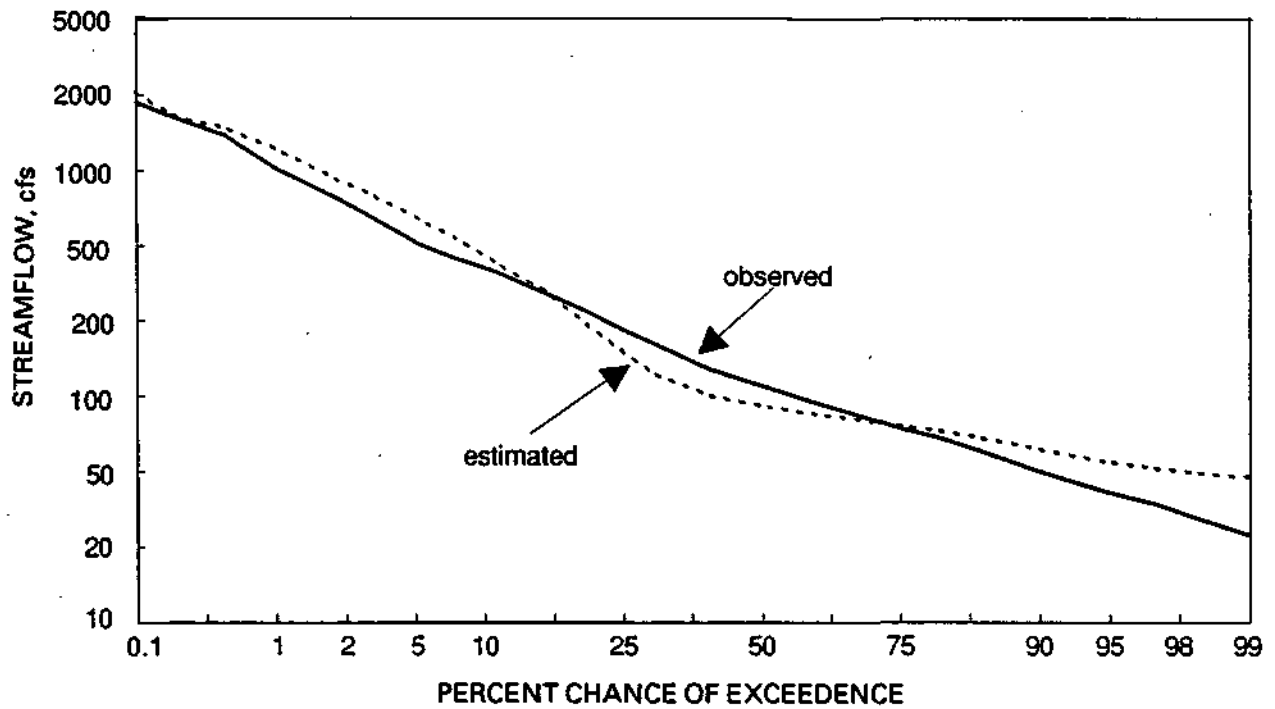


Figure 36. Frequency of daily flows: Nippersink Creek near Spring Grove

**Table 28. Error in Simulated Daily Flows**

*Wilmot Gage: Calibration Period (1974-1987)*

	All Flows	Flood Flows (>2000 cfs)	High Flows (800-2000 cfs)	Medium Flows (300-800 cfs)	Low Flows (<300 cfs)
Bias	-32 cfs (-4.6 %)	+19.cfs (+0.9 %)	-14 cfs (-2.0%)	-64 cfs (-13.3%)	+28 cfs (+17.6%)
Absolute Error	220 cfs (31.4%)	614 cfs (23.4%)	430 cfs (31.7%)	171 cfs (33.6%)	50 cfs (26.4%)
Standard Error	345 cfs (43.8%)	801 cfs (31.2%)	547 cfs (39.8%)	219 cfs (41.0%)	84 cfs (46.5%)

*Spring Grove Gage: Calibration Period (1974-1987)*

	All Flows	Flood Flows (>2000 cfs)	High Flows (800-2000 cfs)	Medium Flows (300-800 cfs)	Low Flows (<300 cfs)
Bias	+3 cfs (+1.8 %)	+3 cfs (+2.3 %)	+5 cfs (+1.3%)	-5 cfs (-3.3%)	+16 cfs (+37.8%)
Absolute Error	67 cfs (39.6%)	265 cfs (34.6%)	151 cfs (50.9%)	44.1 cfs (34.4%)	18 cfs (41.3%)
Standard Error	126 cfs (61.6%)	349 cfs (46.6%)	204 cfs (67.2%)	73 cfs (55.2%)	23 cfs (58.4%)

*Wilmot Gage: Validation Period (1960-1962, 1988-1990)*

	All Flows	Flood Flows (>2000 cfs)	High Flows (800-2000 cfs)	Medium Flows (300-800 cfs)	Low Flows (<300 cfs)
Bias	-19 cfs (-3.0 %)	-39 cfs (-1.9 %)	-78 cfs (-6.8%)	-35 cfs (-7.7%)	+35 cfs (+29.5%)
Absolute Error	209 cfs (39.0%)	759 cfs (25.4%)	405 cfs (35.6%)	231 cfs (33.7%)	78 cfs (48.4%)
Standard Error	350 cfs (56.0%)	1001 cfs (32.6%)	513 cfs (47.1%)	255 cfs (45.2%)	99 cfs (66.7%)

*Spring Grove Gage: Validation Period (1971-1972, 1988-1990)*

	All Flows	Flood Flows (>2000 cfs)	High Flows (800-2000 cfs)	Medium Flows (300-800 cfs)	Low Flows (<300 cfs)
Bias	+17 cfs (+12.9 %)	-10 cfs (-6.1 %)	+28 cfs (+7.7%)	+10 cfs (+10.8%)	+22 cfs (+82.6%)
Absolute Error	60 cfs (44.6%)	286 cfs (34.9%)	127 cfs (41.8%)	58.1 cfs (45.3%)	26 cfs (75.1%)
Standard Error	117 cfs (87.2%)	420 cfs (44.4%)	167 cfs (52.8%)	73 cfs (66.3%)	21 cfs (77.6%)

**Table 29. Annual Maximum Daily Flows for the Fox River at Wilmot: Observed versus Estimated Flow**

Calibrated Years	Maximum 1-day Flow (cfs)		Maximum 7-day Average (cfs)	
	Observed	Estimated	Observed	Estimated
1973	6430	4165	5187	3866
1974	3880	3937	3647	3602
1975	2820	4878	2666	4461
1976	3650	4771	3221	3642
1977	1090	2361	1009	2120
1978	2270	3453	1832	3080
1979	4880	5226	4769	4994
1980	1610	2180	1348	1996
1981	2170	3212	1937	2711
1982	3000	3822	2800	3159
1983	3920	5278	3403	4529
1984	2230	2497	2081	2154
1985	3020	2752	2730	2631
1986	3430	3822	3117	3272
1987	3780	3560	3486	2941
<b>Validation Years</b>				
1951	3660	3634	3083	3369
1952	3930	4628	3607	4038
1960	7100	6811	6104	5985
1961	2180	3598	1937	3067
1962	3940	3012	3757	2738
1972	3250	3600	3057	3503
1988	2260	1926	1900	1766
1989	1780	2807	1387	2138
1990	2730	4534	2509	4209

Note: Annual floods are selected by water year (October 1 - September 30).

For most years, the estimated and observed maximum flows agree reasonably well. In approximately half of the 24 years listed, the estimated maximum runoff is coincident with and falls within 15% of the observed maximum flow. An agreement between the estimated and observed maximum flows is most likely when the observed flood is greater than the median flood, i.e., has a recurrence interval of two years or greater. If the observed flow is greater than the median flood, and the estimated and observed values are significantly different, then the probabilities that the model will overestimate and underestimate are similar.

When the observed maximum flow falls below the median value, the simulated maximum flow has a noticeable tendency to overestimate the observed value. The probability that a simulated storm runoff will exceed the observed amount is particularly increased in circumstances where spatially varied rainfall is observed in the watershed and one or more



**Table 30. Annual Maximum Daily Flows for Nippersink Creek near Spring Grove; Observed versus Estimated Flow**

Calibrated Years	Maximum 1-day Flow (cfs)		Maximum 5-day Average (cfs)	
	Observed	Estimated	Observed	Estimated
1973	1460	1240	1003	897
1974	1920	1477	1267	1250
1975	1020	1408	772	1258
1976	1900	1706	1147	1230
1977	319	896	237	672
1978	946	2318	711	1760
1979	1740	1647	1314	1497
1980	610	1046	466	711
1981	551	1112	432	812
1982	1390	1439	1065	981
1983	1710	2099	1222	1656
1984	1180	1223	877	936
1985	901	896	805	735
1986	2570	2572	2176	2157
1987	1750	1282	1174	835
<b>Validation Years</b>				
1971	3720	1829	1890	1391
1972	1300	1331	1194	1195
1988	1210	621	791	553
1989	590	1333	437	913
1990	837	1446	783	1349

**Note:** Annual floods are selected by water year (October 1 - September 30).

gages register a large precipitation total. Simulated flows from such rainfall events will more likely result in the estimated annual maximum flow during those years that are otherwise dry or lacking major flood events.

Ranked values of the annual flood flows for both gaging stations are presented in table 31. The magnitude of the less frequent (or more highly ranked) events is similar between the historical and simulated records. The magnitude of medium-ranked floods, such as the median annual flood, are generally overestimated by 10% or less. As the frequency of the flood event increases beyond the median flood (and the rank of the event decreases), the difference between the flood magnitude for the simulated and historical records increases.

**Table 31. Ranked Series of Annual Maximum Flows for the Fox River at Wilmot and Nippersink Creek near Spring Grove: Observed versus Estimated Flow**

Fox River Maximum 1-day Flow (cfs)		Fox River Maximum 7-day Flow (cfs)	
Observed	Estimated	Observed	Estimated
7100	6811	6104	5985
6430	5278	5187	4994
4880	5226	4769	4529
3940	4878	3757	4461
3930	4771	3647	4209
3920	4628	3607	4038
3880	4534	3486	3866
3780	4165	3403	3642
3660	3937	3221	3602
3650	3822	3117	3503
3430	3822	3083	3369
3250	3634	3057	3272
3020	3600	2800	3159
3000	3598	2730	3080
2820	3560	2666	3067
2730	3453	2509	2941
2270	3212	2081	2738
2260	3012	1937	2711
2230	2807	1937	2631
2180	2752	1900	2154
2170	2497	1832	2138
1780	2361	1387	2120
1610	2180	1348	1996
1090	1926	1009	1766
Nippersink Creek Maximum 1-day Flow (cfs)		Nippersink Creek Maximum 5-day Flow (cfs)	
Observed	Estimated	Observed	Estimated
3720	2572	2176	2157
2570	2318	1890	1760
1920	2099	1314	1656
1900	1829	1267	1497
1750	1706	1222	1391
1740	1647	1194	1349
1710	1477	1174	1259
1460	1446	1147	1258
1390	1439	1065	1230
1300	1408	1003	1195
1210	1333	877	981
1180	1331	805	936
1020	1282	791	913
946	1240	783	897
901	1223	772	835
837	1112	711	812
610	1046	466	735
590	896	437	711
551	896	432	672
319	621	237	553

## USE OF THE MODEL FOR NEAR REAL-TIME FORECASTING

One of the major purposes of the Fox River hydrologic model is for streamflow forecasting using a near real-time mode. Near real-time modeling uses input data from precipitation events that have just recently occurred. In its use for forecasting, the Fox River model typically uses rainfall information from storms that occurred earlier in the day or on the previous day. This is contrasted with real-time modeling, which simulates the hydrologic response to a precipitation event immediately after its occurrence.

The hydrologic model is adapted for use with forecasting with only a slight modification to the data input. The model user supplies recent data on daily precipitation and mean daily air temperature. Antecedent soil moisture, streamflow, subsurface storage of water, and reservoir levels within the watershed are saved in data files from the previous operation of the model, and these files are used to provide initial conditions for the next model use. This requires that the user provide daily precipitation and temperature data for the entire period since the ending date of the previous model operation. Climatic variables (sunshine, relative humidity, and wind speed), which are not readily available on a near real-time basis, are seasonally averaged. This ordinarily has little effect on the simulated streamflow but may result in slightly higher flows during dry periods.

Given the input of near real-time precipitation and temperature data, the model will predict streamflow conditions for not only the current day, but also for up to six days into the future. In addition to this near-real time forecasting, the model can predict flows future flows using a rainfall prognosis as model input. For example, if the short-term meteorological forecast calls for heavy rainfall over the watershed during the next 24 or 48 hours, the model can predict the effects of this potential (or hypothetical) rainfall on the streamflow. An illustration of a hypothetical rainfall, and its effect on inflows into the Chain of Lakes, is given in figure 37. In this example, four precipitation amounts associated with a hypothetical rainfall are simulated: zero rainfall, a 2-inch rainfall, a 2.5-inch rainfall, and a 3-inch rainfall. An examination of the figure indicates that, for the date simulated (July 10), a 3-inch rainfall would be needed over the entire watershed before streamflows entering the Chain of Lakes would exceed 3,000 cfs. A streamflow prognosis, such as given in this figure, can provide general guidelines for preparation for oncoming storms. Because this flow prediction is based on hypothetical rainfall amounts, and the actual distribution of precipitation over the watershed would not be known until after the rainfall has occurred, the flow prognosis should not be considered a certain or accurate forecast.

For the near real-time operation of the Fox River hydrologic model, the model user must first compile the data that lists the amount of precipitation and air temperatures over the watershed since the last model simulation. Precipitation information can be obtained by one of three methods: 1) precipitation gage telemetry, 2) daily readings from the U.S. National Weather Service (NWS) cooperative raingage network, and 3) by querying (via telephone) individual gage operators. Gage telemetry is a desired source of information because it

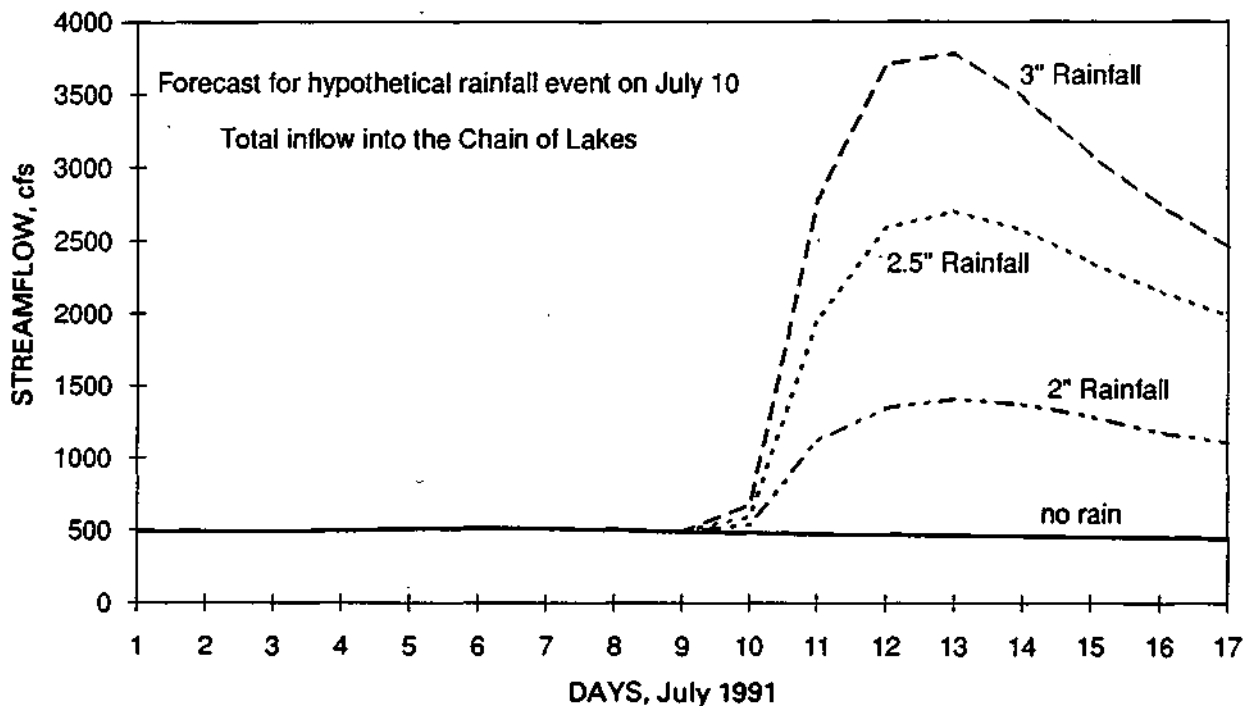


**Figure 37. Prediction of total inflow entering the Chain of Lakes, based on four rainfall prognoses**

provides real-time rainfall information, however, very few precipitation gages near the watershed are presently equipped for telemetry. The NWS data is available in machine-readable format by using either the Midwest Climate Center (MCC) computer, housed at the Illinois State Water Survey, or through the NWS River Forecast Center in Minneapolis. Currently, only seven gages, in or near the Fox River watershed, provide this daily information. These are the Oconomowoc, Mt. Mary College, Milwaukee, Racine, Lake Villa, McHenry Dam, and Chicago O'Hare precipitation gages (figure 5).

The timeliness of the available precipitation information does not significantly impact model accuracy, but it does determine how soon the streamflow can be forecasted. This, in turn, limits how soon McHenry Dam operators react to approaching flood conditions, since the flow forecast provides the technical information needed for them to modify the gate settings.

**Recommended Modifications to the Precipitation Gage Network**

The availability of reliable precipitation data is a major factor in the accurate calibration and application of rainfall-runoff models. The timeliness of the data also impacts how soon anticipatory action may be taken to mitigate flooding. Three types of improvements are recommended for the present precipitation network to improve the accuracy and timeliness of forecasting:

- Improve the overall coverage by adding new gages,
- Add more gaging stations that report daily to the NWS database, and
- Reduce the lag time of reporting, primarily by adding telemetry.

Because of the limited number of gages for which near-real time precipitation information is available, inordinate weight in modeling is given to precipitation measured at each gage. The shortage of data on the distribution of precipitation through the watershed appears to be a primary contributor to model error. Major regions in the watershed lack good gage coverage, especially the western and central portions of the watershed near Nippersink Creek and Honey Creek. To improve the overall gage coverage, a minimum of three well-placed gages are recommended: 1) near Hebron, IL, 2) at either Waterford or Wind Lake, WI, and 3) north of Elkhorn, WI.

Increasing the number of raingages that report near-real time daily rainfall data is of greater concern for forecasting than is reducing the reporting time of gages. Few of the existing daily precipitation gages report to the NWS computer network, from which the near real-time rainfall information can be obtained. A first-step improvement in the rainfall reporting network could be achieved by increasing the number of stations that report in this manner. However, telemetry of gages is of greater value because it can provide real-time information of sub-daily precipitation. And, as the number of gages increases, the timeliness of reporting will become increasingly important.

The addition of telemetry requires that the gage record continuously. New continuous recording gages could be added in lieu of converting existing daily precipitation gages to recording gages. These additional gages would also improve the overall gage coverage. The recommended new gage sites presented above are prime choices for telemetry, which is also suggested for the continuous recording gage at Eagle, WI.

## **SUMMARY**

A hydrologic model that simulates streamflow in the Fox River watershed upstream of South Elgin was developed and calibrated. The model can be used for: 1) forecasting inflows into the Fox Chain of Lakes, to help provide information to assist in the operation of McHenry Dam and 2) as input into the Fox River FEQ unsteady flow-routing model, which estimates the flow stages and discharge rates through the Chain of Lakes and downstream on the Fox River to South Elgin. The development of each of the model's major components, and their application to the Fox River watershed, is described. The model-simulated streamflows are compared with historical flows, and the model errors are examined. Model accuracy is most highly dependent on the amount of information available concerning the distribution of precipitation throughout the watershed. Improvement of the existing precipitation gage network in the watershed is recommended.

## REFERENCES

- Cotter, R.D., R.D. Hutchinson, E.L. Skinner, and D.A. Wentz. 1969. *Water Resources of Wisconsin: Rock-Fox River Basin*. U.S. Geological Survey Hydrologic Investigations Atlas HA-360.
- Cunge, J.A. 1969. On the Subject of a Flood Propagation Computation Method (Muskingum Method). *Journal of Hydraulic Research* 7 (2): 205-230.
- Curtis, G.W. 1977. *Technique for Estimating Magnitude and Frequency of Floods in Illinois*. U.S. Geological Survey Water-Resources Investigations 77-117.
- DeDeur, J.W. 1983. Recent Advances in Urban Hydrology in the USA, *Proceedings, 1983 International Symposium on Urban Hydrology, Hydraulics, and Sediment Control*, Lexington, Kentucky, pp. 1-10.
- Durgunoglu, A., H.V. Knapp, and S.A. Changnon, Jr. 1987. *PACE Watershed Model (PWM): Volume 1, Model Development*. Illinois State Water Survey Contract Report 437.
- Federal Emergency Management Agency (FEMA). 1986. *Flood Insurance Study for McHenry County, Illinois: Unincorporated Areas*. Analysis conducted by the U.S. Army Corps of Engineers, Chicago District.
- Fegeas, R.G., R.W. Claire, K.E. Guptill, K.E. Anderson, and C.A. Hallam. 1983. *Land Use and Land Cover Digital Data*, U.S. Geological Survey Circular 895-E.
- Hoggan, D.H., J.C. Peters, and W. Loehlein. 1987. Real-time Snow Simulation Model for the Monongahela River Basin. *Water Resources Research* 23(6): 1141-1147.
- Huff, F.A., and J.R. Angel. 1989. *Frequency Distributions and Hydroclimatic Characteristics of Heavy Rainstorms in Illinois*. Illinois State Water Survey Bulletin 70.
- Illinois Department of Public Works, Division of Waterways. 1962. *Report on Water Levels and McHenry Dam, Fox Chain of Lakes Region, McHenry and Lake Counties*.
- Illinois Department of Transportation, Division of Water Resources. 1991. *Investigation for Flood Control - Fox River Project FEQ Model - Lake, McHenry, and Kane Counties*.
- James, L.D., and S.J. Burges. 1982. Precipitation-Runoff Modeling: Future Directions. In *Applied Modeling in Catchment Hydrology*, Proceedings of the International Symposium on Rainfall-Runoff Modeling, V.P. Singh (ed.), Water Resources Publications, Littleton, CO, pp. 291-312.
- Knapp, H.V. 1988. *Fox River Basin Streamflow Assessment Model: Hydrologic Analysis*. Illinois State Water Survey Contract Report 454.
- Knapp, H.V., A Durgunoglu, and T.W. Ortel. 1991. *A Review of Rainfall-Runoff Modeling for Stormwater Management*. Illinois State Water Survey Contract Report 516.
- Koussis, A.D. 1980. Comparison of Muskingum Method Difference Schemes. *ASCE Journal of the Hydraulics Division* 106 (HY5): 925-929.

- Kundewicz, Z.W. 1980. Discussion of "Approximate Flood Routing Methods: A Review," by P.E. Weinmann and E.M. Laurenson, *ASCE Journal of the Hydraulics Division* 106 (HY12): 2072-2075.
- Ponce, V.M., R.M. Li, and D.B. Simons. 1978. Applicability of Kinematic and Diffusion Models. *ASCE Journal of the Hydraulics Division* 104 (HY3): 353-360.
- Ponce, V.M., and F.D. Theurer. 1982. Accuracy Criteria in Diffusion Routing. *ASCE Journal of the Hydraulics Division* 108 (HY6): 747-757.
- Ponce, V.M., and V. Yevjevich. 1978. Muskingum-Cunge Method with Variable Parameters. *ASCE Journal of the Hydraulics Division* 104 (HY12): 1663-1667.
- Schaefer, G.C., and D.L. Hey. 1979. *A Re-evaluation of Land Cover Estimates Used in the Northeastern Illinois Planning Commission 208 Project*. Report prepared for the U.S. Environmental Protection Agency by the Northeastern Illinois Planning Commission.
- Schilling, W., and L. Fuchs. 1986. Errors in Stormwater Modeling: A Quantitative Assessment. *ASCE Journal of the Hydraulics Division* 112 (HY2): 111-123.
- Singh, K.P. 1981. *Derivation and Regionalization of Unit Hydrograph Parameters for Illinois (Dam Safety Program)*. Illinois State Water Survey Contract Report 258.
- U.S. Army Corps of Engineers, Chicago District. 1976. *Plan of Study: Fox River and Tributaries, Illinois and Wisconsin*.
- U.S. Army Corps of Engineers, Chicago District. 1978. *Inspection Report, National Dam Safety Program: ILNONAME Dam 562; Wonder Lake, McHenry County, Illinois*.
- U.S. Army Corps of Engineers, Chicago District. 1984. *Interim Report, Fox River and Tributaries, Illinois: Feasibility Report With Final Environmental Impact Statement*.
- U.S. Army Corps of Engineers. 1990. *HEC-1 Flood Hydrograph Package, Users Manual: July 1990*, Hydrologic Engineering Center, Davis, CA, 283 p.
- University of Illinois Agricultural Experiment Station. 1982. *General Soil Map of Illinois*. College of Agriculture in cooperation with the Soil Conservation Service, U.S. Department of Agriculture, Urbana, IL.
- Warwick, J.J., and P. Tadepalli. 1991. Efficacy of SWMM Application. *ASCE Journal of Water Resources Planning and Management* 117 (3): 352-366.
- Younkin, L.M., and W.H. Merkel. 1988. Evaluation of Diffusion Models for Flood Routing. In *Hydraulic Engineering*, Proceedings of the ASCE 1988 National Conference, S.R. Abt and J. Gessler (eds.), pp. 674-680.